Università degli Studi di Firenze

INTERNATIONAL DOCTORATE IN
"Mechanistic and Structural Systems Biology"

CYCLE XXV

COORDINATOR Prof. Roberta Pierattelli

In-cell NMR for structural and functional studies of proteins in their native environment

Settore Scientifico Disciplinare CHIM/03

Doctorate Student
Luchinat Enrico

_____
(signature)

Supervisor
Prof. Banci Lucia

_____
(signature)

Years 2010/2012

This thesis has been approved by the University of Florence,
the University of Frankfurt and the Utrecht University

Table of contents

1. INTRODUCTION

1.1. Aims of the research

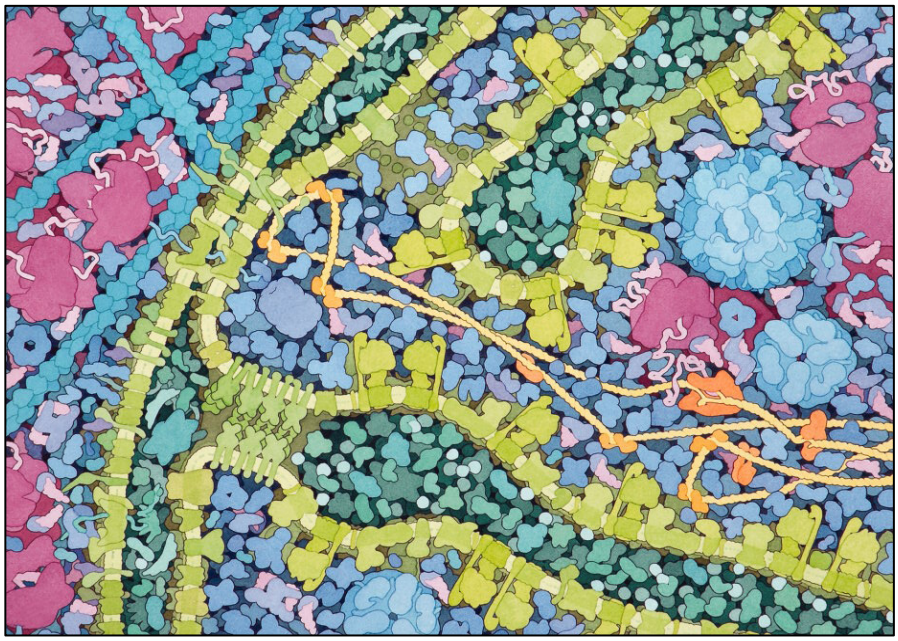

Figure 1. Artistic rendition of a mitochondrion inside a eukaryotic cell. Mitochondrial membranes and membrane proteins (green), proteins of the IMS (teal), proteins of the cytoplasm and of the mitochondrial matrix (blue) and ribosomes (magenta) are shown. From "The Machinery of Life" by David S. Goodsell, 2nd ed., 2009, XII, Springer Ed. Reproduced with permission of Springer.

Structural biology has changed the way in which we look at biological systems. Since the birth of atomic-resolution techniques scientists have started to create a molecular view of living organisms in ever increasing detail. Together with the increasing knowledge of biomolecular structures, also came a better understanding of many biological and pathological mechanisms at molecular level, which opened new ways to design drugs and cure diseases.

However, the global picture of the living cell is still escaping full understanding, due to its intrinsic complexity. The cellular environment is an extremely complex and crowded system, and all the molecular players which act inside are influenced and may be regulated by a myriad of interacting partners (**Figure 1**). In recent years, awareness has grown in the scientific community that is not sufficient anymore to characterize structure, function and interactions of isolated proteins, taken out of the real context:

there is the need for atomic-detail techniques to study proteins in their native environment, i.e. in fully-functional, living cells[1].

Among the atomic-resolution techniques available today, NMR is the most promising one to be extended to complex systems such as living cells, as it is non-destructive, works with samples dissolved or suspended in aqueous solutions at room temperature, and is able to selectively observe a given species in a complex mixture with the help of selective isotopic enrichment. The in-cell NMR approach, which consists in observing a selectively labelled protein or nucleic acid in living cells through high resolution NMR experiments, has indeed proven to be a powerful instrument to obtain structural and functional information *in situ*, thus overcoming the limitation of studying macromolecules isolated from the other cellular components.

After biosynthesis, most proteins need to undergo a series of modifications in order to reach the functional state, such as binding of metal ions and/or other cofactors, and formation of intra- or intermolecular disulfide bonds between cysteine residues, all of which influence the protein folding state and quaternary structure. Such processes are often strictly regulated by the cells; they require the protein to interact with specific partners and chaperones, and are dependent on the specific cellular compartment in which they occur. In order to obtain a biologically meaningful picture of such protein maturation processes, it is therefore important to characterize them in the environment where they really occur.

The aim of this doctorate project is to apply and extend the in-cell NMR approach to study protein folding and maturation processes in living cells. This approach, which still relies on protein overexpression, has been extended to cultured human cells. Observing the proteins in human cells allowed understanding how the correct cellular environment influences protein folding and redox state, how it controls the availability and binding of the metal cofactors, and how it mediates the effect of specific interacting partners in ways which are yet to be modelled *in vitro*. The technique was applied to study the functional processes involving two human proteins, superoxide dismutase 1 (SOD1) and Mia40, both essential proteins for the functioning of the cell, which have different maturation pathways and exert their role in different cellular compartments. The complete sequence of maturation events leading to active SOD1 was followed, both in

E. coli cells, in which the folding and redox state of the apo protein and the zinc-containing species were characterized, and in human cells, where the full process of maturation was reproduced, and the role of its specific metallochaperone CCS in copper delivery and disulfide bond formation was investigated. Finally, the folding state of Mia40 in the cytoplasm was characterized, prior to mitochondrial import, also in dependence of the cytoplasmic redox-regulating proteins glutaredoxin 1 and thioredoxin 1.

1.2. In-cell NMR

In the past years, solution NMR has been applied on cells and tissues to obtain fingerprints of the cellular metabolism, mainly by following changes in intensity and chemical shift of ^{1}H or heteronuclear resonances of small biomolecules (e.g. glucose or ATP)[2,3]. With the increase in resolution and sensitivity of the NMR instruments, provided by higher magnetic fields and cryo-cooled probes, multi-dimensional NMR experiments have become applicable on complex systems such as living cells. The combination of heterologous protein overexpression with selective isotopic labelling and the acquisition of heteronuclear NMR experiments directly on living bacterial cells were at the basis of the first application of the in-cell NMR approach[4]. In the following years, several works have shown the potential of in-cell NMR, and provided a wide range of applicability in the study of macromolecular crowding[5,6], protein structure and folding[7-11], protein-protein interactions[12,13], interaction with drugs[14,15], nucleic acids[16], or other cellular components[6,17], and protein phosphorylation[13,18,19]. Most of the initial research has been limited to proteins overexpressed in *E. coli* cells, due to the high protein concentrations obtainable and to the easiness in growing and handling the cells (**Figure 2 a,b**). Recently, efforts have been undertaken to observe proteins in eukaryotic cells. The main reason for that is that eukaryotic cells provide higher biological significance when studying eukaryotic proteins, as the physiological environment in which those proteins exert their functions in living organisms is matched. Methods have been developed to observe proteins in live eukaryotic cells by NMR, which usually rely on the insertion of pure, isotopically labelled proteins (produced in *E. coli*) from outside

the cells (**Figure 2 c-e**). *Xenopus laevis* oocytes have been used for this purpose[18-21], exploiting their considerable size to physically inject a concentrated solution of labelled protein with a micro-syringe. Other methods, which allow working on human cells, still require the protein to be inserted from outside, either by fusion with a cell-penetrating peptide (e.g. HIV-TAT) to penetrate the plasma membrane[15], or by using pore-forming toxins (e.g. streptolysine O) to permeabilize the membrane to allow protein insertion[22]. A recent work has proposed yeast as a suitable organism for protein overexpression and detection by NMR[23].

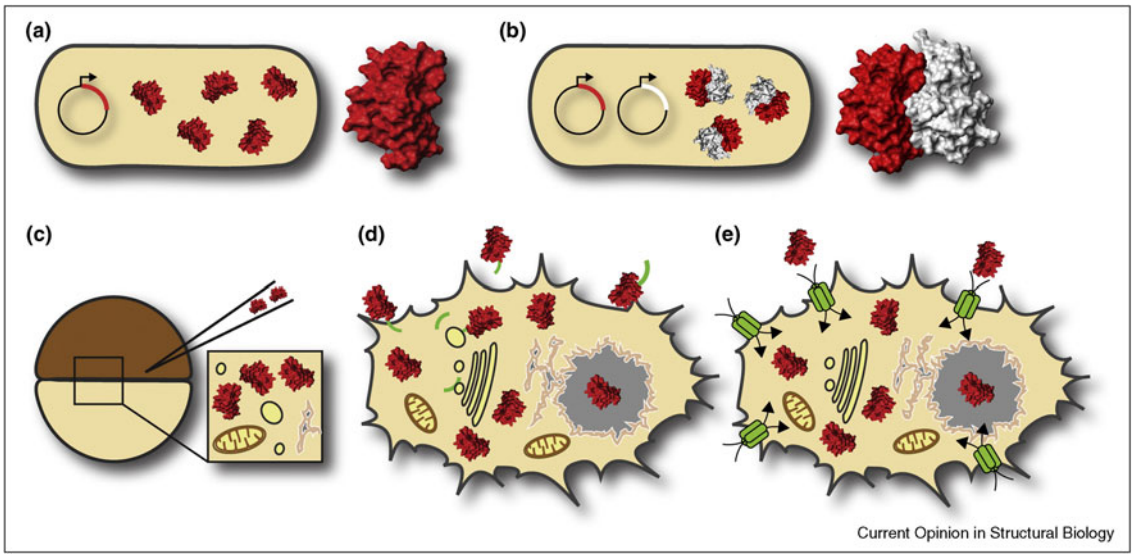

Figure 2. Previously developed approaches to in-cell NMR in bacterial and eukaryotic cells. In *E. coli* cells, one or more proteins are heterologously expressed (a,b). In *X. laevis* oocytes proteins are mechanically inserted by micro-injection (c). In cultured human cells, proteins are inserted either by fusion with a cell-penetrating peptide (d) or by permeabilizing the plasma membrane with pore-forming toxins (e). From Ito Y, Selenko P. Cellular structural biology. *Curr Opin Struct Biol*., 2010, Oct;20(5):640-8.

1.3. Maturation of superoxide dismutase 1

1.3.1. Superoxide dismutase 1

Superoxide dismutase 1 (SOD1) is a well-characterized cuproenzyme which is highly conserved in eukaryotes and also found in some prokaryotes (**Figure 3**). It has an antioxidant role in the cell, as it catalyzes the dismutation of the superoxide anion, which is a toxic by-product of cellular respiration, to molecular oxygen and hydrogen peroxide through the reaction $2O_2^- + 2H^+ \rightarrow H_2O_2 + O_2$[24]. SOD1 is ubiquitously expressed in all tissues in mammals, and is primarily localized in the cytosol, although it has been also found in small amounts in the nucleus, in peroxisomes and in the IMS of mitochondria[25-29]. In order to reach the enzymatically active dimeric form, SOD1 has to undergo several post-translational modifications: the protein has to dimerize and bind zinc and copper ions, and the formation of an intrasubunit disulfide bond between Cys 57 and Cys 146 has to occur[30-33].

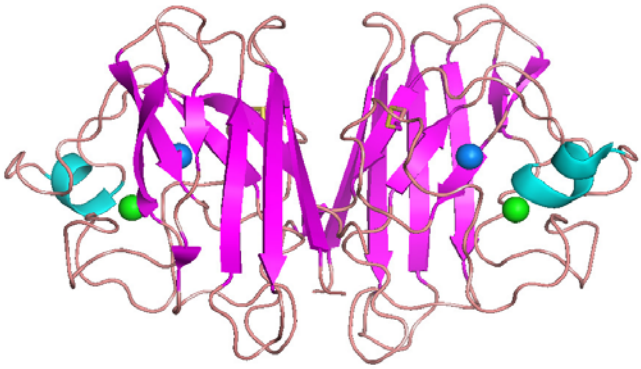

Figure 3. Structure of human Cu,Zn-SOD1.
Solution structure of oxidized, dimeric Cu, Zn superoxide dismutase 1. Copper and zinc ions (blue and green, respectively) are shown as spheres; the disulfide bonds are shown as sticks. Rendered from PDB ID: 1L3N. Banci L. et. al. *Eur. J. Biochem.* 2009, 269: 1905-1915.

The apo protein, the active enzyme and most of the intermediate species have already been structurally characterized by solution NMR[34-36], and some parts of the maturation process have been characterized at molecular level *in vitro*[37]. However, the way in which the whole maturation process occurs *in vivo* is still unknown. Many studies on SOD1 maturation have been carried on with cell cultures or animal models, but they usually relied on indirect assays, such as enzymatic activity assays, which are able to monitor only the fully mature protein[38,39], or assays for functionalized thiols, which distinguish different oxidation states of the cysteines[39,40]. Understanding how human SOD1 reaches its mature form in the cells is of critical importance, because

accumulation and aggregation of immature forms of the protein is linked to the onset of amyotrophic lateral sclerosis (ALS), a neurodegenerative disease which affects 5000-6000 people per year in the U.S. only[*,41-44]. Mutations in the sequence of hSOD1 cause the onset of the familial form of the disesase (fALS), which accounts for 10% of ALS cases[45]. However, aggregation of immature forms of wild-type SOD1 has been also linked to a fraction of the sporadic ALS cases[46]. In the cell, apo-SOD1 is thought to bind zinc spontaneously, whereas it needs a specific chaperone for copper binding and formation of the internal disulfide bond.

1.3.2. Copper chaperone for SOD1

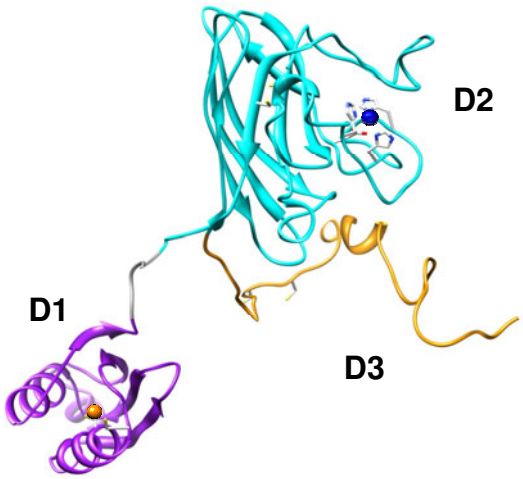

Figure 4. Structure of human CCS.
Structure of a monomer of human CCS. D1 (Atx-like domain) is shown in violet; D2 (SOD-like) in cyan; D3 in yellow. Copper and zinc ions (orange and blue, respectively) are shown as spheres; the cysteines residues are shown as yellow sticks.

To reach the functional form, SOD1 needs a specific chaperone. The copper chaperone for SOD1 (CCS) is a multi-domain metallochaperone whose principal role, in the current model, is that of delivering the copper ion to SOD1 through the formation of a transient SOD1-CCS heterodimer[47,48]. Although CCS-independent maturation of SOD1 has been reported for the human variant (and in some other organisms), the majority of SOD1 present in the human cells requires CCS to become enzymatically active[49,50]. CCS also has disulfide isomerase activity, and it has an active role in the oxidation of SOD1 cysteines[40]. CCS is a dimeric protein and each monomer is made of three distinct domains (**Figure 4**). The N-terminal domain 1 (D1) of human CCS is homologous of the Atx1-like metallochaperones, sharing the same fold, and is responsible for the delivery of a Cu(I) ion to SOD1[51]. Domain 2 (D2) of

[*] http://www.alsa.org/about-als/who-gets-als.html

CCS is structurally similar to SOD1, and is responsible for the formation of a transient heterodimeric complex between SOD1 and CCS, favouring the metal transfer and cysteine oxidation reactions[52]. Although similar to SOD1, D2 does not bind copper (although in humans D2 binds zinc, which is essential for structural stability). The C-terminal domain 3 of CCS (D3) is a short polypeptide chain which lacks secondary structure. It contains a CXC motif, which is responsible for the formation of the disulfide bond between cysteines 57 and 146 of SOD1, through a mechanism which involves the formation of an intermolecular disulfide bond between SOD1 and CCS[52], and requires molecular oxygen *in vitro*[40].

Some aspects of the mechanism of the interaction between SOD1 and CCS have been elucidated at molecular level by NMR *in vitro*[37] (**Figure 5**). Upon interaction of SOD1 with different constructs of CCS, it has indeed been confirmed that D1 of CCS is

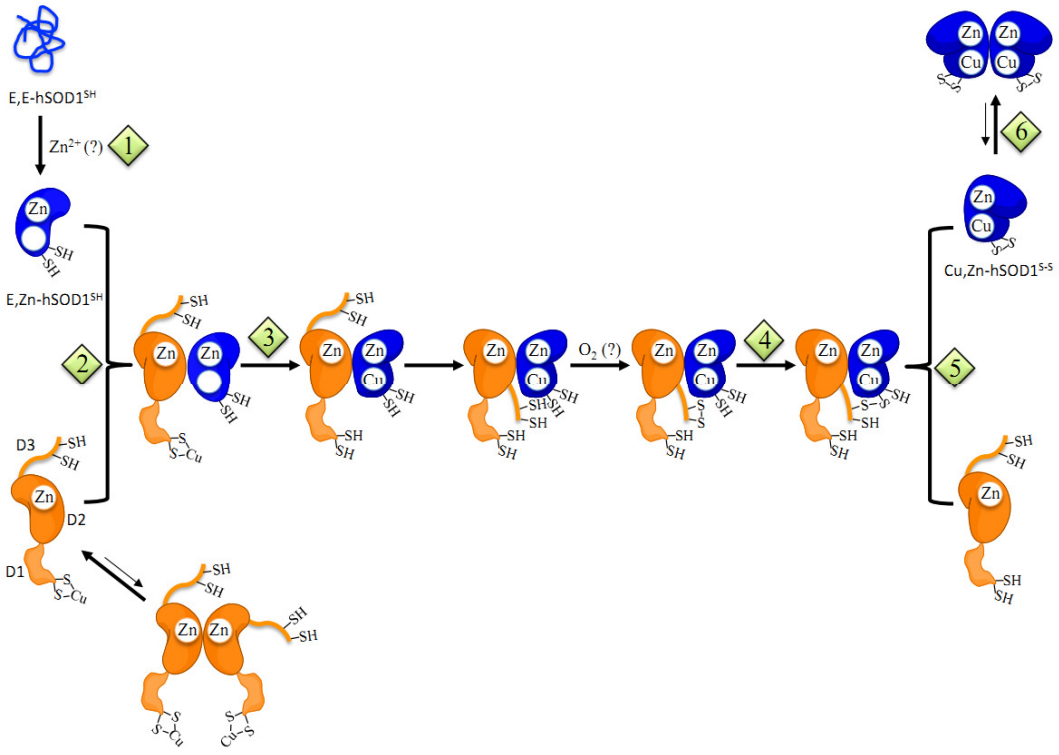

Figure 5. Steps of the interaction of SOD1 with the copper chaperone for SOD1.
A schematic of the steps of CCS-dependent copper binding and formation of the disulfide bonds of SOD1 as reported *in vitro*. (1) Zinc binding occurs spontaneously; (2) a heterodimer between CCS and SOD forms; (3) copper transfer from D1 of CCS occurs before (4,5) exchange of the disulfide bond through interaction with D3 of CCS; (5) active, dimeric Cu,Zn-SOD1 is formed. From (37).

responsible for delivering Cu(I) to E,Zn-SOD1, and the mechanism does not involve D3, as was previously suggested[53]. Instead, D3 is required *in vitro* to oxidize cysteines of Cu,Zn-SOD1^{SH}, but is not able to oxidize those of E,Zn-SOD1^{SH}. No mechanistic details have been reported, however, on the effect of CCS on the SOD1 species in different metallation states *in vivo*.

1.4. Mia40 folding in the cytoplasm

1.4.1. Mitochondrial oxidative folding

Mitochondria are essential organelles found in the cytoplasm of almost all eukaryotic cells. They are the main energy source of the cells, as they generate most of the cells supply of ATP, the main chemical energy vector of living organisms[54]. They are also involved in a range of other processes, such as signalling, cellular differentiation, cell death, cell cycle and cell growth control[55-57]. Mitochondria are small, rod shaped or filamentous organelles, and are organized in several sub-compartments (**Figure 6**). The innermost compartment, the mitochondrial matrix (MM), is enclosed by the inner mitochondrial membrane (IM), which presents invaginations towards the matrix increasing its surface. The IM is enclosed by the outer mitochondrial membrane (OM), which separates mitochondria from the cytosol. Between the two membranes lies the inter-membrane space (IMS). Although some proteins and nucleic acids are encoded in the mitochondrial DNA, (such as subunits of

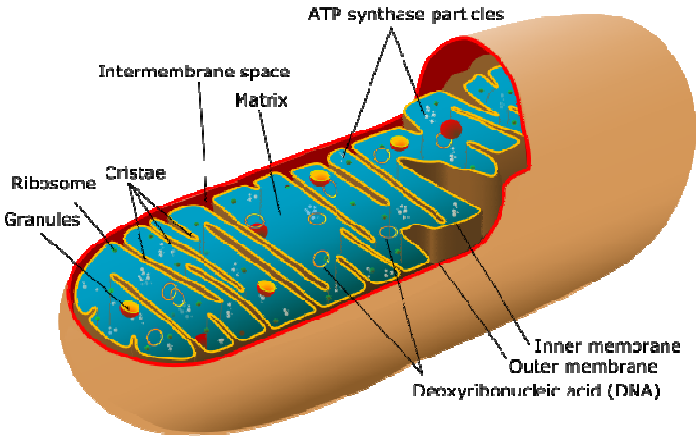

Figure 6. Internal structure of the mitochondrion.
The innermost compartment is the mitochondrial matrix (blue), enclosed by the inner membrane, which invaginates to form *cristae* (yellow). Between the inner membrane and the outer membrane (orange) is enclosed the inter-membrane space (colourless). From Wikimedia Commons.

the respiratory chain complexes, ribosomal RNAs and tRNAs), all other mitochondrial proteins are synthesized in the cytoplasm from nuclear DNA. All these proteins thus have to cross the OM through a multi-subunit translocation complex of the outer membrane (TOM)[58,59]. Some of them are then translocated through another complex in the inner membrane (translocator of the inner membrane, TIM) and reach the matrix[60,61]. A family of small proteins of the IMS, presenting a characteristic coiled-coil helix, coiled-coil helix (CHCH) folding domain, is imported through an independent mechanism[58,62]. They contain CX_nC-CX_nC cysteine motifs, and are imported through the TOM channel as reduced, unfolded polypeptides. In the IMS, these proteins interact with Mia40, which catalyzes folding through the formation of intramolecular disulfide bonds. Once oxidized and folded, they are unable to cross the outer membrane back, and therefore they are trapped in the IMS[63]. Among these small IMS proteins are Cox17, which is a copper chaperone essential for delivering Cu(I), through interaction with Sco1, Sco2 and Cox11, to the Cu_A site of cytochrome c oxidase, the fourth transmembrane complex of the respiratory chain[64-66]; and the small Tim proteins, which are chaperones essential for import and maturation of mitochondrial integral membrane proteins[67-69]. Although the function of several other substrates of Mia40 is still unknown, it is clear that the mitochondrial oxidative folding pathway has a fundamental role for respiration, mitochondrial protein biogenesis and likely other cellular functions.

1.4.2. Mia40

Mia40 is a small protein of the IMS, which is the main component of the oxidative folding pathway of the IMS[70,71]. Like its substrates, it has a CHCH fold, and it presents a CX_9C-CX_9C motif, where the cysteines are paired to form two structural disulfide bonds which hold together two alpha-helices in the mature form[72,73]. In addition, it has an active CPC redox site on the N-terminal side of the alpha-helices, which can form a third disulfide bond, and is crucial for the oxidation of the reduced substrates (**Figure 7**). Mia40 interacts with its substrates, after they enter the IMS through the TOM channel in the unfolded reduced state, through a shallow hydrophobic cleft between the alpha-helices and the CPC motif. An internal targeting signal (ITS)[74] present on the

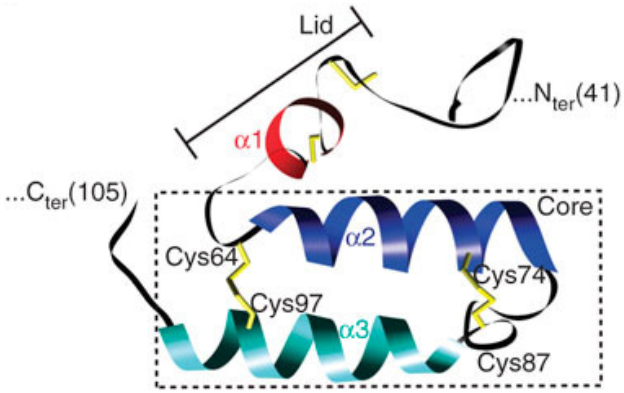

Figure 7. Structure of the folded region of Mia40.
The NMR structure of the central, folded region of oxidized Mia40 is shown. The N-terminal catalytic CPC motif (red) is in the reduced state. The core region containing the twin CX9C motif (blue and cyan) is oxidized and presents a CHCH fold. From (72).

substrate polypeptide binds to the hydrophobic cleft of Mia40 (**Figure 8**), and orients the substrate in a way to expose a cysteine side chain to the active CPC site of Mia40, where a mixed disulfide bond is formed between the substrate cysteine and the docking cysteine of Mia40 (Cys55 in the human variant). It has been shown by NMR that covalent binding to Mia40 induces alpha-helical folding in the substrate in correspondence of the ITS signal interacting with the hydrophobic cleft of Mia40, thus demonstrating the chaperone role of Mia40[73]. A second disulfide exchange reaction then occurs within the substrate, inducing the folding of the second alpha-helix and the release from Mia40, which is now CPC-reduced (**Figure 9**). The reduced active site of Mia40 is re-oxidized by reaction with the Augmenter of Liver Regeneration protein, ALR (human homolog of yeast Erv1), a FAD-linked thiol oxidase, which in turn shuttles electrons to cytochrome oxidase (and eventually to O_2) via reaction with cytochrome *c*[75]. Together, Mia40/ALR form the disulfide relay system of the IMS of mitochondria, regulating the import and folding of small protein substrates which are

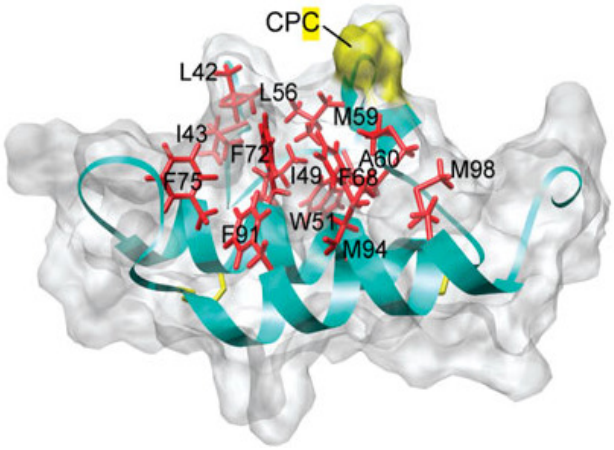

Figure 8. Mia40 hydrophobic cleft.
The conserved residues making up Mia40 hydrophobic cleft are shown (red). The N-terminal lid contains the catalytic CPC motif (yellow), which reacts with the substrates upon their interaction with the cleft. From (72).

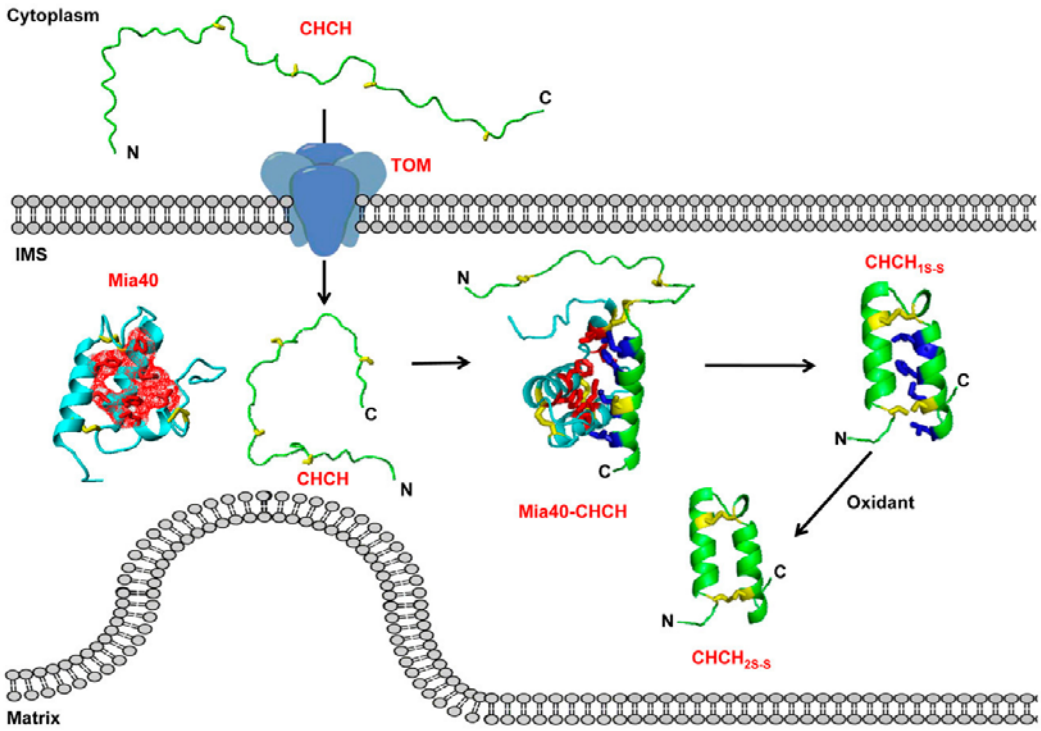

Figure 9. Steps of the oxidative folding mechanism of CHCH domain-containing proteins in the IMS.
Substrates of the oxidative folding pathway are imported in the IMS through the TOM channel in the unfolded state. Upon interaction with Mia40, an intermolecular disulfide bond is formed, inducing the formation of the first α-helix. The oxidized substrate is then released from Mia40. From (73).

essential for mitochondrial function[70,76]. Yeast Mia40 is anchored to the inner mitochondrial membrane by a trasmembrane helix, and is targeted to mitochondria by an N-terminal mitochondrial targeting sequence (MTS)[77,78]. Human Mia40 has evolved differently with respect to the yeast homolog. It is a much smaller, soluble protein (142 amino acids vs. 403 of yeast Mia40), which lacks both the transmembrane segment and the MTS, while the CPC active site and the disulfide-linked alpha-helices are conserved[79]. Consequently, human Mia40 is thought to be imported into the IMS through the same pathway of its substrates, and in the IMS it is likely oxidized by pre-existing Mia40, in a self-propagating fashion[71,80]. In order to translocate to the IMS through the TOM channel, Mia40 needs to be unfolded, and the cysteines in the CX_9C-CX_9C have to be reduced. Therefore, Mia40 must remain unfolded and completely reduced during its entire journey through the cytoplasm, until it is imported into

mitochondria. However, the factors which prevent Mia40 oxidation in the cytoplasm are currently unknown.

1.4.3. Glutaredoxin and thioredoxin systems

The cytoplasm has a redox potential more reducing compared to the IMS, due to the higher ratio between reduced and oxidized glutathione (GSH and GSSG, respectively)[81]. The effect of this reducing environment on cytoplasmic proteins is thought to be exerted by specific redox-regulating pathways, which exploit the reducing pools of GSH, and ultimately NADPH, to catalyze reduction of protein disulfide bonds. These pathways involve the glutaredoxin and thioredoxin systems[82]. Thioredoxins are a family of proteins sharing the same fold (Trx fold), which members are found in all living organisms, from bacteria to higher eukaryotes[83]. In humans, two members of the thioredoxin family, thioredoxin 1 (Trx1) and glutaredoxin 1 (Grx1), exert a thiol oxidoreductase function on a broad range of substrates in the cytoplasm, and have an important role in the cellular thiol regulation and oxidative stress defence [83,84]. Both Trx1 and Grx1 have been shown to reduce disulfide bonds in their substrates, via

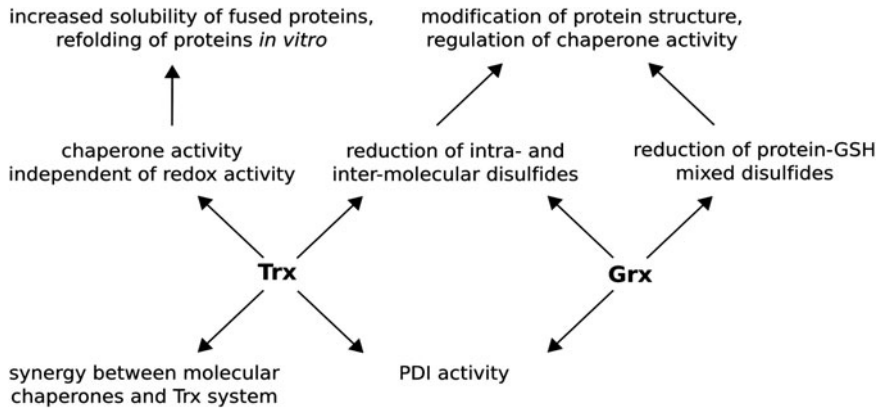

Figure 10. Schematic summary of the functions of the thioredoxin and glutaredoxin systems.
In the cytoplasm, the thioredoxin and glutaredoxin systems have diverse functions. While both Grx1 and Trx1 catalyze the reduction of disulfide bonds, they have different substrates. Grx1 is linked to GSH and glutathione reductase activity, and is also able to reduce mixed protein-GSH disulfides. Trx1 has been shown to have a chaperone activity on certain substrates independent of its redox activity, as an additional way to control protein folding. From Berndt C. et al. Thioredoxins and glutaredoxins as facilitators of protein folding. Biochim Biophys Acta. 2008 Apr;1783(4):641-50.

specific mechanisms (**Figure 10**). The Trx system requires three components: after reducing the substrate, oxidized Trx1 is reduced by thioredoxin reductase, which in turn takes the electrons from NADPH. The Grx system requires four components: oxidized Grx1 is reduced by GSH, producing GSSG. GSSG is then reduced to GSH by glutathione reductase 1, again taking the electrons from NADPH [82]. Therefore, only Grx1 is functionally dependent on the glutathione pool of the environment, while Trx1 is directly dependent on the availability of NADPH. Additionally, Grx1 is also able to react with protein-glutathione mixed disulfide bonds[82,85], and has a potential role in regulating the activity of many cytoplasmic proteins which have been found to be glutathionylated under some conditions such as oxidative stress[86].

Given their broad range of effects, it has been recently hypothesized that the Grx and Trx systems could play a role in keeping in the reduced and unfolded state the substrates of the mitochondrial disulfide relay system, while they are still in the cytoplasm, in order to keep them in an import-competent state[87]. Recently, it was shown in *S. cerevisiae* that the Trx system favours the reduced state of the small Tim proteins in the cytoplasm, and therefore it regulates mitochondrial biogenesis[88]. As Mia40 follows the same maturation pathway through the TOM channel, its redox state may also be regulated by Trx1 and Grx1 in the cytoplasm.

2. METHODS

2.1. In-cell NMR sample preparation

To produce cell samples suitable for NMR detection of protein signals, some general conditions have to be met, which are valid for protein expression in both bacterial and human cells. NMR is an intrinsically insensitive technique, therefore a cell sample must contain a sufficiently high amount of protein to be detected. The lower limit for detection is dependent on the behaviour of the specific protein inside the cells, and on the total acquisition time of the NMR experiment. Moreover, there is a limit for the total duration of the NMR experiments, which is given by the survival time of the cells. To obtain meaningful in-cell NMR data, it is obviously necessary that most of the cells are still intact and alive. High levels of cell death would result in the cellular content being released from broken cells in the external buffer. A solution for both these problems is the use of fast NMR experiments, which enable faster recycling between scans and increase the sensitivity per unit time. A third requirement is high labelling selectivity of the protein with respect to the cells. This condition is needed in heteronuclear experiments, to allow observing the protein signals above the background signals arising from other molecules. To obtain high labelling selectivity, it is important that the expression time, during which the cells grow in labelled medium, is short enough with respect to the growth rate of the cells. In some cases however, there is no need for isotopic labelling, e.g. when the ^{1}H signals to be observed fall in a region of the proton spectrum which is free from cellular background (as in the case of the histidine resonances of SOD1). When working with either *E. coli* or human cell samples, all these requirements are taken into account to optimize the experimental conditions for protein expression.

2.1.1. Bacterial cells

The workflow followed for preparing samples of bacterial cells for in-cell NMR experiments is summarized in **Figure 11**. Competent *E. coli* BL21 cells are transformed with a vector suitable for heterologous protein expression, which contains the gene encoding the protein of interest. The transformed cells are grown in unlabelled LB

growth medium overnight, to generate sufficient biomass for NMR samples. Cells are harvested by mild centrifugation and re-suspended in M9 medium, either uniformly ^{15}N labelled (unlabelled glucose is used as carbon source), or with amino acid-selective labelling (unlabelled glucose is added, plus the other unlabelled 19 amino acids, in order to minimize isotopic scrambling due to the amino acid metabolism). After a short recovery time, protein expression is induced by addition of isopropyl β-D-1-thiogalactopyranoside (IPTG). After the expression phase (4 hours for human SOD1), cells are centrifuged, washed once with clean M9 buffer and re-suspended in 1 pellet volume of M9 buffer with 10% D_2O, producing a ~50% v/v cell slurry which is then placed in the NMR tube. Bacterial cells in M9 buffer remain in suspension for a sufficient time (3-4 hours) for acquiring in-cell NMR experiments. For metal binding experiments, cells are incubated with the metal either during protein expression or immediately after, depending on the metal toxic effects. Incubation with zinc did not have any effect on protein expression, and was carried on during expression of SOD1, while for copper binding experiments cells were incubated with copper after protein

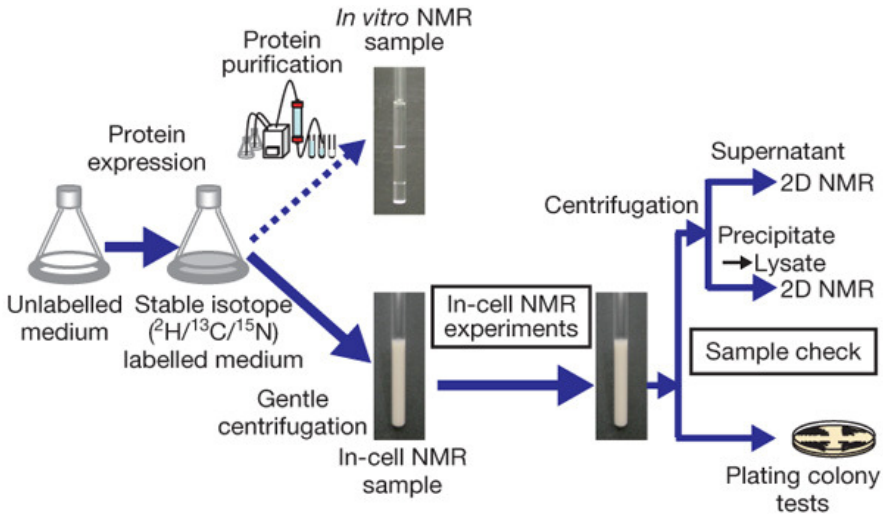

Figure 11. Workflow of an in-cell NMR experiments on *E. coli* cells.
The general protocol to prepare a sample of *E. coli* cells for in-cell NMR is schematically shown (straight arrows). Cells transformed with the gene of interest are first grown in unlabelled medium. After switching to labelled medium, protein expression is induced. Cells are then collected, suspended in buffer and put in the NMR tube. After the NMR experiments, a small sample of cells is taken for plating colony test, and the rest is pelleted again for cell lysis. The supernatant and the cell lysate are checked by NMR. From (9).

expression. After incubation, cells are washed once in M9 buffer by centrifugation. After NMR acquisition, cells are removed from the tube and pelleted. The supernatant is checked by NMR to ensure that no protein leakage due to cell disruption has occurred. Cell lysates are obtained by disrupting the cells through sonication. Cells are suspended in an equal amount of M9 buffer (or other lysis buffer), sonicated and centrifuged, and the supernatant is collected for NMR analysis. A plating test is performed to estimate cell viability after the NMR experiments. Two volumes of the cell slurry, taken before and after the experiments, are sequentially diluted 1:10 in M9 buffer several times. A set of dilutions from both samples (e.g. 10^{-5}-10^{-7}) is plated on LB-agar Petri dishes and incubated overnight. The number of colonies on plates at the same dilution is then counted, and the ratio between the two samples gives an estimate of cell viability.

2.1.2. Human cells

Human cell samples for in-cell NMR are prepared as follows. Cultured human embryonic kidney 293T (HEK293T) cells are continuously propagated in culture flasks for adherent cells, by incubation under controlled 5% CO_2 atmosphere. HEK cells have a doubling time of ~24 h, and are propagated every 3-4 days by 1:10 dilution and plating on a new flask. They maintain unaltered properties for ~20 propagation steps, after which a new cell culture is started from a frozen cell stock. During cell growth, Dulbecco's modified Eagle medium (DMEM) is used, supplemented with 10% foetal bovine serum (FBS), L-glutamine and antibiotics (penicillin and streptomicillin). The expression vector containing the gene of interest is inserted into the cells by transient transfection mediated by branched polyethylenimine (PEI). PEI is a positively charged polymer commonly used as transfection reagent, as it forms large complexes with DNA, with a net positive charge, which are internalized by the cells through endocytosis (**Figure 12**). This method provides high transfection efficiency, as many copies of vector per cell are internalized[89]. A mixture of DNA and PEI in 1:2 ratio (w/w) is incubated for 20' in a small volume of expression medium, to allow the formation of the complex. The mixture is then added to adherent cells and diluted to the final volume with expression medium supplemented with 2% FBS. Protein expression is carried out

in 24-72 h (usually 48 hours gives the optimal balance between expression level and cell growth). For unlabelled cell samples conventional DMEM medium is used, while a homemade equivalent of DMEM is used for amino acid-selective labelling. For ^{15}N labelling, U-^{15}N mammalian medium is used (BioExpress® 6000, CIL). Metal binding experiments are carried on by following the same toxicity criteria followed for *E. coli* cells. Cells are incubated with zinc during the 48 h expression time, whereas copper is added after protein expression, and incubated for additional 18-24 h. For simultaneous co-expression of two proteins, the same transfection protocol is applied, where PEI is mixed with two DNA vectors containing the two genes separately. Once inside the cells, both proteins are expressed. The amount of DNAs can be varied to obtain different expression levels for each protein (although the expression level is not linear with the DNA amount).

To prepare the NMR sample, cells are detached by incubation with trypsin, and washed

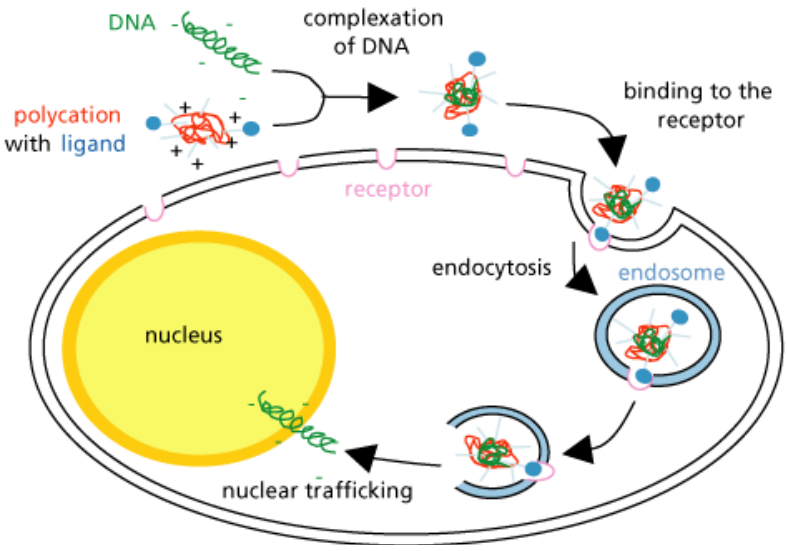

Figure 12. Polymer-mediated DNA transfection.
Schematic representation of cationic polymer-mediated DNA transfection of mammalian cells. A complex is formed between negatively charged DNA and the polymer (e.g. PEI). The complex is internalized by the cells; subsequently the DNA is released and it migrates to the nucleus. From http://www.nano-lifescience.com.

twice in phosphate buffer saline (PBS) buffer through gentle centrifugation. Cells are re-suspended in ~2 pellet volumes of fresh DMEM in 15% D_2O and pipetted in an NMR tube. Cells are sedimented to the bottom with the help of a manual centrifugation device. The human cell sample preparation steps are summarized in **Figure 13**.

After the NMR experiments, cells are re-suspended in their supernatant and pelleted again out of the tube. As with *E. coli* cells, the supernatant is checked by NMR for protein leakage. Cell disruption is obtained by 6-8 freeze-thaw cycles in liquid nitrogen on the cells suspended in PBS. After centrifugation, the supernatant containing the cytoplasmic extract is recovered. Cell viability is estimated by staining with trypan blue. The trypan blue dye selectively stains damaged or dead cells, as is able to diffuse through damaged cell membranes, and accumulates in the cytoplasm. Conversely, the plasma membrane of healthy cells is not permeable to the dye. Two aliquots of cells taken before and after the NMR experiment are diluted and incubated with trypan blue. They are then laid on a Burker chamber (or hemocytometer), and counted under a microscope. The ratio of stained over total cells gives an estimate of cell death. On average, dead cells increase from 5-6% before NMR to 8-9% after ~2 hours of NMR

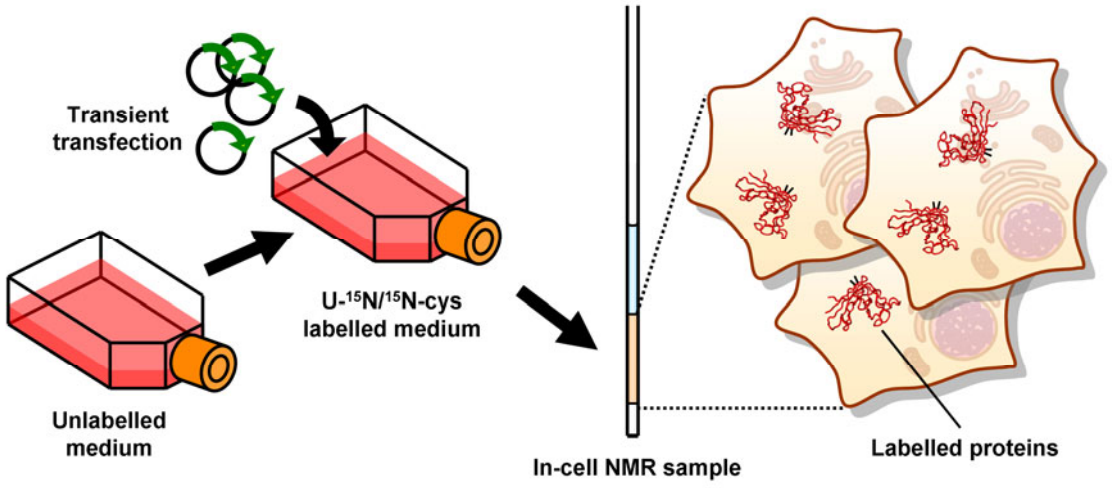

Figure 13. Workflow of an in-cell NMR experiment on *E. coli* cells.
A sample of cultured human cells for in-cell NMR is prepared as shown. Cells are first grown in unlabelled medium. They are then transiently transfected with pHLsec vector containing the gene of interest, and the medium is replaced with isotopically labelled medium. After protein expression (usually 48 h), the cells are collected, washed in PBS and put in a 3 mm Shigemi NMR tube. In-cell NMR experiments are then acquired.

experiments. Comparing the NMR spectra of the supernatant with the in-cell NMR spectra, a cell death lower than 10% is considered acceptable.

2.2. NMR experiments

NMR is an intrinsically insensitive technique. Although this limit has been much mitigated by the advent of cryoprobes and more powerful spectrometers, many heteronuclear NMR experiments, which are commonly used on labelled samples of complex molecules such as proteins, can last several hours, or even days when diluted samples are analyzed. Therefore, only a subset of these NMR experiments can be applied on living cell samples without incurring in cell disruption. Fast recycling NMR experiments provide a way to overcome this limitation.

2.2.1. SOFAST-HMQC

The Heteronuclear ^{1}H-^{15}N Single Quantum Coherence (^{1}H-^{15}N HSQC) is a commonly used 2D experiment which correlates the chemical shift of amide protons with that of the corresponding nitrogen atom[90]. It provides a unique fingerprint of the backbone of a protein, and is often used as a starting point for more complex heteronuclear experiments for backbone resonance assignment. The band-Selective Optimized Flip-Angle Short-Transient heteronuclear multiple quantum coherence ^{1}H-^{15}N SOFAST-HMQC is a fast-recycling pulse sequence which provides the same information, in about 30% of the time with respect to standard ^{1}H-^{15}N experiments at the same S/N ratio[91] (**Figure 14**). It relies on enhanced spin-lattice relaxation to increase the repetition rate of the

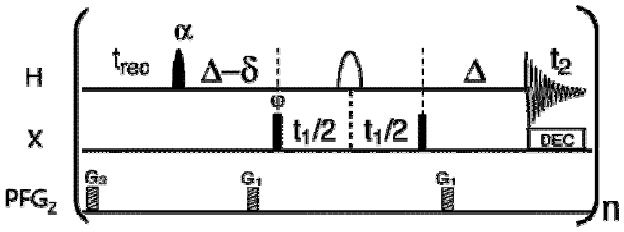

Figure 14. SOFAST-HMQC pulse sequence. Band-selective shaped pulses are used on the proton channel, to selectively perturb the amide protons. The proton excitation pulse (filled symbol) is given at the flip angle α, and has a polychromatic PC9 shape. The inversion pulse (open symbol) is given as a RE-BURP symmetric shape. From (91).

experiment without losing S/N. By use of band-selective pulses on the proton channel, only the amide resonances are perturbed during the pulse sequence, leaving the water proton and the aliphatic proton resonances unperturbed, and significantly shortening the T_1 of the amide protons. Additionally, an optimized flip angle is used, which allows for more efficient excitation at high repetition rates. By varying the length of the shaped pulses, and the offset with respect to the water resonance, the excitation window can be tuned on the amide resonance range of the specific protein, and cleaner water suppression can be obtained. The recycle delay of the experiment is then adjusted to maximise S/N ratio per unit time. In experimental conditions of this work, adjusting the excitation pulse length did not increase the S/N ratio, therefore a 90° shaped pulse was used.

^{1}H-^{15}N SOFAST-HMQC experiments applied on cell samples expressing ^{15}N labelled proteins provide spectra with good S/N ratio in ~30' on *E. coli* cells, while ~1 hour is necessary for human cell samples where the protein concentration is in the tens-of-µM range.

2.2.2. ^{1}H NMR spectra

In principle, proteins expressed in *E. coli* or human cells could be detected with ^{1}H-only NMR experiments. The obvious problem in not using heteronuclear experiments is that no filter is applied to observe the protein, which is then obscured by the signals arising from other cellular components. In some instances however, a set of protein resonances falls in a region of the ^{1}H spectrum which is free from background signals, and ^{1}H NMR spectra can be of use, without any labelling scheme being required. In the case of the histidine protons of SOD1, which provide useful information on the protein metallation state, sequences with a binomial pulse for water suppression (3-9-19 pulse train) provide the highest sensitivity. By differently manipulating proton magnetization at different offsets from the water resonance, water protons can be flipped back on the z-axis while keeping the histidine protons on the plane, thus avoiding magnetization losses due to proton exchange with water.

2.3. Protein purification

2.3.1. Human SOD1

U-^{15}N labelled samples of human SOD1 in different metallation and redox state are used as *in vitro* references, to interpret the in-cell NMR data. SOD1 is produced by heterologous expression in *E. coli*. After cell lysis, a first purification step is performed with anionic exchange chromatography with DEAE Sepharose resin; the protein is eluted in a gradient of NaCl. The fractions containing SOD1 are collected for a second step of purification with size-exclusion chromatography (SEC) with Superdex75 resin. The fractions containing pure SOD1 are collected and concentrated. To obtain apo-SOD1, protein demetallation is carried on in several dialysis steps against sodium acetate buffer supplemented with EDTA at increasing pH (starting from ~3.5), in order to remove both copper and zinc ions by decreasing the histidines affinity for the metals. Finally, the buffer is exchanged against phosphate buffer at pH=7. To obtain E,Zn-SOD1, one equivalent per monomer of zinc is added at pH=5. For copper binding, one equivalent of copper is added at neutral pH. To produce the reduced-cysteine species, 50 mM DTT is incubated at pH>7.

2.3.2. Human Mia40

Mia40 is produced by heterologous expression in *E. coli*, as a fusion protein with His-tagged maltose-binding protein (MBP) to increase protein yield and solubility. In a first purification step, the fusion construct is loaded on a Hi-Trap Ni-chelating resin and eluted in 400 mM imidazole. Mia40 is then cut from MPB by incubation with Tobacco Etch Virus (TEV) protease, and the reaction mixture is loaded again on Ni-chelating resin to remove the His-tagged MBP. Finally, two SEC steps are performed in phosphate buffer at pH=7 to obtain pure Mia40. Reduction of the structural disulfide bonds of Mia40 is performed by incubating Mia40 at 95° 10’ with 10 mM DTT in phosphate buffer.

3. RESULTS

3.1. In-cell NMR in **E. coli** *to Monitor Maturation Steps of hSOD1*

In all living organisms, most proteins need to undergo a series of modifications, in order to reach the functional state, after they are synthesized in the cytoplasm. Such maturation steps include binding of cofactors such as small molecules or metal ions, change in the cysteines redox state with formation of disulfide bonds, and formation of quaternary structure. These processes may be deeply influenced by the intracellular environment, therefore, for their correct understanding, it is necessary to study them inside the cells, with an atomic-detail technique. In this work, the first steps of maturation of human superoxide dismutase 1 (hSOD1) were characterized in *E. coli* cells. The cytoplasm of *E. coli* is used as a model of the eukaryotic cytoplasm, having similar macromolecular crowding, pH and redox potential. By overexpressing SOD1 in *E. coli* cells, different maturation states were characterized. When expressed in absence of metal ions, SOD1 was found in the partially unfolded, monomeric apo state. In that state, only part of the amide resonances was detected in-cell, corresponding to the residues of the flexible loops, while the resonances of the structured part were broadened beyond detection. This effect could be due to weak, non-specific interactions occurring between the apo protein and other cellular components, which would slow down the tumbling of the structured part broadening the signals. When SOD1 was expressed in presence of zinc ions in the culture medium, it bound zinc and dimerized. Interestingly, zinc binding in cells was selective, as only the species with one zinc ion per monomer was detected (E,Zn-SOD1), whereas purified SOD1 easily binds a second zinc ion to the copper binding site, giving rise to a mixture of species. By expressing selectively ^{15}N-cysteine labelled SOD1, the cysteine redox state in-cell was determined. Both the apo and the zinc-containing protein were in the reduced state in the cytoplasm, thus indicating that disulfide bond formation does not occur spontaneously after the zinc-binding step, but likely requires copper binding and/or the intervention of the specific copper chaperone (CCS).

OPEN ACCESS Freely available online

PLoS one

In-cell NMR in *E. coli* to Monitor Maturation Steps of hSOD1

Lucia Banci[1,2]*, Letizia Barbieri[1,2], Ivano Bertini[1,2]*, Francesca Cantini[1,2], Enrico Luchinat[1,2]

1 Magnetic Resonance Center, University of Florence, Sesto Fiorentino, Italy, **2** Department of Chemistry, University of Florence, Sesto Fiorentino, Italy

Abstract

In-cell NMR allows characterizing the folding state of a protein as well as posttranslational events at molecular level, in the cellular context. Here, the initial maturation steps of human copper, zinc superoxide dismutase 1 are characterized in the *E. coli* cytoplasm by in-cell NMR: from the apo protein, which is partially unfolded, to the zinc binding which causes its final quaternary structure. The protein selectively binds only one zinc ion, whereas *in vitro* also the copper site binds a non-physiological zinc ion. However, no intramolecular disulfide bridge formation occurs, nor copper uptake, suggesting the need of a specific chaperone for those purposes.

Citation: Banci L, Barbieri L, Bertini I, Cantini F, Luchinat E (2011) In-cell NMR in *E. coli* to Monitor Maturation Steps of hSOD1. PLoS ONE 6(8): e23561. doi:10.1371/journal.pone.0023561

Editor: Andreas Hofmann, Griffith University, Australia

Received May 6, 2011; **Accepted** July 20, 2011; **Published** August 24, 2011

Copyright: © 2011 Banci et al. This is an open-access article distributed under the terms of the Creative Commons Attribution License, which permits unrestricted use, distribution, and reproduction in any medium, provided the original author and source are credited.

Funding: This work was supported by the Italian FIRB PROTEOMICA MIUR contract RBRN07BMCT, and is part of the JRA2 of the Bio-Nuclear Magnetic Resonance project (European Commission's FP7, project number 261863). The funders had no role in study design, data collection and analysis, decision to publish, or preparation of the manuscript.

Competing Interests: The authors have declared that no competing interests exist.

* E-mail: bertini@cerm.unifi.it (IB); banci@cerm.unifi.it (LB)

Introduction

Folding and maturation of proteins characterized by post-translational modifications and formation of quaternary structure is a complex process which progresses through a number of well concerted events. A deep understanding of such processes requires their characterization at molecular level in a cellular context.

In-cell NMR has the unique ability to acquire structural and conformational information of biomolecules in their native cellular environment at atomic level [1,2]. It has been previously shown that the bacterial cytoplasm is a good model of the eukaryotic one, especially to study the effects of molecular crowding on protein folding and non-specific interactions [3], as they have similar pH and redox potential [4–6].

Within this frame, we have characterized by in-cell NMR the wild-type human copper, zinc superoxide dismutase 1 (hSOD1) protein, as well as the initial steps towards its maturation.

hSOD1 is a 32 kDa homodimeric protein involved in the cellular defence against oxidative stress. It is physiologically expressed at relatively high concentrations in human cells, and it exerts its function in the cytoplasm, in the nucleus and in the mitochondrial IMS [7]. In order to reach its mature form, hSOD1 has to incorporate one Zn^{2+} ion and one catalytic Cu^{+} ion per subunit. Additionally, two conserved cysteine residues (Cys 57 and 146) form an intramolecular disulfide bridge during the protein maturation process.

Apo-hSOD1 has been recently linked to the familial form of amyotrophic lateral sclerosis (fALS), a fatal motor neurodegenerative disease [8–10]. The immature form of hSOD1, i.e. without the metal ions and with a misfolded structure, is believed to play a pivotal role in ALS pathology [11,12]. Therefore folding and metal insertion are important factors to be investigated in the cellular environment.

In this work, we characterized the state of hSOD1, analyzing samples of *E. coli* cells overexpressing hSOD1 protein, in its initial state after expression, and its initial maturation steps through zinc uptake and disulfide bond formation and we determined how this affects the tertiary and quaternary structure of the protein. This study sheds some light on the folding state of the non-mature protein as well as on the process of zinc uptake and protein folding in the cellular environment.

Results

Folding state of apo-hSOD1 in the cytoplasm

$^{1}H,^{15}N$-SOFAST-HMQC spectra [13] were acquired on cell samples overexpressing hSOD1 in a metal-free medium. The spectra were then recorded again on the cleared lysates after cell lysis. The in-cell NMR spectrum shows mainly peaks in the 8.0–8.3 ppm (^{1}H) region. In addition, few more dispersed peaks are visible, at lower S/N ratio (Figure 1 A). When the cells are lysed, still maintaining the sample in anaerobic conditions, a few other dispersed peaks appear, indicating the presence of some structured regions of the protein, while most of the peaks are still in the "unfolded" region. The spectrum of the latter species compares well with that of the monomeric apo form with reduced cysteines, E,E-hSOD1^{SH-SH}(Figure 1 B) which also shows many peaks in the region of unstructured peptides, overall corresponding to the ones that remain visible in the in-cell spectrum of the protein. This therefore indicates that, once the newly produced protein is in the cytoplasm and in the absence of metal ions, it is in a reduced, metal-free state.

Several interpretations of the in-cell NMR spectrum of apo-hSOD1 are possible: apo-hSOD1 could be completely unfolded in the cytoplasm; in this case all the NH cross-peaks would be overlapped in the "unfolded" region of the spectrum. The protein

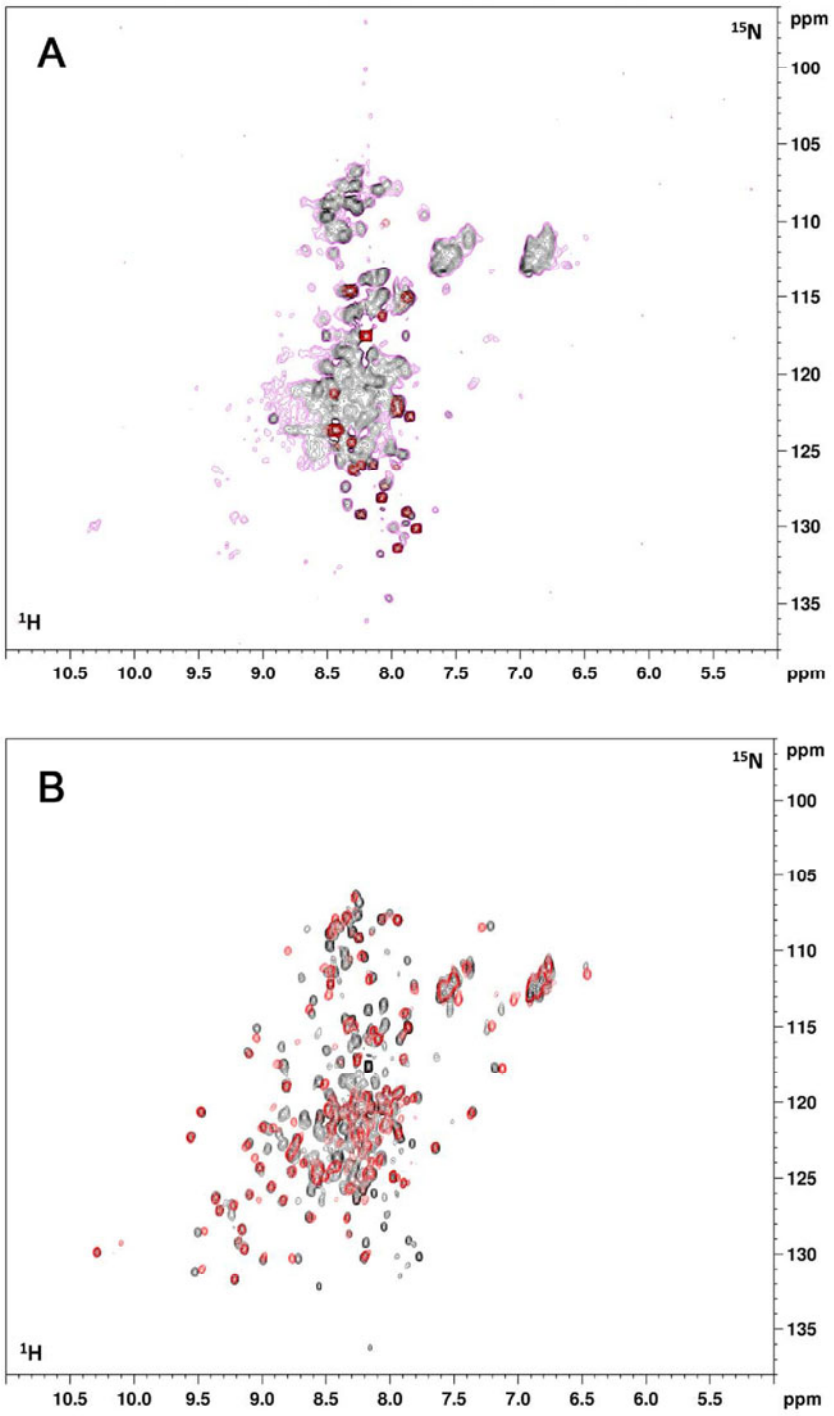

Figure 1. In-cell NMR spectra of apo-hSOD1 and of cell lysate. (A) In-cell ^{1}H-^{15}N SOFAST-HMQC spectrum of *E. coli* cells expressing hSOD1 in defect of Zn(II). Two different thresholds are shown (black, purple). At lower threshold (purple) some weak and broad signals are visible, while only signals in the unfolded region of the spectrum are visible at higher threshold (black). Signals belonging to other cellular components are overlaid in red. These are always present in all in-cell spectra. (B) Overlay of the ^{1}H-^{15}N SOFAST-HMQC spectrum of a cell lysate without addition of Zn(II) (black), and the ^{1}H-^{15}N HSQC of an *in vitro* sample of E,E-hSOD1^{SH-SH} (red).
doi:10.1371/journal.pone.0023561.g001

could be only partially unfolded, as is the case of *in vitro* E,E-hSOD1$^{SH\text{-}SH}$ [14], and the cross-peaks of the folded region could be lost as a consequence of chemical or conformational exchange phenomena in the NMR timescale. Alternatively, the loss of the signals could be a consequence of interactions with other components of the cellular environment, like membranes, bacterial heat shock proteins or DNA. Finally, the in-cell NMR species could be an oligomer of apo-hSOD1.

To determine whether apo-hSOD1 is completely unfolded in the cytoplasm, the in-cell NMR spectrum was compared to the *in vitro* NMR spectrum of E,E-hSOD1$^{SH\text{-}SH}$ denatured with guanidinium chloride (Figure 2 A). The latter spectrum also shows only signals in the region typical of unfolded proteins, but is somewhat different from the in-cell NMR spectrum. The cross peak of the side-chain NH of Trp 32 for example, which in the folded protein is located in a β-strand of the hSOD1 β-barrel, falls at different chemical shifts in the two spectra (Figure 2 B) and in particular in the cytoplasmic species it has the same chemical shift as in the *in vitro* E,E-hSOD1$^{SH\text{-}SH}$. This indicates that in the cellular environment apo-hSOD1 is not completely unfolded, but the signals of the folded part are lost.

The loss of those signals could be caused by chemical or conformational exchanges phenomena involving the protein amides. In this case, the low S/N ratio of the signals should be increased at different magnetic field strength and temperature. SOFAST-HMQC spectra of cell samples expressing apo-hSOD1

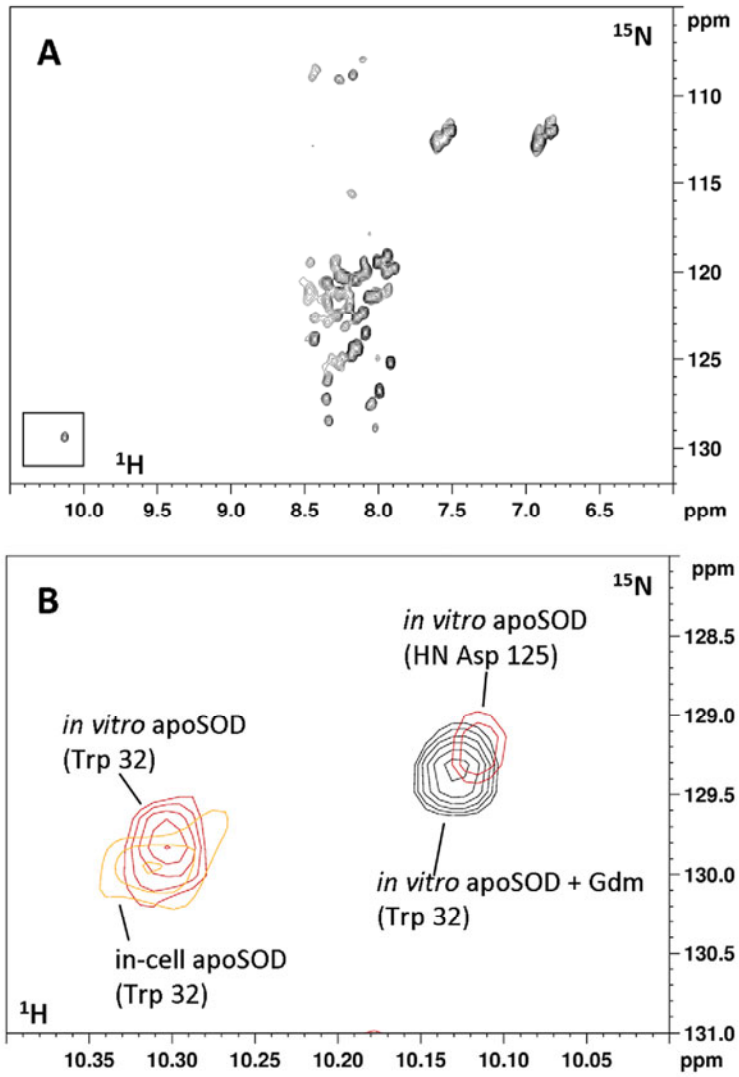

Figure 2. Trp 32 side chain of denatured *in vitro* apo-hSOD1. (A) ^{1}H-^{15}N HSQC of an *in vitro* sample of E,E-hSOD1$^{SH\text{-}SH}$ denatured with 0.5 M guanidinium chloride. (B) Zoom of the (A) spectrum showing the signal of Trp 32 (black). Overlaid are the in-cell NMR spectrum of apo-hSOD1 (orange) and the *in vitro* spectrum of non-denatured E,E-hSOD1$^{SH\text{-}SH}$.
doi:10.1371/journal.pone.0023561.g002

were acquired at 500 MHz at 315 K and at 800 MHz at 288 K and 298 K. In both cases no increase of the S/N ratio of the signals was observed (data not shown), disfavouring this hypothesis.

The possibility of apo-hSOD1 forming aggregates in the cells was also taken into account. Apo-hSOD1 is known to give rise, both *in vivo* and *in vitro*, to soluble oligomeric species, and eventually to fibrils [11,15]. It has been shown that the formation of soluble oligomers of apo-hSOD1 *in vitro* leads to the complete loss of the signals in the HSQC spectrum. This is most true for fibrils, which are insoluble species. Therefore, the presence of several signals in the "unfolded" region of the in-cell NMR spectrum, and the fact that the missing signals are completely recovered after cell lysis, excludes the possibility that oligomers of apo-hSOD1 have formed in the cytoplasm.

Apo-hSOD1 in the cytoplasm could be interacting to some extent with cellular components. Such interactions would lead to the formation of high molecular weight complexes, determining the broadening beyond detection of the signals. In this situation, only the amide signals of the unstructured regions are observable, as they might not interact with the cellular components and therefore move freely with respect to the slow-tumbling complex. Upon cell lysis these interactions are released, the protein becomes free and tumbles faster. The interactions have to be weak enough, in order to be disrupted upon sonication and subsequent dilution of the cell content in M9 buffer (~1:2 dilution).

The line broadening effect could be better explained considering the multiplicity of weak interactions in which apo-hSOD1 is involved. hSOD1 is overexpressed, and is more abundant than any other cellular species (~850 μM in the cytoplasm). Therefore all the different interactions involve some hSOD1 molecules at any given time. In fact we can think of many sub-populations of apo-hSOD1, each experiencing a different chemical environment, thus having different chemical shifts. This "cellular anisotropy" causes an inhomogeneous broadening of different amount for each NH cross-peak. The peaks of the folded part have larger chemical shift dispersion and are thus made invisible by the cellular anisotropy.

Zinc binding properties of cytoplasmic hSOD1

$^{1}H,^{15}N$-SOFAST-HMQC spectra were acquired on cell samples overexpressing hSOD1 in a minimal medium supplied with different amounts of $ZnSO_4$. The concentration of zinc in the medium ranged from 10 μM to 1 mM in the expression medium; this is always in excess with respect to the total amount of hSOD1 expressed. When cells are grown in the presence of extra zinc added in the expression medium, the in-cell NMR spectra of hSOD1 show remarkable differences with respect to those of in-cell hSOD1 expressed without added zinc (Figure 3 A). The appearance of several dispersed peaks, together with the disappearance (or decrease in intensity) of some signals in the 'unfolded' region, indicates that hSOD1 inside the bacterial cells binds zinc when this is added to the culture medium in excess relatively to the total amount of protein expressed. This in-cell NMR spectrum compares very well with that of E,Zn-hSOD1^{SH-SH} (the species with one zinc ion bound to the zinc binding site), and not with that of Zn,Zn-hSOD1^{SH-SH} (the non-physiological species with two zinc ions bound to both metal binding sites). Among the various signals, the NH signals from Gly 61 and Thr 135, which are close to the metal binding sites, have chemical shift values which are indicative of the metal binding state of the protein, i.e. of which metal site is occupied by which metal ion. In the in-cell NMR spectra these signals have chemical shifts very close to those observed in the E,Zn-hSOD1^{SH-SH} *in vitro* spectrum (combined chemical shift difference ^{1}H-^{15}N: $\Delta\delta G61 = 0.015$, $\Delta\delta T135 = 0.029$), while are more distant from the corresponding signals of the Zn,Zn-hSOD1^{SH-SH} form ($\Delta\delta G61 = 0.169$, $\Delta\Delta\delta T135 = 0.123$) (Figure 3 B, Figure S1). This is a striking result as it indicates that hSOD1 in the cytoplasm has a higher selectivity than *in vitro* in the binding site mode. Indeed, when sub-stoichiometric amounts up to 1 equivalent of zinc are added to E,E-hSOD1 *in vitro* at physiological conditions (pH around 7), mixtures of E,E-hSOD1, E,Zn-hSOD1 and Zn,Zn-hSOD1 species are formed, while when 2 equivalents of zinc per subunit are added only Zn,Zn-hSOD1 is formed. Instead in the cytoplasm hSOD1 binds zinc only in its native binding site, giving only E,Zn-hSOD1 species, while zinc binding to the copper site does not occur, and Zn,Zn-hSOD1 species is not detected (within the sensitivity of the NMR experiment). Moreover, this effect is seen regardless of the concentration of zinc added to the medium, even at 1 mM.

After the in-cell NMR experiments, the cell samples were washed with metal-free medium in order to remove the external zinc, and NMR spectra of the cleared cell lysates were acquired. Only the species Zn,Zn-hSOD1^{SH-SH} was detected. Apparently, an excess of zinc is still present inside the cells, which is made available upon cell lysis and binds at the hSOD1 copper binding site.

Cysteine redox state determination

hSOD1, when is either in the cytoplasm or in the cell lysate, without addition of zinc has all its cysteines in the reduced state, as monitored from ^{1}H-^{15}N signals of selectively labelled cysteines.

After cysteine oxidation by air exposure, the spectrum shows the four peaks of the cysteines, with that of Cys 57 only detectable below 298K. Cys 57 and 146 have chemical shifts equal to those previously assigned in the *in vitro* dimeric E,E-hSOD1^{S-S} species [16] and indicative of their oxidized state. After reduction of the same sample with DTT, the peaks shift back to the chemical shift they have in the cells and in the cell lysate, therefore confirming the reduced state of Cys 57 and 146 in the cytoplasm (Figure 4 A–C). The same analysis, repeated for cells and lysates when hSOD1 is expressed in the presence of Zn(II), shows that also in the case of E,Zn-hSOD1, Cys 57 and 146 in the cytoplasm are reduced (Figure 4 D–F).

The redox state of the cysteines is further confirmed by reaction with AMS performed directly on the cell culture and on the cell lysate after the NMR experiments (Figure S2, Information S1).

Quaternary structure of hSOD1

The spectra of the ^{15}N-cysteine labelled protein provide evidences on the quaternary structure of hSOD1 in the cellular cytoplasm. Indeed disulfide bond formation and protein dimerization are tightly linked processes. *In vitro*, the species E,E-hSOD1^{SH-SH} is monomeric, while both E,E-hSOD1^{S-S} and E,Zn-hSOD1^{SH-SH} are homodimers [14,17]. In the NMR spectra of both *in vitro* ^{15}N-cysteine labelled E,E-hSOD1 and E,Zn-hSOD1, the amide cross-peak of Cys 146 has a large chemical shift difference between the two redox states (Figure 4 B,D). This difference is expected, as Cys 146 is directly involved in the disulfide formation. On the other hand, the cross-peak of Cys 6 has a similar behaviour upon disulfide formation in E,E-hSOD1, but changes little in the case of E,Zn-hSOD1 (Figure 4 C,F). This is because Cys 6 is located close to the interaction surface of the homodimer. Upon E,E-hSOD1 dimerization as a consequence of disulfide bond formation, Cys 6 changes its chemical environment, whereas in E,Zn-hSOD1, which is always dimeric regardless of the oxidation state, it remains unchanged. Therefore the chemical shift of Cys 6 is a marker of the quaternary structure of hSOD1. The chemical shift of Cys 6 of both in-cell E,E-hSOD1^{SH-SH} and E,

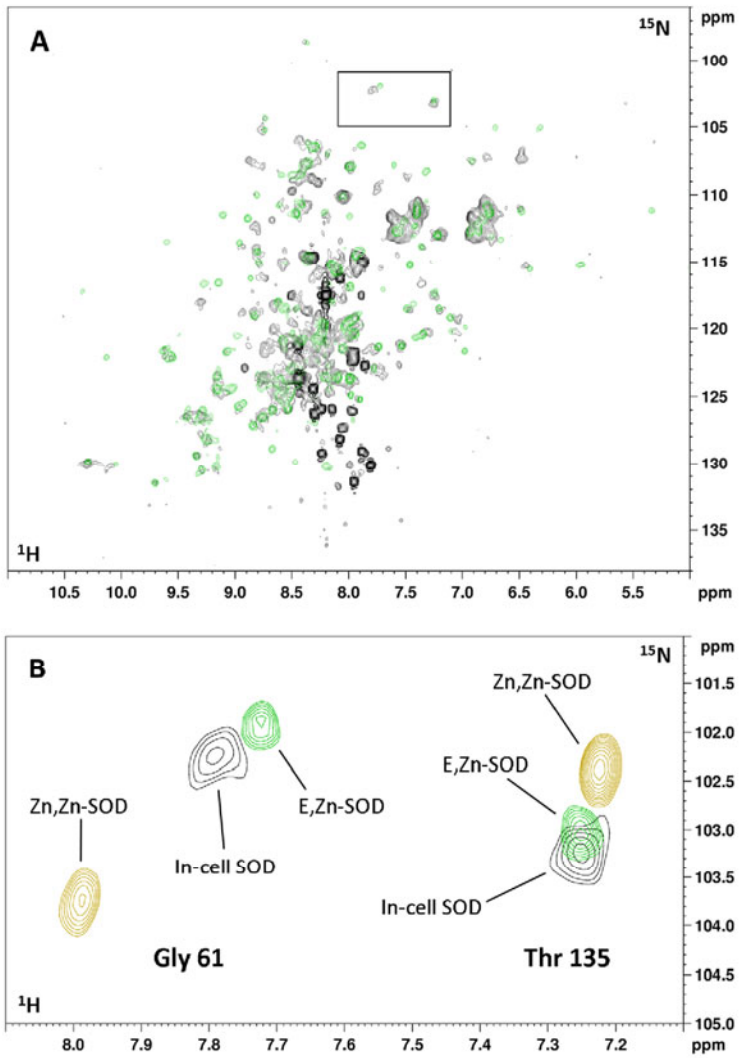

Figure 3. In-cell NMR spectra of hSOD1 with added Zn(II). (A) Overlay of the in-cell ^{1}H-^{15}N SOFAST-HMQC spectrum of *E. coli* cells expressing hSOD1 in presence of Zn(II) (black), and 1H-15N HSQC spectrum of an *in vitro* sample of E,Zn-hSOD1$^{S\text{-}S}$ (green). (B) Zoom of the (A) spectrum showing the peaks of Gly 61 and Thr 135 in-cell (black), *in vitro* E,Zn-hSOD1$^{S\text{-}S}$ (green) and *in vitro* Zn,Zn-hSOD1$^{S\text{-}S}$ (yellow).
doi:10.1371/journal.pone.0023561.g003

Zn-hSOD1$^{SH\text{-}SH}$ species matches that of the corresponding *in vitro* species, thus suggesting that in the cytoplasm E,E-hSOD1$^{SH\text{-}SH}$ is in the monomeric state, while E,Zn-hSOD1$^{SH\text{-}SH}$ is in the dimeric state, confirming that the *in vitro* findings hold true also inside the cell.

Discussion

The process leading a newly synthesized protein to acquire its final, functional state could involve several steps which consist of protein folding to its tertiary and possibly quaternary structure, cofactor binding and post-translational modifications. In most of the cases these steps have been characterized at molecular level only *in vitro*, where protein is isolated in an environment which might be far from the physiological one. In-cell NMR is a quite powerful method to characterize in detail those processes directly in living cells. Indeed, the atomic resolution of the technique, which can be applied to labelled proteins while inside living cells, allows us not only to analyze the folding and organization properties of a protein but also to look at the status of individual residues and the interaction with cofactors.

hSOD1 needs to undergo a number of events after its synthesis, i.e. needs to bind one zinc and one copper ion per molecule, to form a disulfide bond and to dimerize. In this work we have analyzed the protein state directly in the cytoplasm of *E. coli* cells, before it undergoes those maturation steps. Then, by adding zinc to the external medium, we have been able to monitor the changes in tertiary and quaternary structure following the binding of zinc.

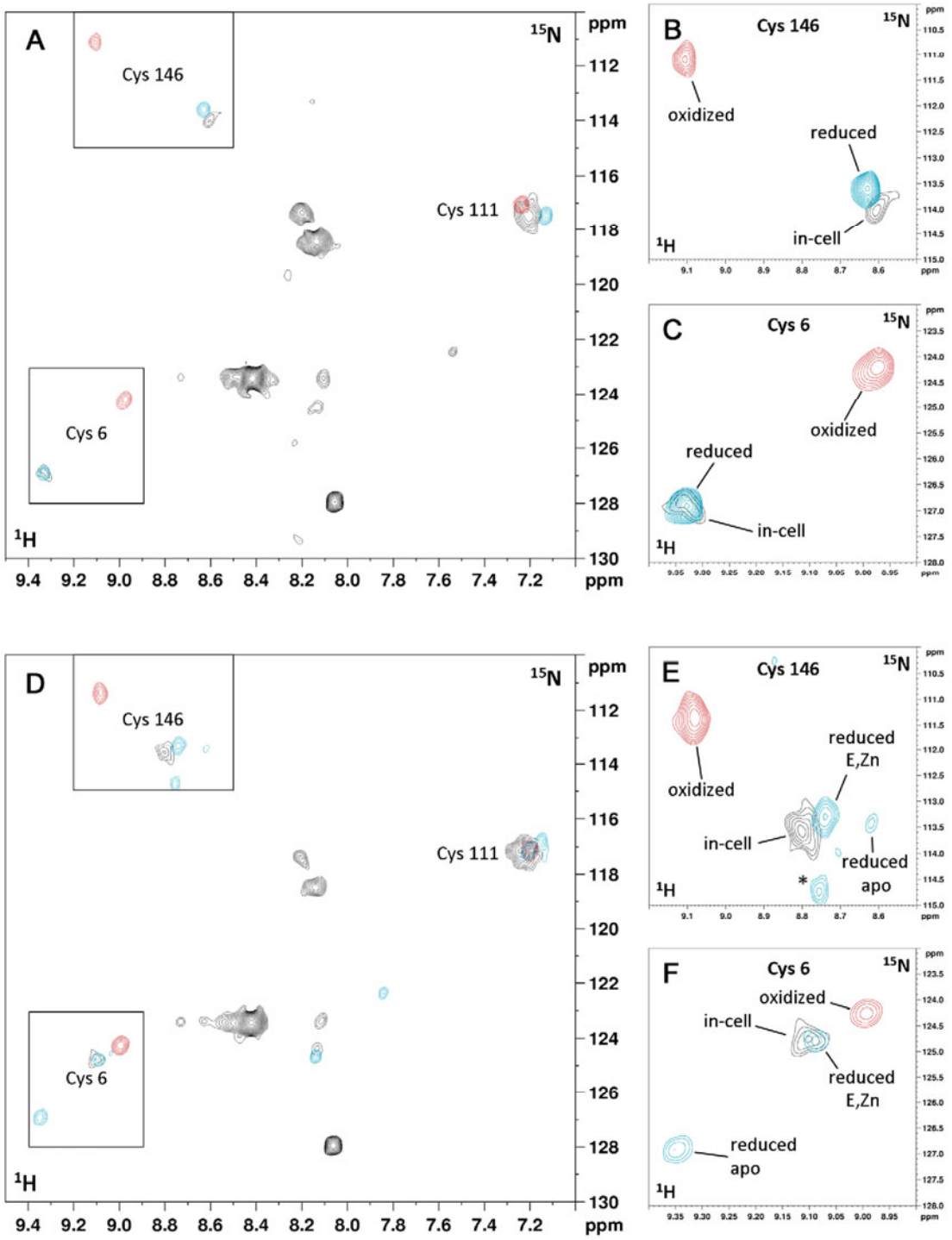

Figure 4. In-cell and *in vitro* NMR spectra of ^{15}N cysteine-labelled E,E-hSOD1 and E,Zn-hSOD1. (A) Overlay of ^{1}H-^{15}N SOFAST-HMQC in-cell spectrum (black) of ^{15}N cysteine-labelled E,E-hSOD1, oxidized E,E-hSOD1 purified from the lysate (red), same sample reduced with DTT (blue). (B,C) Detailed views of (A) showing Cys 146 and Cys 6 amide cross-peaks. (D) Overlay of ^{1}H-^{15}N SOFAST-HMQC in-cell spectrum (black) of ^{15}N cysteine-

labelled E,Zn-hSOD1, oxidized E,Zn-hSOD1 purified from the lysate (red), same sample reduced with DTT (blue). (E,F) Detailed views of (D) showing Cys 146 and Cys 6 amide cross-peaks. When DTT is added to the sample of E,Zn-hSOD1$^{S\text{-}S}$, E,Zn-hSOD1$^{SH\text{-}SH}$ is detected, together with E,E-hSOD1$^{SH\text{-}SH}$ and other species (indicated with an asterisk).
doi:10.1371/journal.pone.0023561.g004

Additionally, we have shown that during this process the cysteines involved in the intramolecular disulfide bridge are in the reduced state. Structural information was obtained by comparing the in-cell NMR spectra with spectra recorded *in vitro* on single, defined protein states.

We have shown that apo-hSOD1 in the cytoplasm is monomeric, reduced and in a partially unstructured state. This is the species which has been suggested and is believed to pass the outer membrane of mitochondria, reaching the IMS where it is trapped upon interaction with the copper chaperone for SOD (CCS) [18]. Interestingly, apo-hSOD1 in the *E. coli* cytoplasm appears to be interacting with different cellular components, giving rise to a distribution of conformations which causes the broadening of part of the NH signals.

A striking result of the present characterization is the in cell selectivity for zinc binding. We have shown that when zinc is added in excess to the culture medium, hSOD1 binds only one equivalent of zinc in its native site, while *in vitro* both metal binding sites are able to bind zinc with comparable affinity. The selective binding of only one zinc ion per subunit occurs only in the intact cells, as when they are lysed and hSOD1 is exposed to an excess of zinc, it binds two equivalents per subunit. Zinc uptake is known to be tightly regulated in the cytoplasm of *E. coli*. While the concentration of free zinc is reported to be less than one atom per cell, the total amount of zinc present is thought to be distributed among other cellular species, either zinc binding proteins or small molecules [19]. It is therefore possible that in this regulated environment zinc binding to hSOD1 becomes highly selective towards the zinc binding site, contrarily to what occurs *in vitro*. Conversely, when the cells are lysed the zinc distribution is not controlled anymore and, if zinc in excess is present, Zn,Zn-hSOD1 species is formed.

To reach its mature state, E,Zn-hSOD1$^{SH\text{-}SH}$ still has to bind a copper ion per monomer and the disulfide bridge has to form. However, in most of Gram-negative bacteria, such as *E. coli*, no copper proteins are known to localize in the cytoplasm, and indeed these organisms have copper efflux pumps to remove copper from the cytoplasm, while no protein is present for cytoplasmic copper uptake [20]. Therefore hSOD1 cannot bind copper after zinc, even if copper is added to the culture medium. Copper binding of course can occur in the cytoplasm of eukaryotic cells, which have systems to regulate cytoplasmic copper intake [21–23], provided the CCS chaperone is present.

Concerning the cysteine redox state, we have shown that after zinc binding the formation of the disulfide bridge still does not occur. This suggests that in the eukaryotic cells the disulfide formation process is also mediated by CCS, and it may be concomitant to the copper loading.

Methods

Cell samples preparation

For uniform ^{15}N labelling, BL21(DE3) Gold *E. coli* strain was used, transformed with a pET28a plasmid containing the WT hSOD1 gene sequence without any additional tag. For selective ^{15}N-cysteine labelling, the auxotroph strain BL21(DE3) CysE was transformed with a pET21 plasmid containing the same WT hSOD1 gene sequence.

Cell samples for in-cell NMR were prepared by adapting a reported protocol [24] (Information S2).

For expression of selective ^{15}N-cysteine labelled WT hSOD1 the samples were prepared as described above, but a M9-based reconstituted medium was used [25], containing ^{15}N-cysteine and the other 19 unlabelled amino acids.

Concentration of hSOD1 inside the cytoplasm after 4 h of overexpression was determined by measuring the absorption of the hSOD1 band on a coomassic-stained SDS-PAGE. A purified hSOD1 sample of known concentration (200 uM) was run on the same gel at different dilutions to provide a calibration curve. hSOD1 is ~850 μM in the cytoplasm, while in the lysate sample hSOD1 is ~350 uM.

Purified hSOD1 samples preparation

Pure WT hSOD1 protein was prepared following an existing protocol [26] (Information S3).

The removal of the metals to obtain E,E-hSOD1$^{S\text{-}S}$ was achieved by dialyzing several times a diluted solution of hSOD1 against 10 mM EDTA in 50 mM acetic acid at pH 3.5. After removal of EDTA E,Zn-hSOD1$^{S\text{-}S}$ and Zn,Zn-hSOD1$^{S\text{-}S}$ were then obtained by adding at pH 5.5 one and two equivalents of $ZnSO_4$, respectively.

To obtain E,E-hSOD1$^{SH\text{-}SH}$ and E,Zn-hSOD1$^{SH\text{-}SH}$, the E,E-hSOD1$^{S\text{-}S}$ and E,Zn-hSOD1$^{S\text{-}S}$ were incubated 1 h at 37°C with 50–60 mM of DTT; 1 mM EDTA was added to the sample of E,E-hSOD1$^{SH\text{-}SH}$ to prevent binding of any metal present in traces. DTT concentration was then brought to 2 mM by dialysis against oxygen-free phosphate buffer. Zn,Zn-hSOD1$^{SH\text{-}SH}$ was obtained by adding $ZnSO_4$ in excess (4 equivalents) to a sample of reduced E,E-hSOD1$^{SH\text{-}SH}$.

The final NMR samples obtained were in 20 mM phosphate buffer at pH 7.5; protein concentration ranged between 0.1 and 0.3 mM (referred to the monomer). All NMR spectra were acquired at Bruker Biospin 600 and 800 MHz spectrometers. The latter is equipped with a cryo-cooled TXI probe.

In-cell NMR experiments

We performed a series of in-cell NMR experiments in which protein expression was induced in M9 medium either without zinc or with increasing amounts of $ZnSO_4$ (from 10 μM up to 1 mM). 2D ^{1}H,^{15}N-SOFAST-HMQC spectra were acquired at 310K. The total acquisition time for each cell sample ranged from 1 to 3 h. After the acquisition, the cells were gently centrifuged and collected to be lysed. The supernatant was then checked in the same experimental conditions, in order to exclude the presence of any signal arising from the protein leaked out of the cells (**Figure S3**). After cell lysis by sonication and centrifugation, 2D ^{1}H,^{15}N-SOFAST-HMQC spectra were acquired on the cleared cell lysate.

The cysteine redox state inside the cells and in the cell lysate was determined via NMR by monitoring the ^{1}H and ^{15}N chemical shifts of the ^{15}N-labelled cysteines. After lysis of the in-cell NMR sample, the protein contained was roughly purified with DEAE anion exchange resin, and left exposed to air for >2 h to allow cysteine oxidation. Finally, *in vitro* reduction of the cysteines was performed with 50 mM DTT.

In vitro NMR experiments

Either 2D ^{1}H,^{15}N-HSQC spectra or both ^{1}H,^{15}N-HSQC and ^{1}H,^{15}N-SOFAST-HMQC spectra were acquired on the *in vitro*

^{15}N-labelled samples of WT hSOD1 at 310K. The linewidth of the HSQC crosspeaks is 10% smaller on average than that of the SOFAST-HMQC crosspeaks, while the crosspeak intensities are comparable, the chemical shifts being the same. Unfolding of an *in vitro* sample of E,E-hSOD1$^{SH\text{-}SH}$ was performed by adding increasing amounts of guanidinium chloride up to 0.5 M, and was monitored with 2D ^{1}H,^{15}N-HSQC spectra acquired at 600 MHz. ^{15}N R_1 and R_2 relaxation measurements [27] were performed at 600 MHz on the ^{15}N labelled E,E-hSOD1$^{SH\text{-}SH}$ sample. The τ_m estimated from R_2/R_1 ratios ($\tau_m = 11.1 \pm 1.5$ μs) confirmed that the protein was in the monomeric state [14].

Supporting Information

Figure S1 Combined Chemical Shift Difference (CCSD) plot of in-cell vs. *in vitro* zinc-bound hSOD1 NMR spectra. CCSD plot of a subset of amide resonances of hSOD1 showing that the in-cell+zinc hSOD1 species is more similar to *in vitro* E,Zn-hSOD$^{SH\text{-}SH}$ compared to *in vitro* Zn,Zn-hSOD1$^{SH\text{-}SH}$. CCSDs between in-cell+zinc hSOD1 and Zn,Zn-hSOD$^{SH\text{-}SH}$ (blue) are higher on average than CCSDs between in-cell+zinc hSOD1 and E,Zn-hSOD$^{SH\text{-}SH}$ (orange). Amide cross-peaks of residues Gly 61 and Thr 135 (marked with an asterisk) are shown in **Figure 3B**. CCSDs were calculated using the formula: $CCSD = \sqrt{\frac{1}{2}\left(\Delta\delta^{1}H\right)^{2} + \frac{1}{2}\left(\Delta\delta^{15}N/5\right)^{2}}$.
(TIF)

Figure S2 Cysteine redox state determined by reaction of hSOD1 with AMS. Non-reducing SDS-PAGE of AMS reaction performed on cell cultures expressing hSOD1 both in presence and in defect of Zn(II) in the medium (right). AMS reaction on *in vitro* samples (left) of reduced and oxidized hSOD1 is showed as a reference.
(TIF)

Figure S3 Supernatant after centrifugation of the cell sample. ^{1}H-^{15}N SOFAST-HMQC spectrum of the supernatant collected after centrifugation of an in-cell NMR sample of hSOD1. The threshold has been lowered to show the very low S/N ratio of the signals detected.
(TIF)

Information S1 Reaction with AMS.
(DOC)

Information S2 Cell and lysate samples preparation.
(DOC)

Information S3 hSOD1 purification protocol.
(DOC)

Author Contributions

Conceived and designed the experiments: L. Banci IB EL. Performed the experiments: L. Barbieri FC EL. Analyzed the data: L. Barbieri FC EL. Wrote the paper: L. Banci L. Barbieri IB FC EL.

References

1. Reckel S, Hänsel R, Löhr F, Dötsch V (2007) In-cell NMR spectroscopy. Prog NMR Spectrosc 51: 91–101.
2. Selenko P, Wagner G (2007) Looking into live cells with in-cell NMR spectroscopy. J Struct Biol 158: 244–253.
3. Dedmon MM, Patel CN, Young GB, Pielak GJ (2002) FlgM gains structure in living cells. Proc Natl Acad Sci U S A 99: 12681–12684.
4. Ritz D, Beckwith J (2001) Roles of thiol-redox pathways in bacteria. Annu Rev Microbiol 55: 21–48.
5. Wilks JC, Slonczewski JL (2007) pH of the cytoplasm and periplasm of Escherichia coli: rapid measurement by green fluorescent protein fluorimetry. J Bacteriol 189: 5601–5607.
6. Hu J, Dong L, Outten CE (2008) The redox environment in the mitochondrial intermembrane space is maintained separately from the cytosol and matrix. J Biol Chem 283: 29126–29134.
7. Sturtz LA, Diekert K, Jensen LT, Lill R, Culotta VC (2001) A fraction of yeast Cu,Zn-superoxide dismutase and its metallochaperone, CCS, localize to the intermembrane space of mitochondria. A physiological role for SOD1 in guarding against mitochondrial oxidative damage. J Biol Chem 276: 38084–38089.
8. Lindberg MJ, Tibell L, Oliveberg M (2002) Common denominator of Cu/Zn superoxide dismutase mutants associated with amyotrophic lateral sclerosis: Decreased stability of the apo state. Proc Natl Acad Sci USA 99: 16607–16612.
9. Furukawa Y, O'Halloran TV (2005) Amyotrophic Lateral Sclerosis Mutations Have the Greatest Destabilizing Effect on the Apo- and Reduced Form of SOD1, Leading to Unfolding and Oxidative Aggregation. J Biol Chem 280: 17266–17274.
10. Cozzolino M, Pesaresi MG, Amori I, Crosio C, Ferri A, et al. (2009) Oligomerization of mutant SOD1 in mitochondria of motoneuronal cells drives mitochondrial damage and cell toxicity. Antioxid Redox Signal 11: 1547–1548.
11. Banci L, Bertini I, Girotto S, Martinelli M, Vieru M, et al. (2007) Metal-free SOD1 forms amyloid-like oligomers: a possible general mechanism for familial ALS. Proc Natl Acad Sci USA 104: 11263–11267.
12. Furukawa Y, Kaneko K, Yamanaka K, O'Halloran TV, Nukina N (2008) Complete loss of post-translational modifications triggers fibrillar aggregation of SOD1 in the familial form of amyotrophic lateral sclerosis. J Biol Chem 283: 24167–24176.
13. Schanda P, Kupce E, Brutscher B (2005) SOFAST-HMQC experiments for recording two-dimensional heteronuclear correlation spectra of proteins within a few seconds. J Biomol NMR 33: 199–211.
14. Arnesano F, Banci L, Bertini I, Martinelli M, Furukawa Y, et al. (2004) The unusually stable quaternary structure of human SOD1 is controlled by both metal occupancy and disulfide status. J Biol Chem 279: 47998–48003.
15. Chattopadhyay M, Valentine JS (2009) Aggregation of copper-zinc superoxide dismutase in familial and sporadic ALS. Antioxid Redox Signal 11: 1603–1614.
16. Banci L, Bertini I, Boca M, Calderone V, Cantini F, et al. (2009) Structural and dynamic aspects related to oligomerization of apo SOD1 and its mutants. Proc Natl Acad Sci U S A 106: 6980–6985.
17. Banci L, Bertini I, Cantini F, D'Amelio N, Gaggelli E (2006) Human SOD1 Before Harboring the Catalytic Metal: Solution Structure of Copper-Depleted, Disulfide-Reduced Form. J Biol Chem 281: 2333–2337.
18. Kawamata H, Manfredi G (2010) Import, maturation, and function of SOD1 and its copper chaperone CCS in the mitochondrial intermembrane space. Antioxid Redox Signal 13: 1375–1384.
19. Outten CE, O'Halloran TV (2001) Femtomolar sensitivity of metalloregulatory proteins controlling zinc homeostasis. Science 292: 2488–2492.
20. Rensing C, Grass G (2003) Escherichia coli mechanisms of copper homeostasis in a changing environment. FEMS Microbiol Rev 27: 197–213.
21. Banci L, Bertini I, Ciofi-Baffoni S, Kozyreva T, Zovo K, et al. (2010) Affinity gradients drive copper to cellular destinations. Nature 465: 645–648.
22. Kim BE, Nevitt T, Thiele DJ (2008) Mechanisms for copper acquisition, distribution and regulation. Nat Chem Biol 4: 176–185.
23. Finney LA, O'Halloran TV (2003) Transition Metal Speciation in the Cell: Insights from the Chemistry of Metal Ion Receptors. Science 300: 931–936.
24. Serber Z, Selenko P, Haensel R, Reckerl S, Loehr F, et al. (2006) Investigating macromolecules inside cultured and injected cells by in-cell NMR spectroscopy. Nat Protoc 1: 2701–2709.
25. Cheng H, Westler WM, Xia B, Oh BH, Markley JL (1995) Protein expression, selective isotopic labeling, and analysis of hyperfine-shifted NMR signals of Anabaena 7120 vegetative [2Fe-2S]ferredoxin. Arch Biochem Biophys 316: 619–634.
26. Banci L, Benedetto M, Bertini I, Del Conte R, Piccioli M, et al. (1998) Solution structure of reduced monomeric Q133M2 Copper, Zinc Superoxide Dismutase. Why is SOD a dimeric enzyme? Biochemistry 37: 11780–11791.
27. Farrow NA, Muhandiram R, Singer AU, Pascal SM, Kay CM, et al. (1994) Backbone dynamics of a free and phosphopeptide-complexed Src homology 2 domain studied by 15N NMR relaxation. Biochemistry 33: 5984–6003.

Figure S1.

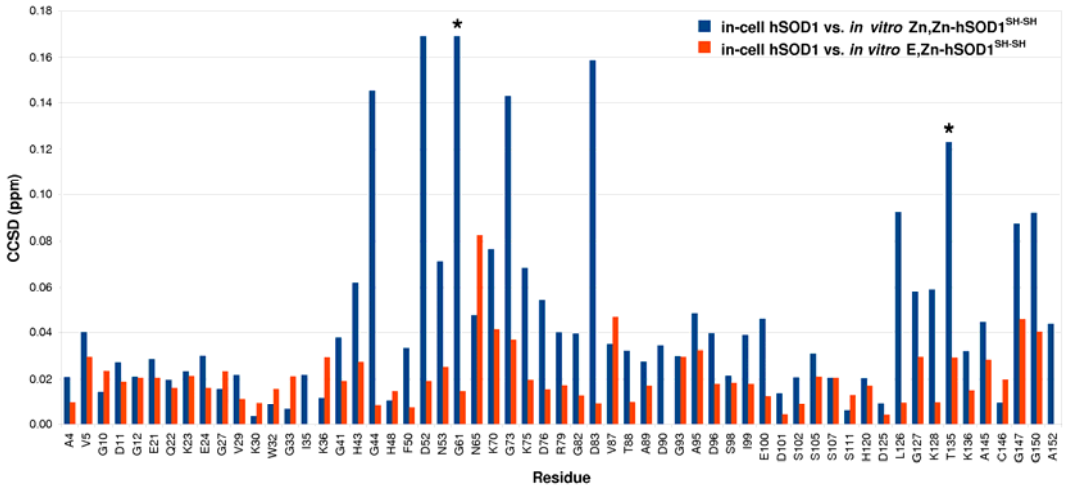
in-cell hSOD1 vs. *in vitro* Zn,Zn-hSOD1^{SH-SH}
in-cell hSOD1 vs. *in vitro* E,Zn-hSOD1^{SH-SH}
CCSD (ppm)
0.18
0.16
0.14
0.12
0.10
0.08
0.06
0.04
0.02
0.00
*
*
A4 V5 G10 D11 G12 E21 Q22 K23 E24 G27 V29 K30 W32 G33 I35 K36 G41 H43 G44 H48 F50 D52 N53 G61 N65 K70 G73 K75 D76 R79 G82 D83 V87 T88 A89 D90 G93 A95 D96 S98 I99 E100 D101 S102 S105 S107 S111 H120 D125 L126 G127 K128 T135 K136 A145 C146 G147 G150 A152
Residue

Figure S2.

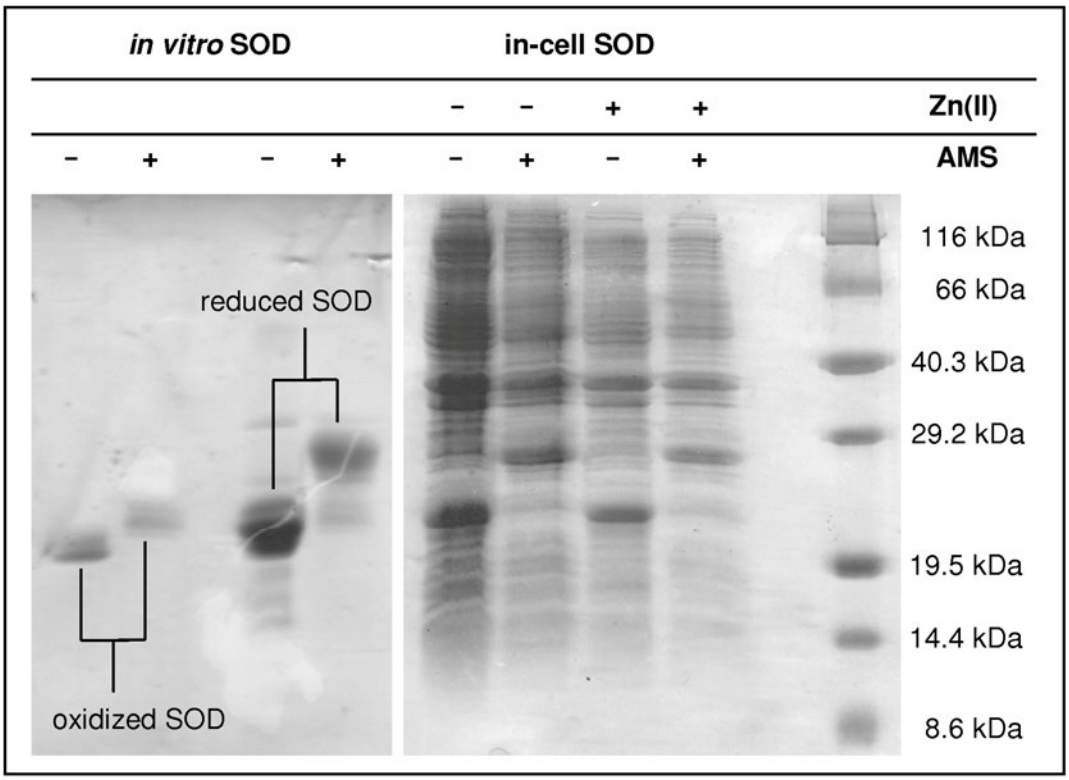
in vitro SOD
in-cell SOD
Zn(II)
AMS
reduced SOD
oxidized SOD
116 kDa
66 kDa
40.3 kDa
29.2 kDa
19.5 kDa
14.4 kDa
8.6 kDa

Figure S3.

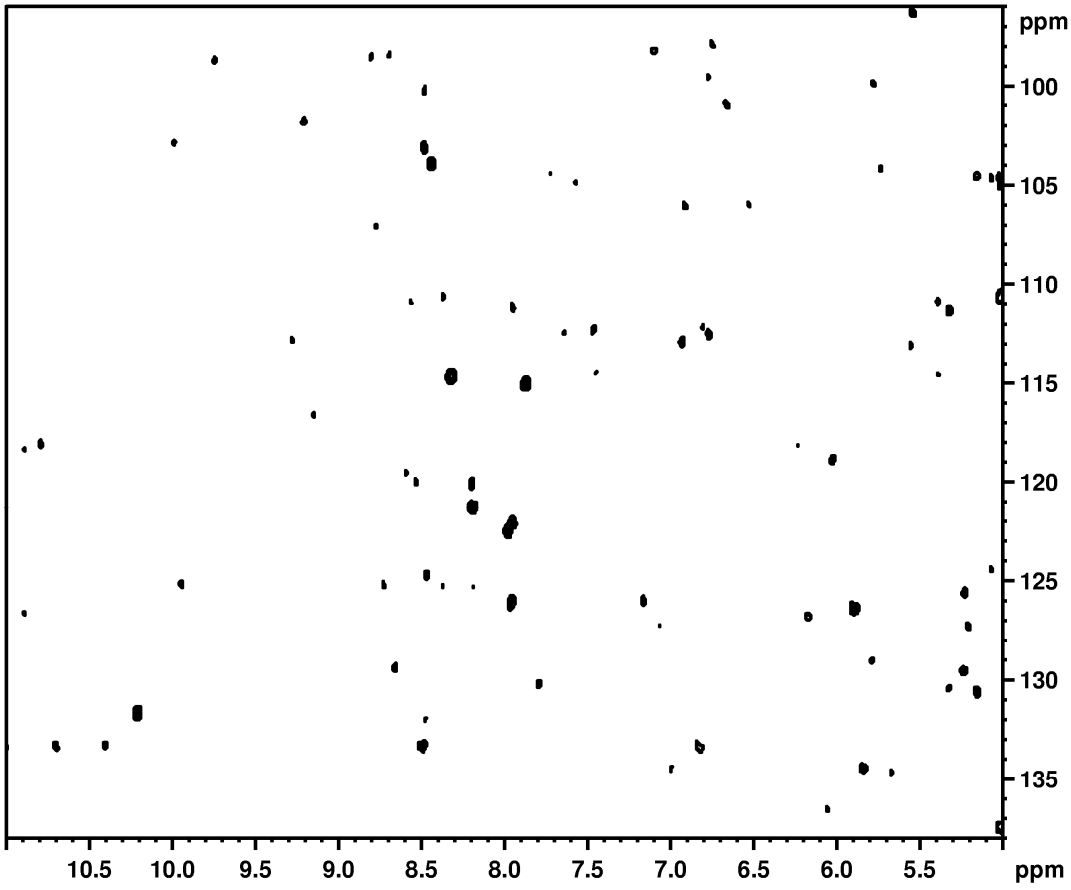
ppm
100
105
110
115
120
125
130
135
10.5
10.0
9.5
9.0
8.5
8.0
7.5
7.0
6.5
6.0
5.5
ppm

Supporting Information S1. Reaction with AMS

Reaction with 4-acetamido-4'-maleimidylstilbene-2,2'-disulfonic acid (AMS) was performed directly on cell samples in oxygen-free conditions [1]. 1 mL of cell culture was precipitated with 10% trichloroacetic acid (TCA), washed with 80 µL acetone and re-suspended in 100 µL 100 mM Tris pH 7 + 2% SDS. 10 µL of the mixture obtained was incubated 1 h at 37°C with 20 mM AMS, and finally run on a non-reducing SDS-PAGE. The same reaction was performed on *in vitro* samples of $hSOD1^{S\text{-}S}$ and $hSOD1^{SH\text{-}SH}$. 20 µL of an *in vitro* protein sample (0.2 mM) were precipitated with 10% TCA, washed with 40 µL acetone and re-suspended in 50 µL 100 mM Tris pH 7 + 2% SDS. 10 µL of the mixture obtained was incubated 1 h at 37°C with 20 mM AMS.

References

1. Kobayashi T, Ito K (1999) Respiratory chain strongly oxidizes the CXXC motif of DsbB in the Escherichia coli disulfide bond formation pathway. EMBO J. 18: 1192-1198.

Supporting Information S2. Cell and lysate samples preparation

Cell samples preparation

The M9 buffer used in all cell cultures was checked through ICP-AES for traces of zinc. The concentration of Zn^{2+} was below the detection limit of 0.04 µM.

Cell samples for in-cell NMR were prepared as follows: a cell culture was grown overnight at 30°C in 35 mL of LB medium. After gentle centrifugation (3000 g) for 20 minutes, the cells were re-suspended in 50 mL of M9 minimal medium [M9 buffer (7 g/L K_2HPO_4, 3 g/L KH_2PO_4, 0.5 g/L NaCl, pH 7.4), 2 mM $MgSO_4$, 0.1 mM $CaCl_2$, 1 mg/L biotin, 1 mg/L thiamine, antibiotic] containing 1 g/L $(^{15}NH_4)_2SO_4$ and 3 g/L of unlabelled glucose to obtain an OD_{600} of ~1.6. After 10 min recovery time, overexpression was induced with 0.5 mM IPTG, and carried out at 30°C for 4 h. The cells were washed once with 50 mL of metal-free M9 buffer in order to remove nutrients, metal ions and any excreted by-product, and they were harvested through gentle centrifugation. The pellet was then re-suspended in metal-free M9 buffer until 500 µL of a ~50% v./v. cell slurry were obtained. 50 µL of D_2O were added, and the final volume was put in a 5 mm NMR tube.

Cell lysates preparation

Cleared cell lysates for in-cell NMR experiments were prepared as follows: after removal of the supernatant to be checked by NMR, the cell pellet was re-suspended in an equal volume of metal-free M9 buffer. The cells were then lysed by ultrasonication. Then the lysate was centrifuged at 18000 g for 20 minutes, the supernatant was collected and its volume was brought to 500 µL with M9 buffer. 50 µL of D_2O were then added. The final dilution of the cytoplasm in M9 buffer is around 1:2.

Supporting Information S3. hSOD1 purification protocol

Pure hSOD1 protein was prepared as follows: a cell culture (BL21(DE3) Gold (Stratagene), transformed with a pET28a plasmid containing the WT hSOD1 gene) was grown overnight at 30°C in 750 mL LB, harvested and re-suspended in 2.25 L ^{15}N-labelled M9 medium. After 4 h from induction with 0.5 mM IPTG at 30°C the cells were harvested and re-suspended in 20 mM Tris, pH 8 buffer for lysis. The cleared lysate was loaded on an anion exchange column (DEAE Sepharose Fast Flow resin, GE Healthcare) for a first purification of hSOD1 by elution with NaCl gradient. The collected fractions containing hSOD1 (checked by SDS-PAGE) were further purified by gel filtration (Superdex75 16/60 column, GE Healthcare) in 20 mM Tris, 100 mM NaCl, pH 8 buffer. Fractions containing pure hSOD1 were collected. $ZnSO_4$ was added to the protein solution to increase hSOD1 stability, and 1 mM DTT was added in all buffers to prevent protein aggregation through disulfide bridges.

3.2. Atomic-resolution monitoring of protein maturation in live human cells

Understanding protein functional processes requires atomic-level description of all players, ideally in their real cellular context. The in-cell NMR approach is perhaps the most suitable to give important information at the atomic scale on protein structure and dynamics in a cellular environment. While *E. coli* cells can be used to characterize proteins either alone or with an interacting partner, they may not fully reproduce the true intracellular conditions of eukaryotic cells. Many eukaryotic proteins require specific chaperones to obtain their correct fold, or to be targeted to specific cellular compartments. Also, the availability of metal cofactors is strictly controlled by the cell, which has complex metal homeostasis pathways. In this work, the complete sequence of maturation of human SOD1 was characterized in living human cells by NMR. The protein expression approach was extended to cultured human cells, by adapting a protocol for transient protein expression in mammalian cells to obtain sufficient intracellular levels of labelled protein to be detected by NMR. In addition to the initial folding states of SOD1, the processes of copper uptake and disulfide bond formation were investigated. By growing cells in defect of metal ions, apo-SOD1 was obtained, in analogy with what was seen in *E. coli* cells. When zinc was supplemented, E,Zn-SOD1 quantitatively formed, again in a selective manner. Incubation with copper ions only resulted in partial formation of Cu,Zn-SOD1, suggesting that the increased protein production would overload the cellular machinery, preventing complete maturation of SOD1. This in turn allowed the effect of copper chaperone for SOD1 to be studied, by co-expressing both proteins at comparable levels. Interestingly, while co-expression of CCS had a minor effect in increasing the amount of Cu,Zn-SOD1 upon cell incubation with copper, it strongly affected the amount of oxidized SOD1 formed. Indeed, even without supplementing copper, half of the total SOD1 had the disulfide bond formed, while in combination with copper 100% of SOD1 was oxidized in presence of CCS. This result highlighted the need of intracellular CCS for disulfide bond formation, and also suggested a possible mechanism for CCS to oxidize the E,Zn-SOD1 species, through a copper-independent mechanism which was not observed *in vitro.*

Atomic-resolution monitoring of protein maturation in live human cells

Lucia Banci[1,2,*], Letizia Barbieri[1], Ivano Bertini[1,2], Enrico Luchinat[1], Erica Secci[1], Yuguang Zhao[3], A. Radu Aricescu[3,*]

Affiliations:

[1]CERM, Magnetic Resonance Center, University of Florence, Via Luigi Sacconi 6, 50019, Sesto Fiorentino, Florence, Italy.

[2]Department of Chemistry, University of Florence, Via della Lastruccia 3, 50019, Sesto Fiorentino, Florence, Italy.

[3]Division of Structural Biology, Wellcome Trust Centre for Human Genetics, University of Oxford, Roosevelt Drive, Oxford, UK.

* To whom correspondence should be addressed. L.B. (banci@cerm.unifi.it), A.R.A. (radu@strubi.ox.ac.uk).

SUBMITTED

Abstract

Structural studies of biological molecules are typically carried out in vitro, far from the physiological conditions of the cellular context. Here we describe the maturation process of a protein, human superoxide dismutase 1 (SOD1), observed directly in live human cells using high-resolution NMR. We could thus follow at atomic resolution the complete sequence of events in the SOD1 post-translational modification: zinc binding, homodimer formation, copper uptake and oxidation of the intrasubunit disulfide bond. Co-expression of the copper chaperone for SOD1 (CCS) revealed its essential role in catalyzing the SOD1 intramolecular disulfide bond oxidation, through both copper-dependent and independent mechanisms. The approach described here is applicable to a broad range of proteins, and opens up a new way to study physiological events, in molecular detail, within a cellular environment.

Functional understanding of cellular processes requires a detailed characterization of molecular players, their structural and dynamic properties, and their networks of interactions. Biomolecules should ideally be characterized within their cellular milieu, to match the physiological environment including pH, redox potential, viscosity, and the presence of all relevant interaction partners. A new approach to structural biology is therefore needed to explore the cellular context with atomic resolution techniques. In principle, in-cell NMR[1-5] represents an ideal method to monitor protein structure during functional processes, in "close to physiological" conditions. However, in practical terms, one must overcome a number of technological limitations in order to: 1) express (or co-express, where appropriate) isotopically labelled proteins within cells derived from a suitable organism: human proteins, for example, should be endogenously synthesised and studied within human cells; 2) establish experimental conditions to maintain cellular viability inside the NMR tube and to reduce data acquisition time, while increasing measurement sensitivity. We sought to address these challenges and attempt to directly monitor the steps involved in post-translational modifications of a

model protein, human superoxide dismutase 1 (SOD1), within live human cells. Furthermore, we aimed to define the role of the copper chaperone for SOD1 (CCS), which was proposed to make a major contribution to SOD1 maturation[6,7]. A correct understanding of this process is important considering the fundamental role played by SOD1 in the cellular defence against oxidative stress[8]. Impaired SOD1 maturation has been linked to disease states, including the onset of amyotrophic lateral sclerosis[9-11]. Finally, we further assessed the general applicability of this approach to other human proteins.

We expressed human SOD1 transiently in HEK293T cells[12] and modulated its expression levels by varying the amount of transfected cDNA (see Methods). We estimated the endogenous concentration of SOD1 in HEK293T cells, under our culture conditions, to be 10±2 μM (Supplementary Fig. 1). Previously, levels up to 40 μM SOD1 have been reported in the cytoplasm of mammalian cells[13,14]. Following recombinant expression, the maximal intracellular SOD1 monomer concentration we could achieve was 360±30 μM (Supplementary Fig. 2). However, we could still detect SOD1 by in-cell NMR at intracellular concentrations 45±10 μM. The distribution of SOD1 was assessed in isolated nuclear, cytoplasmic and mitochondrial fractions from cellular extracts. Independently of the total protein level, the majority of SOD1 is present in the cytoplasm (Supplementary Fig. 3). Less than 1% of total SOD1 is localized in the mitochondrial fraction (Supplementary Fig. 3), a value somewhat lower than previously reported[15,16].

When cells were grown in medium without supplements of zinc or copper ions, two forms of SOD1 could be detected, in similar amounts: the monomeric, metal-free species (apo-SOD1) and the dimeric species with one Zn^{2+} ion bound to each subunit (E,Zn-SOD1) (Supplementary Fig. 4a); the NMR data were analyzed by taking advantage of previous *in vitro* spectra and backbone assignments[17,18]. This mixture of species is likely due to the presence of residual zinc in the culture media (calculated around 4.5 μM in 10% foetal bovine serum (FBS)-supplemented medium and 1 μM in 2% FBS-supplemented medium[1]). Cysteines 57 and 146, forming an intrasubunit

[1] Zinc concentrations were taken from Sigma-Aldrich Media Expert (http://www.sigmaaldrich.com/life-science/cell-culture/learning-center/media-expert.html)

disulfide bond in the mature enzyme, were reduced in both species as revealed by NMR spectra of the ^{15}N-Cys selectively labelled proteins (Fig. 1a). The presence of only these two species was further confirmed by NMR spectra acquired on cell extracts (Supplementary Fig. 4b). The ^{1}H-^{15}N SOFAST-HMQC spectrum of the metal-free SOD1 species was consistent with its equivalent produced in *E. coli* cells without addition of metal ions[19], only the crosspeaks of the less structured parts being detected.

Addition of Zn^{2+} to the culture medium eliminated signals from the apo-SOD1 species in the spectra of the ^{15}N-Cys selectively labelled protein (Fig. 1b). The uniformly-^{15}N labelled cell sample yielded a good quality spectrum of E,Zn-SOD1 (Fig. 1c), which could be improved after removing the background signals arising from non-selective labelling of cellular components, by subtracting a spectrum of cells transfected with the empty vector (Supplementary Fig. 5). Therefore, *in vivo*, Zn^{2+} ions are efficiently uptaken by cells and bound in stoichiometric amounts, specifically to the native binding site of the dimeric SOD1 species, as further confirmed by ^{1}H-^{15}N crosspeak analysis (Supplementary Fig. 6). On the contrary, when reduced apo-SOD1 was exposed to Zn^{2+} ions *in vitro* or in cell lysates, even at sub-stoichiometric concentrations, a mixture of apo-SOD1, E,Zn-SOD1 and Zn,Zn-SOD1 forms was generated[19]. Therefore, site-selectivity of Zn^{2+}-binding can only be achieved within a cellular context.

Prokaryotes have simple mechanisms for copper uptake and excretion[20], while in eukaryotic cells these processes are tightly regulated[21,22]. Accordingly, when copper was added as Cu(II) salt to the culture medium of *E. coli* cells it was readily and stoichiometrically bound to recombinantly expressed SOD1, forming Cu(I),Zn-SOD1 (Supplementary Fig. 7a,c). Cu(II) was therefore reduced to Cu(I) and bound SOD1 only in this redox state. Importantly, Cu(I) added to *E. coli* cells either as an acetonitrile or glutathione complex did not become available to E,Zn-SOD1 (Supplementary Fig. 7d). In-cell NMR spectra also show that in *E.coli* the SOD1 intrasubunit disulfide bridge is oxidized in a sizable fraction (around 50%, Supplementary Fig. 7b). Unlike bacteria, copper entrance in eukaryotic cells and its delivery to copper-binding proteins require a number of steps, involving specific chaperones responsible of its intracellular trafficking[23-25]. When HEK293T cells overexpressing SOD1 were incubated for 24 h

with 100 µM Cu(II) in the medium (the highest concentration of copper that still allowed good cell viability during the NMR experiment), only around 25% of the total SOD1 protein incorporated copper, again in the Cu(I) state (Fig. 2a). The remaining protein fraction contained only one zinc ion per subunit, as observed from the ^{1}H histidine signals in the 1D ^{1}H NMR spectrum (Fig. 2a and 2b). Additionally, the spectra of the ^{15}N-Cys selectively labelled protein showed only ~20% SOD1 intrasubunit disulfide bond formation (Fig. 3a). Copper incorporation of SOD1 in eukaryotes was shown to be dependent on the CCS protein[26-28]. Although a basal expression-level of the hCCS gene does occur during normal cell growth, it is likely that the amount of SOD1 produced in our experimental setup was too high to allow for complete copper insertion via the CCS-dependent pathway. However, a CCS-independent copper insertion pathway has also been reported for human SOD1[29,30] and might have contributed to the partial formation of Cu(I),Zn-SOD1 observed (Fig 2a).

Simultaneous overexpression and isotopic enrichment of both hSOD1 and hCCS was accompanied by a reduction in the overall SOD1 expression levels (Supplementary Fig. 2). Nevertheless, the signals of SOD1 were still easily identified (Fig. 3b and 3c), with minimum interference from CCS due to the larger molecular mass of the latter. Intracellular protein concentration in these experiments ranged between 70±10 µM and 45±10 µM SOD1, and between 50±10 µM and 15±3 µM CCS (Supplementary Fig. 2). Co-expression of SOD1 and CCS in zinc supplemented medium resulted in dimeric, zinc-containing, SOD1 species. No difference in SOD1 metal content was found with respect to the cell sample with basal CCS level (Supplementary Fig. 8). However, spectra recorded from cells co-expressing the two proteins revealed a partial oxidation (around 50%) of the SOD1 intrasubunit disulfide bond (Fig. 3b), as monitored on ^{15}N-Cys selectively labelled proteins. This result is consistent with a mechanism of CCS-mediated SOD1 disulfide oxidation which, unexpectedly, does not require copper insertion into SOD1.

When cells co-expressing SOD1 and CCS were incubated for 24h in Cu(II) containing medium, a higher ratio of Cu(I),Zn-SOD1 vs E,Zn-SOD1 was obtained (~1:1, Fig. 2d) compared with cell samples with basal CCS level, indicating that CCS promotes copper incorporation in SOD1. The redox state of hSOD1 cysteines 57 and

146 is affected by both overexpression of CCS and presence of copper. Indeed, when cells overexpressing both hSOD1 and CCS were incubated with Cu(II), the intrasubunit disulfide bridge of hSOD1 was completely oxidized (Fig. 3c).

We next attempted to explore the above mechanism at lower concentrations of SOD1 and CSS, as close as possible to the reported physiological levels[13,14]. At 45±10 μM SOD1 and 15±3 μM CCS, complete disulfide formation in E,Zn-SOD1 was observed (Supplementary Fig. 9a and 9d), whereas additional incubation with copper resulted in the complete formation of oxidized Cu(I),Zn-SOD1 (Supplementary Fig. 9b and 9c). These results suggest that only the relative amounts of species are affected by recombinant protein expression levels, but not the sequence of maturation events. We speculate that even lower levels of SOD1, undetectable by NMR, would result in the complete formation of mature SOD1, even with the endogenous levels of CCS and copper. In such conditions, however, no information on the intermediate maturation steps would be obtained. By overexpressing only SOD1, the components of its maturation pathway are not sufficiently abundant to complete the process, and thus intermediate SOD1 maturation states are detected. Furthermore, by selectively increasing single components (e.g. CCS, or copper), specific steps of SOD1 maturation can be recovered, and different SOD1 states detected. With this "knock-in" approach (as it works the opposite of the conventional knock-out approach), combined with some *a priori* knowledge of the components involved, we can understand which of them are necessary for each step of the process.

The key steps of SOD1 maturation observed by in-cell NMR are schematically summarized in Fig. 3d. Specifically, we found that: apo-SOD1 is largely unfolded and monomeric in the HEK293T cytoplasm; zinc uptake occurs without the need of any chaperone; copper uptake and oxidation of the Cys57-Cys146 disulfide bond occur partially in the cells exposed to Cu(II) (which is reduced to Cu(I)); copper loading and the complete oxidation of the above mentioned cysteines is achieved in cells co-expressing SOD1 and CCS. Importantly, our experiments also reveal that, within a physiological context, CCS is able to oxidize the intramolecular SOD1 disulfide bond in the absence of copper bound to SOD1. This finding, while consistent with the previously reported effect of CCS overexpressed *in vivo* in promoting SOD1 disulfide

bond formation[31], demonstrates that the cysteine oxidation step can occur *in vivo* independently of copper transfer, thus differing from the mechanism observed *in vitro*[32].

We sought to establish whether the approach described here is applicable to proteins beyond hSOD1. We selected four other proteins [Mia40, Atox1, glutaredoxin-1 (Grx1) and thioredoxin (Trx)] with different properties such as those relative to protein fold, binding of metal ions and redox potential of cysteine residues. Following the same protocol established for SOD1 and CCS, all these targets were highly expressed (Supplementary Fig. 10a). They were visible in the ^{1}H NMR spectra above the cellular background, and Mia40 and Atox1 could be detected on ^{1}H-^{15}N SOFAST-HMQC spectra on uniformly ^{15}N labelled cell samples (Supplementary Fig. 10b,c). Grx1 and Trx only became visible upon cell lysis, suggesting that some interaction occurs in the cytoplasm which makes the protein tumbling slower on average, thus broadening the amide crosspeaks beyond detection (Supplementary Fig. 10d,e). Such molecules may be successfully characterized through different kinds of NMR techniques (such as solid-state MAS NMR for slow tumbling proteins)[33].

Successful application of in-cell NMR to proteins expressed endogenously in mammalian cells relies on efficient transfection of the cell population, relatively high expression levels of the molecule of interest, applicability of different labelling strategies and maintenance of cell integrity during the experiment. All these aspects have been successfully addressed in this study, allowing us to follow a functional process such as the maturation steps, metal uptake processes and protein oxidation of hSOD1 directly in live human cells. We also determined the sequential, physiological order of the events in the SOD1 post-translational modification process, information that cannot be retrieved *in vitro*. To our knowledge this is the first time a complete protein maturation process has been followed in a living cell, in atomic detail. Importantly, this strategy may be applicable for many other protein targets, and thus opens the way for a broad range of molecular level, in-cell structural studies of proteins.

Acknowledgements:

This work was supported by the Access to Research Infrastructures activities in the 7th Framework Programme of the EC (Bio-NMR - Contract 261863 and P-CUBE – Contract 227764), and by the Italian MIUR-PRIN 2009 'Biologia strutturale meccanicistica: avanzamenti metodologici e biologici'. We would like to thank E.Y. Jones and D.I. Stuart for critically reading the manuscript and providing advice. A.R.A. is an MRC Career Development Award fellow.

Author contributions:

L.Banci, I.B., A.R.A. conceived the work, L.Banci, L.Barbieri, E.L. and A.R.A. designed the experiments; L.Barbieri, and Y.Z. grew and transfected the human cells; L.Barbieri cloned the genes and produced the cell samples of SOD1, CCS, Atox1, Grx1, Trx; E.S. produced the cell sample of Mia40; L. Barbieri and E.L produced and analyzed the *E. coli* cell samples; E.L. performed the NMR experiments and analyzed the data; L.Banci, L.Barbieri, I.B., E.L., and A.R.A. wrote the paper.

Competing financial interests:

The authors declare no competing financial interests.

Additional information:

Supplementary information (eleven figures) is available in the online version of the paper. Correspondence and requests for materials should be addressed to L. Banci or A.R.A.

Figures:

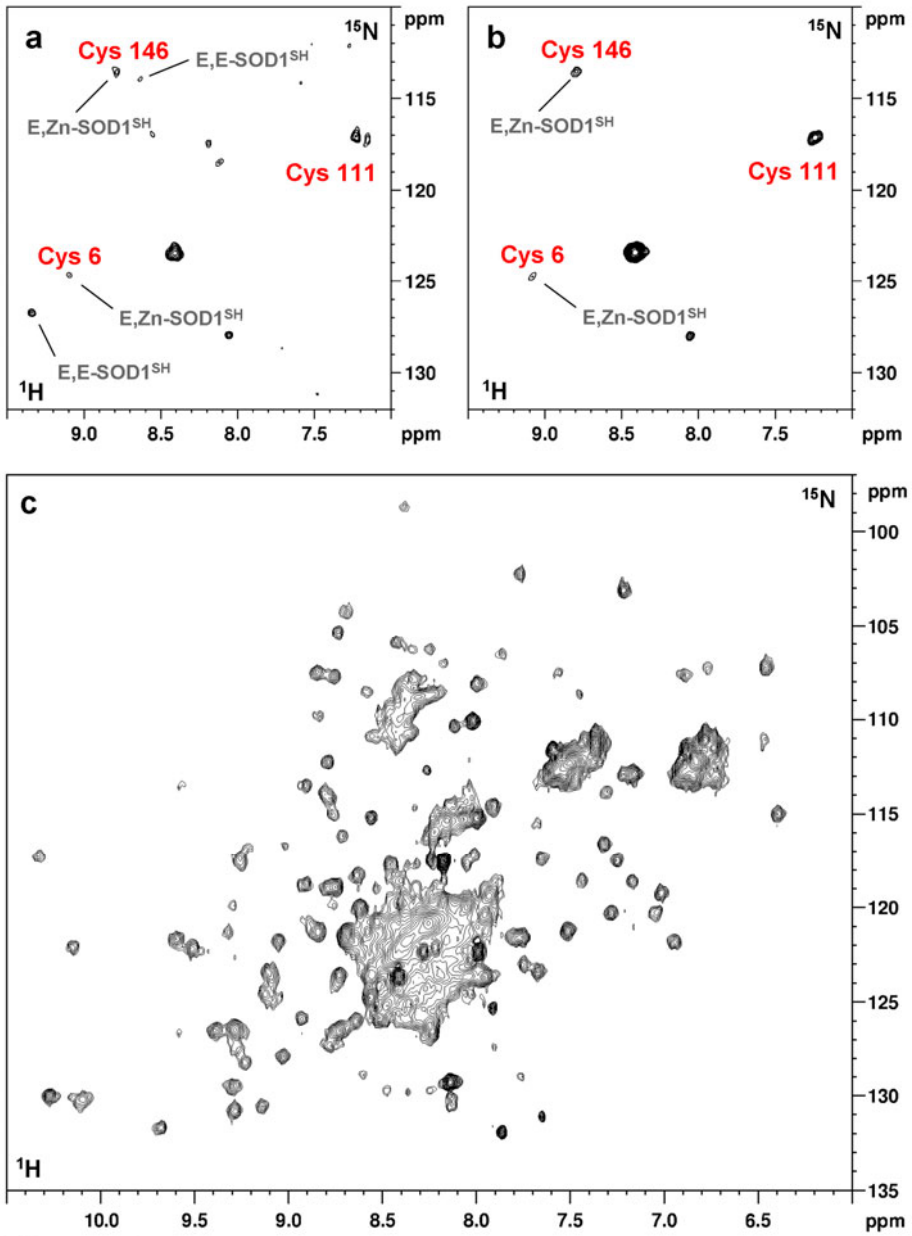

Figure 1

Figure 1. Zn(II) added to the culture medium promotes binding of one Zn^{2+} ion per apo-SOD1 subunit in the cytoplasm. ^{1}H-^{15}N SOFAST HMQC spectra were acquired on human cells expressing ^{15}N-cysteine labelled SOD1: **a**, in absence of metals; **b**, with Zn(II) added to the culture medium. Assigned cysteine residues are indicated in red. When two species of SOD1 are present, dark grey labels indicate the species to which each crosspeak belongs (E,E-$SOD1^{SH}$: reduced apo-SOD1; E,Zn-$SOD1^{SH}$: reduced SOD1 containing one Zn^{2+} ion per subunit). Unlabelled crosspeaks correspond to cellular background signals; **c**, ^{1}H-^{15}N SOFAST HMQC acquired on human cells expressing uniformly ^{15}N-labelled SOD1 in Zn(II)-supplemented medium. The region between 8.0 and 8.5 (^{1}H) ppm contains overlapped signals arising from non-specific labelling of the cells, which can be subtracted to obtain a cleaner spectrum (Supplementary Fig. 5). By comparing the chemical shift of the assigned crosspeaks in the in-cell spectrum with backbone assignments of SOD1 in different metallation and redox state *in vitro*[17,18] it was possible to assess the species present in the cytoplasm (Supplementary Fig. 6).

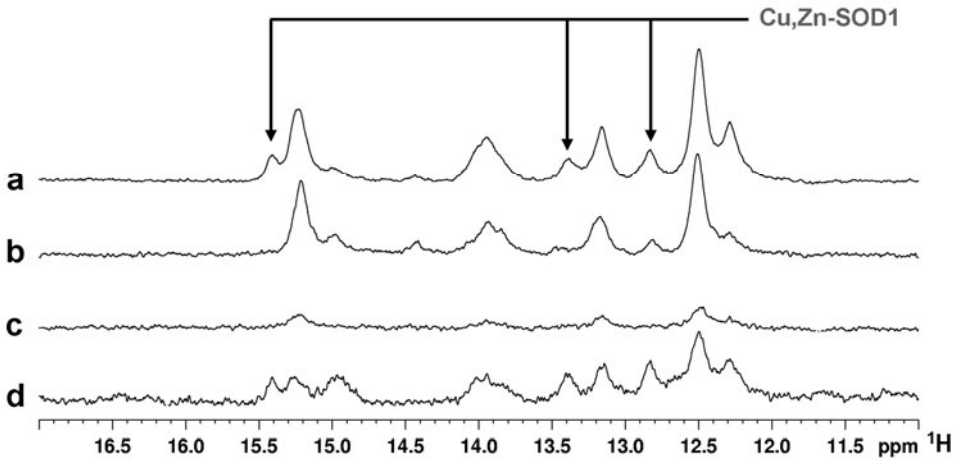

Figure 2

Figure 2. Cu(II) addition to the culture medium induces Cu(I) binding to a fraction of cytoplasmic SOD1. Histidine region of ^{1}H NMR spectra were acquired on human cells expressing unlabelled SOD1: **a**, in Zn(II)-supplemented medium, after incubation with Cu(II); **b**, in Zn(II)-supplemented medium without incubation with Cu(II); **c**, in medium without added metals. **d**, ^{1}H NMR spectrum of human cells co-expressing SOD1 and CCS in Zn(II)-supplemented medium, after incubation with Cu(II). Histidine protons unambiguously assigned to Cu(I),Zn-SOD1 species are indicated.

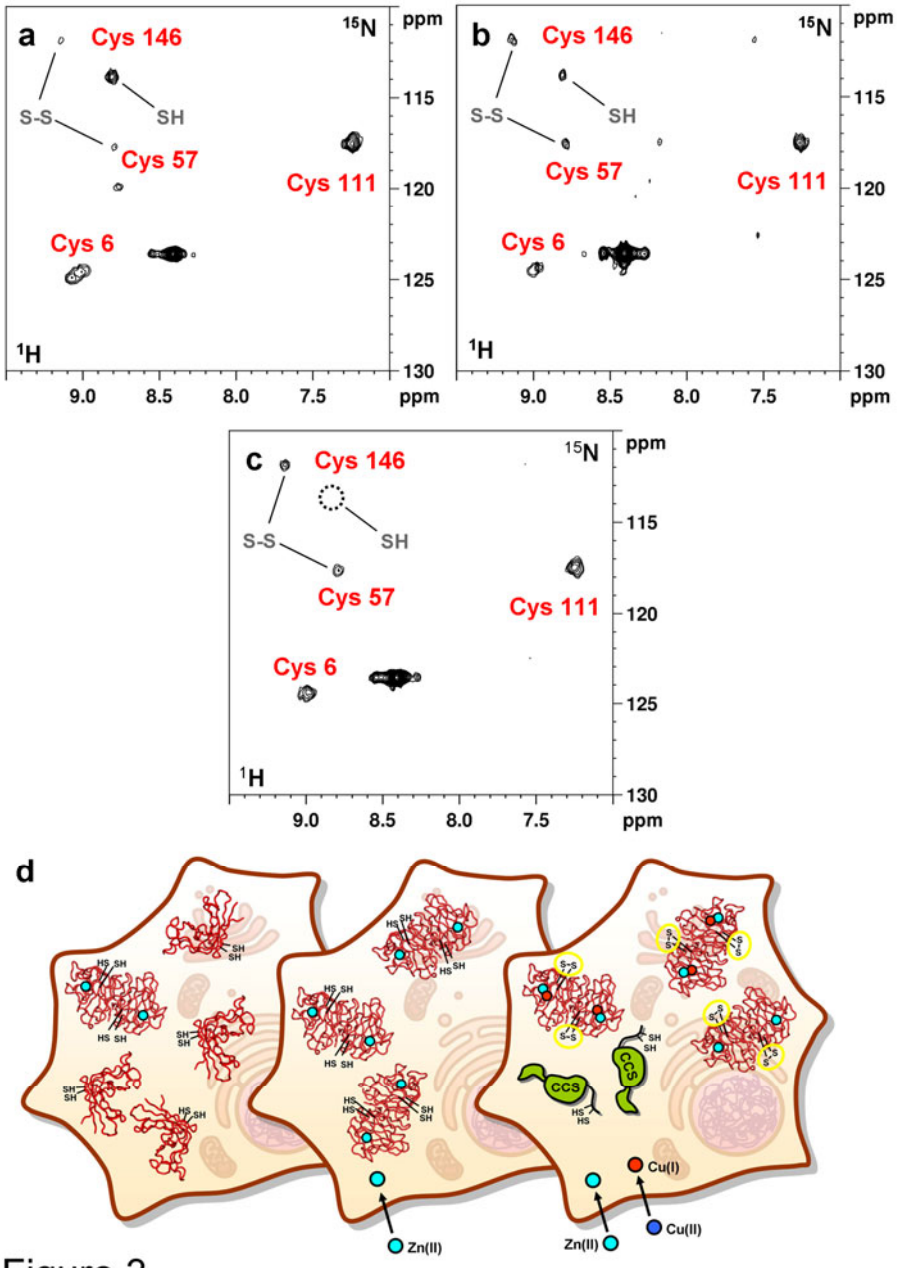
a
Cys 146
S-S
SH
Cys 57
Cys 111
Cys 6
15N
ppm
115
120
125
130
1H
9.0
8.5
8.0
7.5
ppm
b
Cys 146
S-S
SH
Cys 57
Cys 111
Cys 6
15N
ppm
115
120
125
130
1H
9.0
8.5
8.0
7.5
ppm
c
Cys 146
S-S
SH
Cys 57
Cys 111
Cys 6
15N
ppm
115
120
125
130
1H
9.0
8.5
8.0
7.5
ppm
d
CCS
CCS
Cu(I)
Cu(II)
Zn(II)
Zn(II)

Figure 3

Figure 3. The redox state of SOD1 is influenced by both copper binding and the presence of CCS. ^{1}H-^{15}N SOFAST HMQC spectra were acquired on human cells: **a**, expressing ^{15}N-cysteine labelled SOD1 in Zn(II)-supplemented medium, after incubation with Cu(II); **b**, co-expressing ^{15}N-cysteine labelled SOD1 and CCS in Zn(II)-supplemented medium; **c**, co-expressing ^{15}N-cysteine labelled SOD1 and CCS in Zn(II)-supplemented medium, after incubation with Cu(II). Assigned cysteine residues are indicated in red. When two species of SOD1 are present, dark grey labels indicate the disulfide redox state of each species. Unlabelled crosspeaks are cellular background signals. **d**, drawing summarizing SOD1 maturation steps. Left cell: SOD1 expressed in cells with no addition of metals is present mainly it the apo form, which is monomeric and partially unfolded. A fraction of SOD1 binds the zinc present in the expression medium. Central cell: when Zn(II) (cyan) is added to the expression medium SOD1 quantitatively binds one zinc ion per monomer and dimerizes; the intrasubunit disulfide bridge is completely reduced. Right cell: when both Zn(II) and Cu(II) (blue) are added to the expression medium, and CCS is co-expressed, a fraction of SOD1 binds Cu(I) (orange); the disulfide bridge is completely oxidized (yellow circles).

Methods:

Constructs

For constructing the mammalian expression plasmids, genes encoding full-length human SOD1 (amino acids 1-154, GenBank accession number: NP_000445.1), CCS (amino acids 1-274, GenBank accession number: NP_005116.1), Mia40 (amino acids 1-142, GenBank accession number: NP_001091972.1), Atox1 (amino acids 1-68, GenBank accession number: NP_004036.1), glutaredoxin-1 (amino acids 1-106, GenBank accession number: NP_001112362.1) and thioredoxin (amino acids 1-105, GenBank accession number: NP_003320.2) were amplified from cDNA by PCR and sub-cloned into the pHLsec[12] vector between *EcoRI* and *XhoI* restriction-enzyme sites. All clones were verified by DNA sequencing.

Cell culture and transfection

HEK293T cells were maintained in Dulbecco's Modified Eagle's Medium (DMEM high glucose, D6546, Sigma) supplemented with L-glutamine, antibiotics (penicillin/streptomycin) and 10% foetal bovine serum (FBS, Gibco) in uncoated 75 cm^2 plastic flasks, and were incubated at 310 K, 5% CO_2 in a humidified atmosphere. Cells were transiently transfected with the pHLsec plasmid containing the hSOD1 cDNA using polyethylenimine (PEI), as described elsewhere[12]. Different DNA:PEI ratios were tested for maximizing protein expression (PEI was kept constant at 50 µg/flask), and an optimal ratio of 1:2 was found (25 µg/flask DNA, 50 µg/flask PEI). For co-expression of SOD1 and CCS, cells were transfected with plasmids containing hSOD1 and hCCS constructs in different amounts and ratios. The highest expression of both proteins was obtained by transfecting in a 1:1:2 hSOD1:hCCS:PEI ratio, thus doubling the total DNA amount. Lower expression levels of SOD1 were obtained by transfecting cells with a 1:4 hSOD:PEI ratio. To decrease the expression levels of both proteins, cells were transfected with a 1:1:4 hSOD1:hCCS:PEI ratio. PEI was always kept constant at 50 µg/flask. Different times of SOD1 expression were tested (1, 2, 3, 6 days), and the highest amount of protein was reached after 2 days (48 hours) of expression. During protein expression, cells were incubated at 310 K in 75 cm^2 flasks. Commercial DMEM media were used for unlabelled in-cell NMR samples:

BioExpress6000 medium (CIL) was used for uniform ^{15}N labelling, while for selective ^{15}N-cysteine labelling a reconstituted medium was prepared following the DMEM (Sigma) reported composition, in which ^{15}N-cysteine was added together with all the other unlabelled components. All expression media were supplemented with 2% FBS. Zn(II) was supplemented as $ZnSO_4$, which was added to the expression media to a final concentration of 10 μM immediately after transfection. Cu(II) was supplemented as $CuCl_2$, added to a final concentration of 100 μM after 48 hours of protein expression, and incubated for 24 hours. Protein expression levels were monitored by comparing the protein band intensities in the cell extracts with bands of *in vitro* samples of known concentration run on Coomassie-stained SDS-PAGE.

Human cell samples for in-cell NMR

Samples for in-cell NMR were prepared following a reported protocol[3] with some variations: HEK293T cells from a 75 cm^2 culture flask were detached with trypsin-EDTA 0,05% (Gibco) and resuspended in 20 mL DMEM containing 10% FBS to inactivate trypsin. Cells were gently centrifuged (800 g), resuspended in 10 mL PBS, washed once with PBS and finally resuspended in one cell pellet volume of DMEM medium supplemented with 90 mM glucose, 16 mM HEPES buffer, 20% D_2O (for a final 10% D_2O amount). The cell suspension was transferred to a 3 mm Shigemi NMR tube; the glass plunger was not used. Cells were allowed to settle at the bottom of the tube, thus filling up the active coil volume. The supernatant was kept during the NMR experiments to obtain good field homogeneity. After the experiments, cells were resuspended in the supernatant, removed from the NMR tube and spun down again to collect the medium for protein leakage check (Supplementary Fig. 11). Cells were lysed by freeze/thaw method after suspending them in one pellet volume of PBS buffer supplemented with 0.5 mM EDTA and AEBSF (4-(2-Aminoethyl) benzenesulfonyl fluoride hydrochloride). The lysate was centrifuged at 16000 g, 30', 4°C and the cleared cell extract was collected for NMR and SDS-PAGE analysis.

NMR experiments

NMR experiments were acquired at a 950 MHz Bruker Avance™ III spectrometer equipped with a CP TCI CryoProbe™. 1D ^{1}H and 2D $^{1}H,^{15}N$-SOFAST-HMQC[34] spectra were acquired at 305K. The total acquisition time for each cell sample ranged from 1 to 2 h. The supernatant of each cell sample was checked in the same experimental conditions, in order to exclude the presence of any signal arising from the protein leaked out of the cells. In the above experimental conditions, very low protein signal was detected in the external medium (< 10% of the signal in cells). The same NMR spectra were also acquired on the cell extracts. Cell viability before and after NMR experiments was assessed by Trypan Blue staining[35]. Cell viability remained above 90%, as damaged cells ranged from 3% before the experiments to 8% after the experiments.

***E. coli* cell samples**

*S*amples of *E. coli* cells expressing human SOD1 were prepared as previously described[19]. For copper incorporation experiments, after 4 h expression of SOD1 cells were incubated with either 100 μM $Cu(II)SO_4$, Cu(I)-acetonitrile complex or Cu(I)-glutathione complex for 15'. Cells were then washed once with M9 buffer and collected for NMR sample preparation. NMR spectra on *E. coli* cell samples were acquired at 305K at an 800 MHz Bruker Biospin™ spectrometer equipped with a TXI CryoProbe™.

References

1. Reckel,S., Hänsel,R., Löhr,F. & Dötsch,V. *Prog. NMR Spectrosc.* **51**, 91-101 (2007).

2. Burz,D.S. & Shekhtman,A. *Plos ONE* **3**, e2571 (2008).

3. Inomata,K. *et al. Nature* **458**, 106-109 (2009).

4. Ogino,S. *et al. J. Am. Chem. Soc.* **131**, 10834-10835 (2009).

5. Selenko,P. *et al. Nat. Struct. Mol. Biol.* **15**, 321-329 (2009).

6. Wong,P.C. *et al. Proc. Natl. Acad. Sci. USA* **97**, 2886-2891 (2000).

7. Culotta,V.C., Yang,M. & O'Halloran,T.V. *Biochim. Biophys. Acta* **1763**, 747-758 (2006).

8. Michiels,C., Raes,M., Toussaint,O. & Remacle,J. *Free Radic. Biol. Med.* **17**, 235-248 (1994).

9. Lindberg,M.J., Tibell,L. & Oliveberg,M. *Proc. Natl. Acad. Sci. USA* **99**, 16607-16612 (2002).

10. Furukawa,Y. & O'Halloran,T.V. *J. Biol. Chem.* **280**, 17266-17274 (2005).

11. Banci,L. *et al. Proc. Natl. Acad. Sci. USA* **104**, 11263-11267 (2007).

12. Aricescu,A.R., Lu,W. & Jones,E.Y. *Acta Crystallogr. D. Biol. Crystallogr.* **62**, 1243-1250 (2006).

13. Chang,L.Y., Slot,J.W., Geuza,H.J. & Crapo,J.D. *J. Cell Biol.* **107**, 2169-2179 (1988).

14. Rakhit,R. *et al. J. Biol. Chem.* **279**, 15499-15504 (2004).

15. Crapo,J.D., Oury,T., Rabouille,C., Slot,J.W. & Chang,L.Y. *Proc. Natl. Acad. Sci. USA* **89**, 10405-10409 (1992).

16. Sturtz,L.A., Diekert,K., Jensen,L.T., Lill,R. & Culotta,V.C. *J. Biol. Chem.* **276**, 38084-38089 (2001).

17. Banci,L., Bertini,I., Cramaro,F., Del Conte,R. & Viezzoli,M.S. *Biochemistry* **42**, 9543-9553 (2003).

18. Banci,L., Bertini,I., Cantini,F., D'Amelio,N. & Gaggelli,E. *J. Biol. Chem.* **281**, 2333-2337 (2006).

19. Banci,L., Barbieri,L., Bertini,I., Cantini,F. & Luchinat,E. *Plos ONE* **6**, e23561 (2011).

20. Rensing,C. & Grass,G. *FEMS Microbiol. Rev.* **27**, 197-213 (2003).

21. Rae,T.D., Schmidt,P.J., Pufahl,R.A., Culotta,V.C. & O'Halloran,T.V. *Science* **284**, 805-808 (1999).

22. Kim,B.E., Nevitt,T. & Thiele,D.J. *Nat. Chem. Biol.* **4**, 176-185 (2008).

23. Puig,S. & Thiele,D.J. *Curr. Opin. Chem. Biol.* **6**, 171-180 (2002).

24. Banci,L. *et al. Nature* **465**, 645-648 (2010).

25. Banci,L., Bertini,I., Cantini,F. & Ciofi-Baffoni,S. *Cell. Mol. Life Sci.* **67**, 2563-2589 (2010).

26. Schmidt,P.J. *et al. J. Biol. Chem.* **274**, 23719-23725 (1999).

27. Furukawa,Y., Torres,A.S. & O'Halloran,T.V. *EMBO J.* **23**, 2872-2881 (2004).

28. Caruano-Yzermans,A.L., Bartnikas,T.B. & Gitlin,J.D. *J. Biol. Chem.* **281**, 13581-13587 (2006).

29. Carroll,M.C. *et al. Proc. Natl. Acad. Sci. USA* **101**, 5964-5969 (2004).

30. Leitch,J.M., Yick,P.J. & Culotta,V.C. *J. Biol. Chem.* **284**, 24679-24683 (2009).

31. Proescher,J.B., Son,M., Elliott,J.L. & Culotta,V.C. *Hum. Mol. Genet.* **17**, 1728-1737 (2008).

32. Banci,L. *et al. Proc. Natl. Acad. Sci. USA* **109**, 13555-13560 (2012).

33. Reckel,S., Lopez,J.J., Löhr,F., Glaubitz,C. & Dötsch,V. *ChemBioChem* **13**, 534-537 (2012).

34. Schanda,P. & Brutscher,B. *J. Am. Chem. Soc.* **127**, 8014-8015 (2005).

35. Freshney,R. Culture of Animal Cells: A Manual of Basic Technique. Alan R. Liss, Inc., New York, (1987).

Supplementary Information

for

Atomic-resolution monitoring of protein maturation in live human cells

Lucia Banci[1,2,*], Letizia Barbieri[1], Ivano Bertini[1,2], Enrico Luchinat[1], Erica Secci[1], Yuguang Zhao[3], A. Radu Aricescu[3,*]

Contains Supplementary Figures 1 to 11.

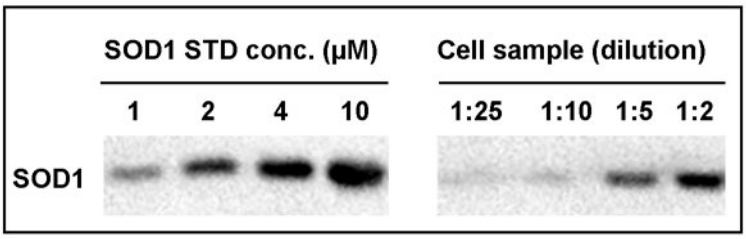

Supplementary Figure 1. Endogenous SOD1 levels in untransfected HEK293T cells were measured by Western Blot analysis. Untransfected HEK293T cells were analyzed by Western Blot, and the endogenous amount of SOD1 was estimated by comparing band intensities with different dilutions of a sample of pure SOD1 at known concentration. SOD1 was stained using a rabbit anti-human SOD1 polyclonal primary antibody (BioVision) diluted 1:100 at 2μg/mL and a goat anti-rabbit IgG-peroxidase secondary antibody for detection (Sigma), diluted at 1:80000.

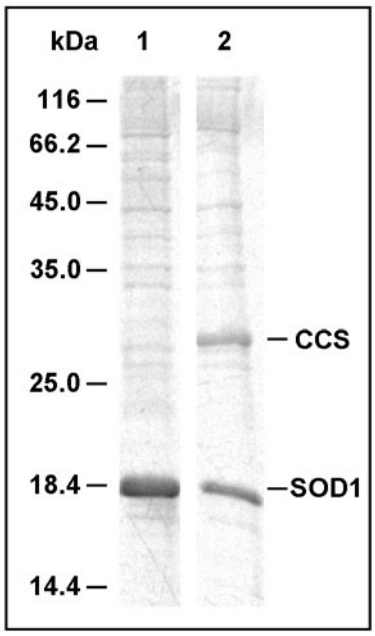

Supplementary Figure 2. Overexpression of SOD1 and CCS in human cells. Coomassie-stained SDS-PAGE of cell extracts from NMR samples of human cells expressing SOD1 (lane 1) and co-expressing SOD1 and CCS (lane 2) in Zn(II)-supplemented medium. Cell extracts were obtained by freeze/thaw lysis followed by centrifugation. Protein bands and reference molecular weights are indicated. Protein concentration was estimated by comparing band intensities with serial dilutions of a pure SOD1 sample at known concentration, run on the same SDS-PAGE.

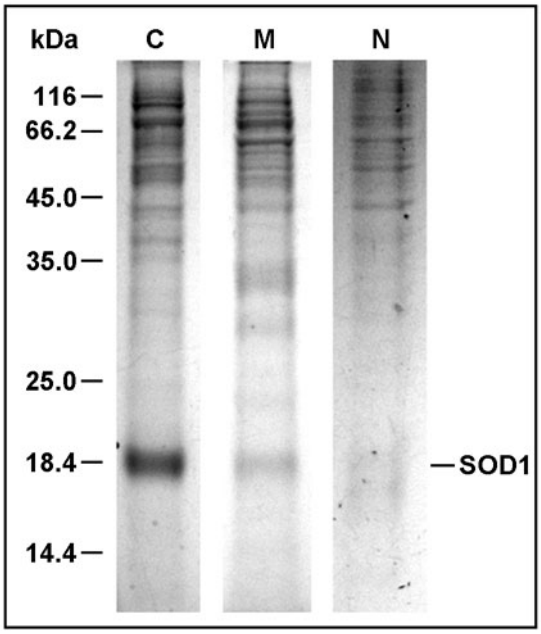

Supplementary Figure 3. Cellular fractionation shows that SOD1 is present mainly in the cytoplasm. Coomassie-stained SDS-PAGE of sub-cellular fractions obtained from human cells expressing SOD1 using a mitochondria isolation kit for cultured cells (Thermo Scientific). The nuclear fraction was obtained by washing once the pellet obtained after cell rupture, and resuspending it in PBS buffer. C = cytoplasm; M = mitochondria; N = nuclei. Relative dilutions are 1:16 (C), 1:1 (M), 1:10 (N) respectively. SOD1 concentration was estimated via SDS-PAGE by comparing each fraction at different dilutions with a *in vitro* sample of SOD1 of known concentration.

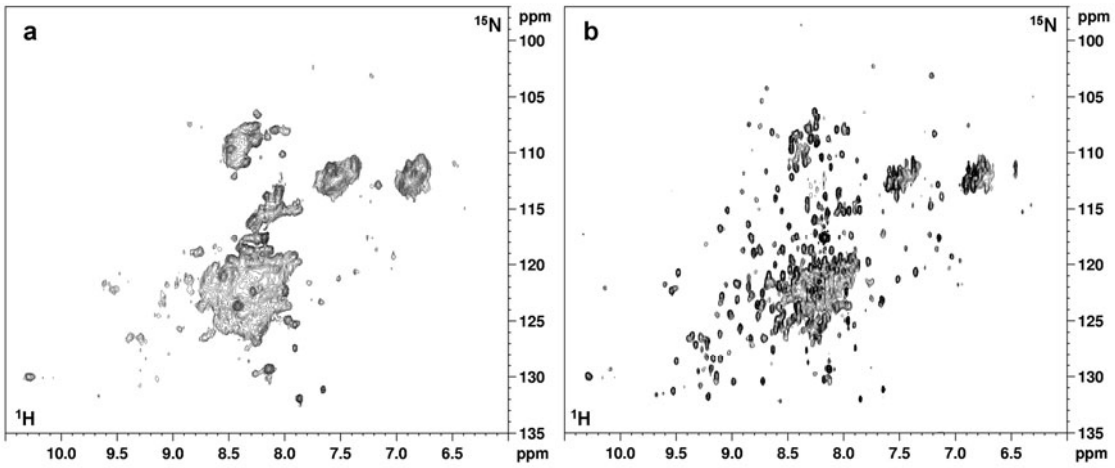

Supplementary Figure 4. SOD1 is present both in the metal-depleted form (apo-SOD1^{SH}) and in the zinc-containing form (E,Zn-SOD1^{SH}) in cells without metal supplementation of tissue culture media. ^{1}H-^{15}N SOFAST HMQC spectra were acquired: **a**, on human cells expressing uniformly ^{15}N-labelled SOD1; **b**, on the corresponding cell extract. In the in-cell NMR spectrum (**a**) only the the crosspeaks of the unfolded region of apo-SOD1^{SH} are detected, (at 8.0-8.5 ppm ^{1}H, above the cellular background signals) while the peaks of the folded region are broadened beyond detection. Most of the crosspeaks of apo-SOD1^{SH} are detected in the cell extract (**b**), together with those of E,Zn-SOD1^{SH}, while no crosspeaks from other species are detected.

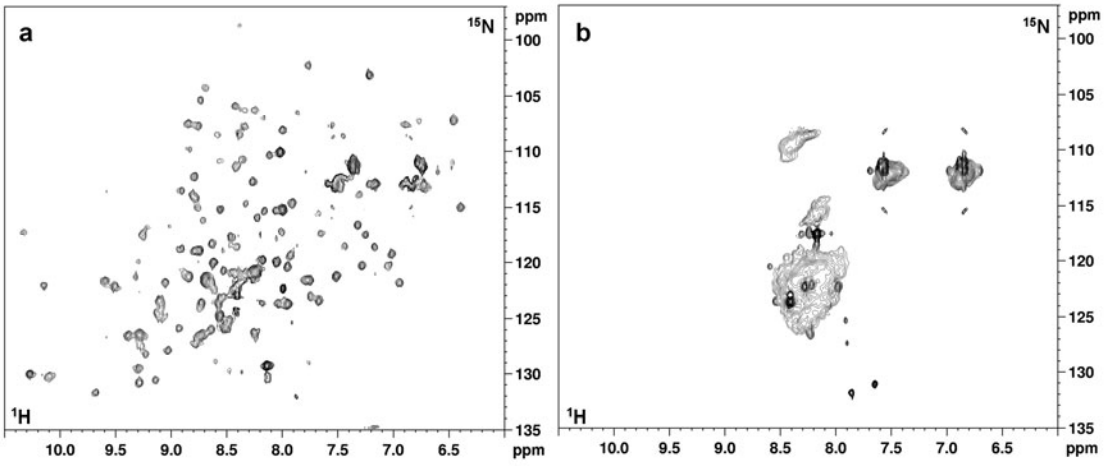

Supplementary Figure 5. Spectral crowding is reduced by subtracting the background signals arising from the non-selective labelling of cellular components. **a**, ^{1}H-^{15}N correlation spectrum of cytoplasmic E,Zn-SOD1^{SH} free of background signals obtained by subtracting to the ^{1}H-^{15}N SOFAST-HMQC spectrum shown in Figure 1c the spectrum **b**, of a cell sample transfected with the empty pHLsec vector, containing only signals from cellular components. The two spectra were acquired in the same experimental conditions.

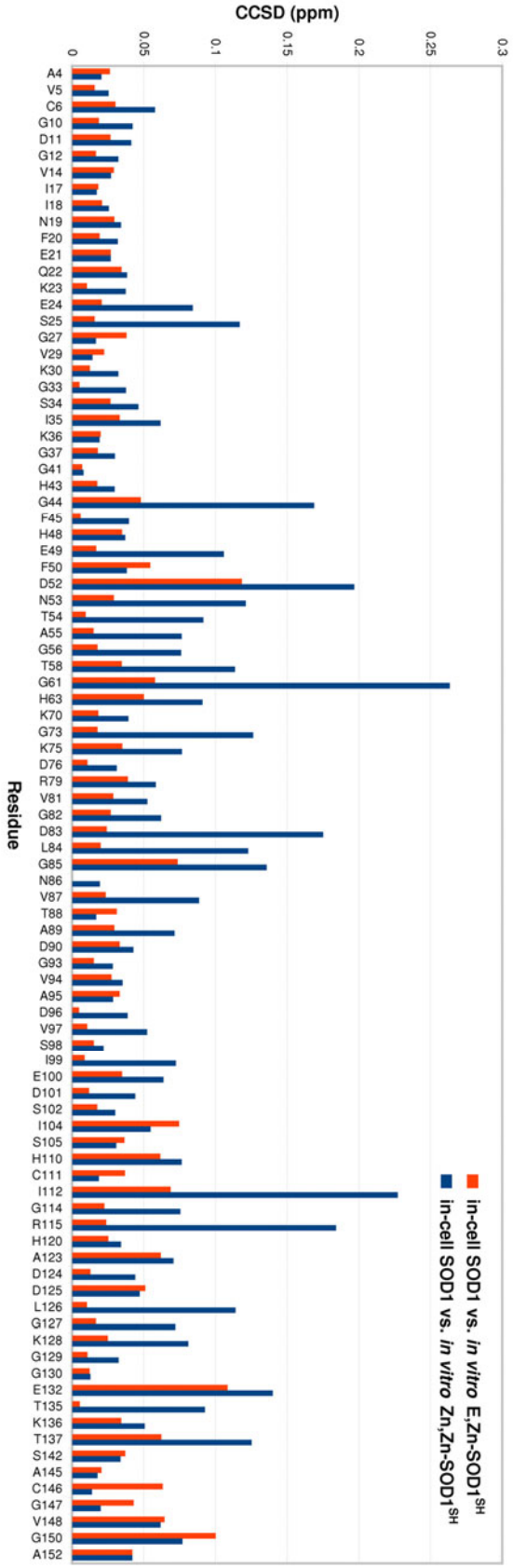
CCSD (ppm)
0
0.05
0.1
0.15
0.2
0.25
0.3
Residue
A4
V5
C6
G10
D11
G12
V14
I17
I18
N19
F20
E21
Q22
K23
E24
S25
G27
V29
K30
G33
S34
I35
K36
G37
G41
H43
G44
F45
H48
E49
F50
D52
N53
T54
A55
G56
T58
G61
H63
K70
G73
K75
D76
R79
V81
G82
D83
L84
G85
N86
V87
T88
A89
D90
G93
V94
A95
D96
V97
S98
I99
E100
D101
S102
I104
S105
H110
C111
I112
G114
R115
H120
A123
D124
D125
L126
G127
K128
G129
G130
E132
T135
K136
T137
S142
A145
C146
G147
V148
G150
A152
in-cell SOD1 vs. in vitro E,Zn-SOD1SH
in-cell SOD1 vs. in vitro Zn,Zn-SOD1SH

Supplementary Figure 6. Combined Chemical Shift Difference (CCSD) plot of in-cell SOD1 vs. in vitro E,Zn-SOD1 and Zn,Zn-SOD1. CCSD plot of a subset of ^{1}H-^{15}N resonances of SOD1 showing that the cytoplasmic zinc-containing SOD1 species corresponds to *in vitro* E,Zn-SOD1^{SH}. CCSDs between cytoplasmic SOD1 and Zn,Zn-SOD1^{SH} (blue) are higher on average than CCSDs between cytoplasmic SOD1 and E,Zn-SOD1^{SH} (orange). CCSDs were calculated using the formula: $CCSD = \sqrt{\frac{1}{2}\left(\Delta\delta^{1}H\right)^{2} + \frac{1}{2}\left(\Delta\delta^{15}N/5\right)^{2}}$.

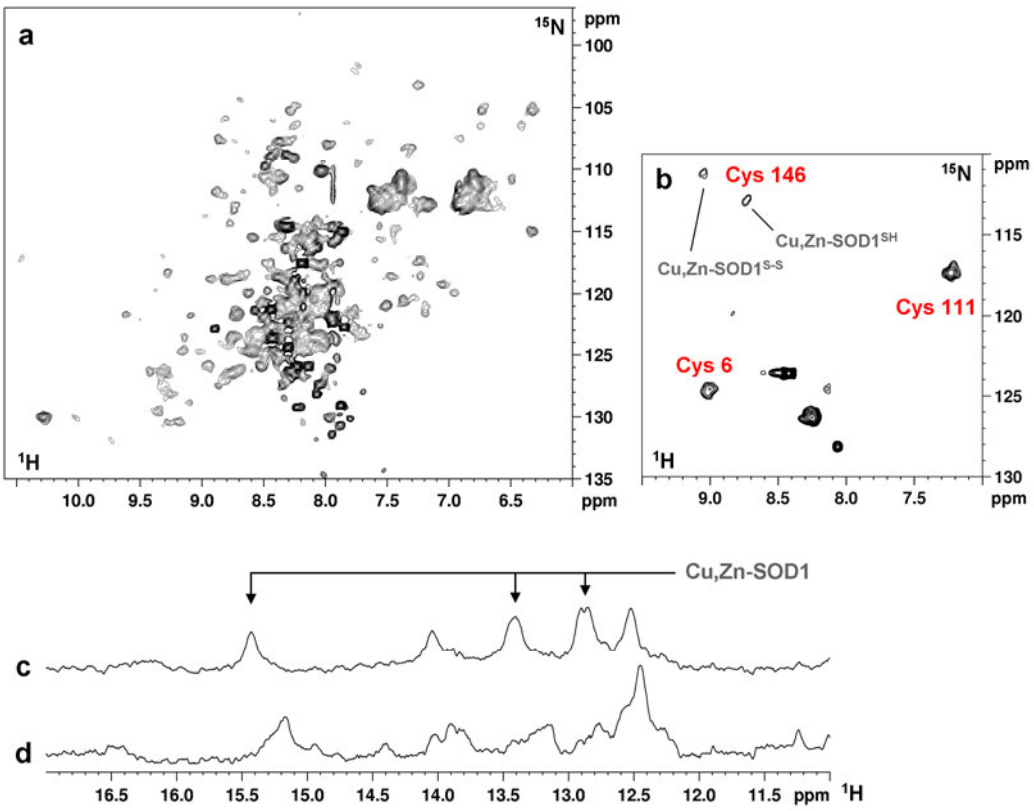

Supplementary Figure 7. Cu(II) addition to *E. coli* cells induces formation of Cu(I),Zn-SOD1 and partial disulfide oxidation. ^{1}H-^{15}N SOFAST HMQC spectra of *E. coli* cells expressing: **a**, uniformly ^{15}N-labelled SOD1; **b**, ^{15}N-cysteine labelled SOD1 in Zn(II)-supplemented medium, after incubation with Cu(II). Assigned cysteine residues in **b** are indicated in red. When two species of SOD1 are present, dark grey labels indicate the disulfide redox state of each species. Unlabelled crosspeaks are cellular background signals; **c**, ^{1}H histidine NMR spectrum of *E. coli* cells expressing SOD1 incubated with Cu(II); **d**, NMR spectrum of *E. coli* cells expressing SOD1 incubated with Cu(I)-acetonitrile complex.

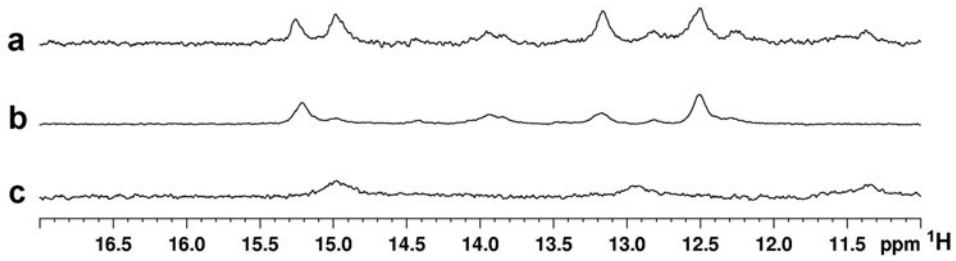

Supplementary Figure 8. Histidine region of ^{1}H NMR spectra acquired on human cells co-expressing SOD1 and CCS. a, cells co-expressing unlabelled SOD1 and CCS; **b**, expressing unlabelled SOD1 (scaled down to match the intensity of SOD1 peaks in **a**); **c**, expressing unlabelled CCS. Cell samples were transfected in Zn(II)-supplemented medium.

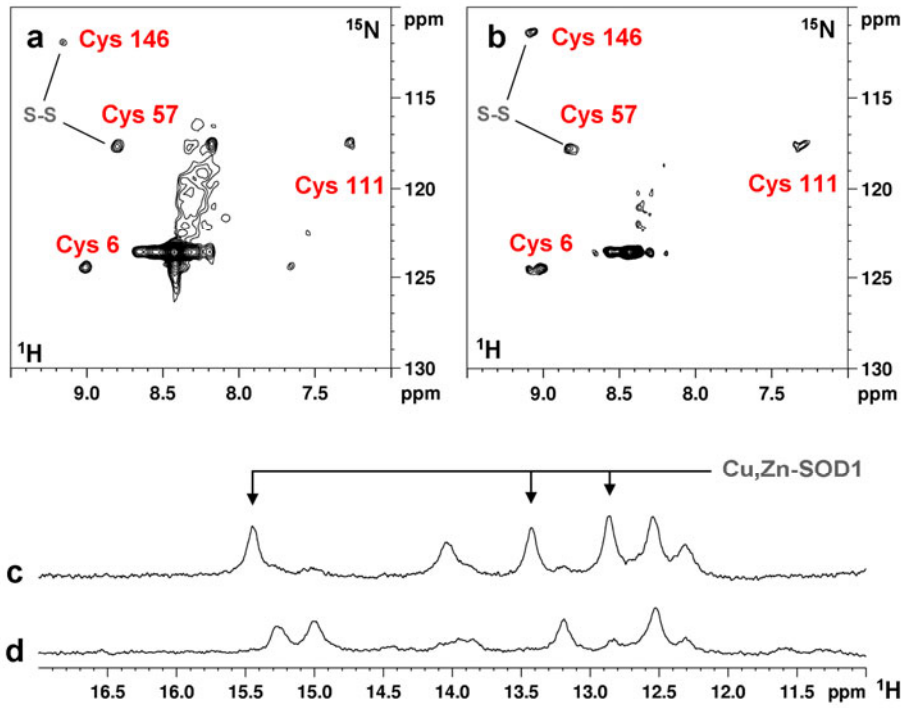

Supplementary Figure 9. When SOD1 is expressed at lower amounts, CCS catalyzes the complete formation of the disulfide bond, and incubation with copper results in the complete formation of Cu,Zn-SOD1. ^{1}H-^{15}N SOFAST HMQC spectra were acquired on human cells expressing lower amounts of SOD1 (45 ± 10 µM) and CCS (15 ± 3 µM): **a**, ^{15}N-cysteine labelled SOD1 and CCS in Zn(II)-supplemented medium; **b**, ^{15}N-cysteine labelled SOD1 and CCS in Zn(II)-supplemented medium, after incubation with Cu(II). Assigned cysteine residues are indicated in red. In both spectra, the cysteine crosspeaks of reduced SOD1 are not detected. Histidine region of ^{1}H NMR spectra acquired on the same cells: **c**, after incubation with Cu(II); **d**, without incubation with Cu(II). Histidine protons unambiguously assigned to Cu(I),Zn-SOD1 species are indicated. Complete copper delivery to SOD1 is observed.

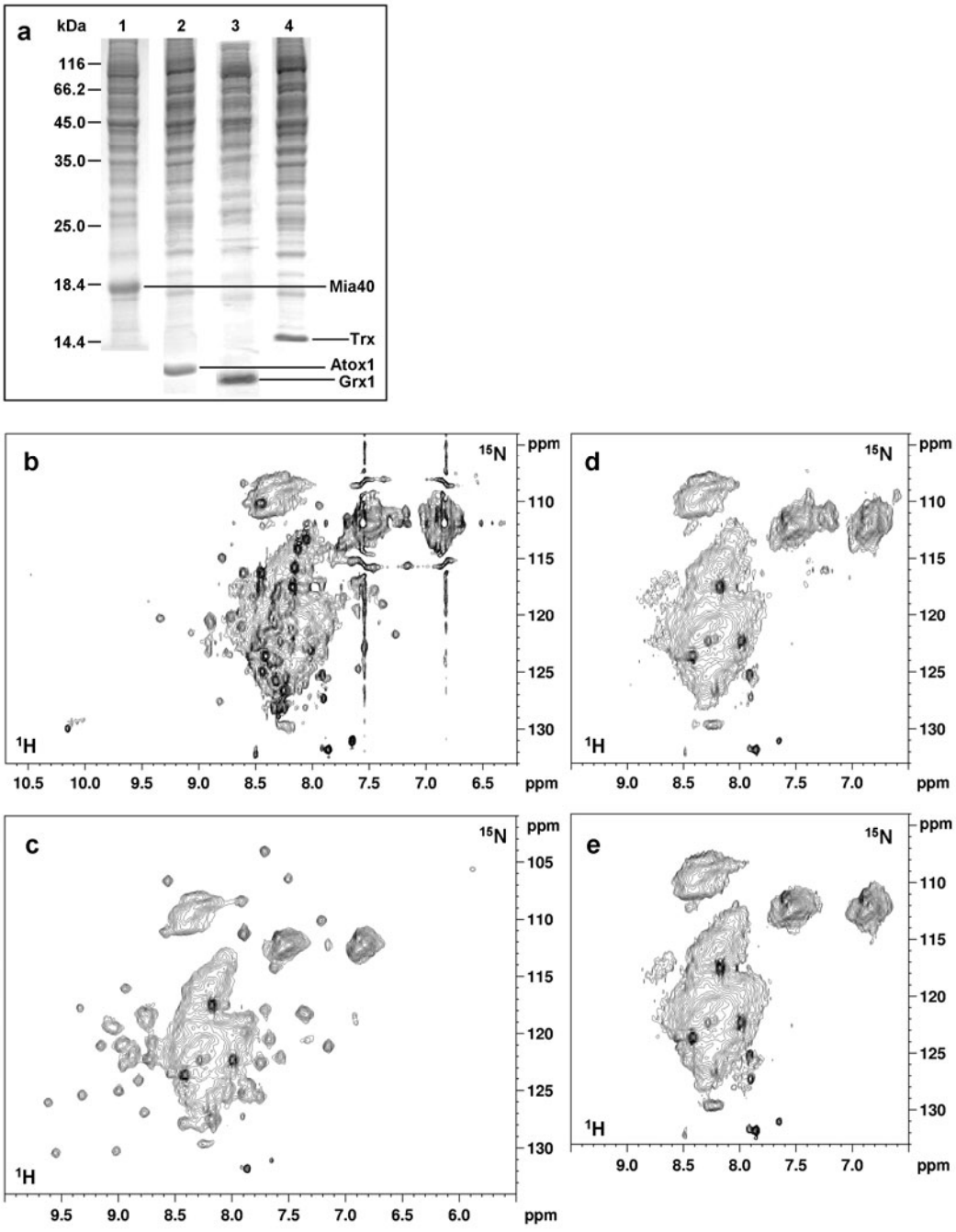
a
kDa
1
2
3
4
116
66.2
45.0
35.0
25.0
18.4
14.4
Mia40
Trx
Atox1
Grx1
b
c
d
e
15N
1H
ppm

Supplementary Figure 10. In-cell NMR detection of non hSOD1 protein targets. a, Coomassie-stained SDS-PAGE of cell extracts showing the overexpression of Mia40 (lane 1), Atox1 (lane 2), glutaredoxin-1 (Grx1, lane 3) and thioredoxin (Trx, lane 4); **b**, ^{1}H-^{15}N SOFAST HMQC spectrum of HEK293T cells expressing U-^{15}N labelled Mia40; **c**, ^{1}H-^{15}N SOFAST HMQC spectrum of HEK293T cells expressing U-^{15}N labelled Atox1; **d**, ^{1}H-^{15}N SOFAST HMQC spectrum of HEK293T cells expressing U-^{15}N labelled glutaredoxin-1; **e**, ^{1}H-^{15}N SOFAST HMQC spectrum of HEK293T cells expressing U-^{15}N labelled thioredoxin. Mia40 (**b**) and Atox1 (**c**) are clearly detected above the cellular background, while glutaredoxin-1 (**d**) and thioredoxin (**e**) are not detected due to slow tumbling in the cytoplasm.

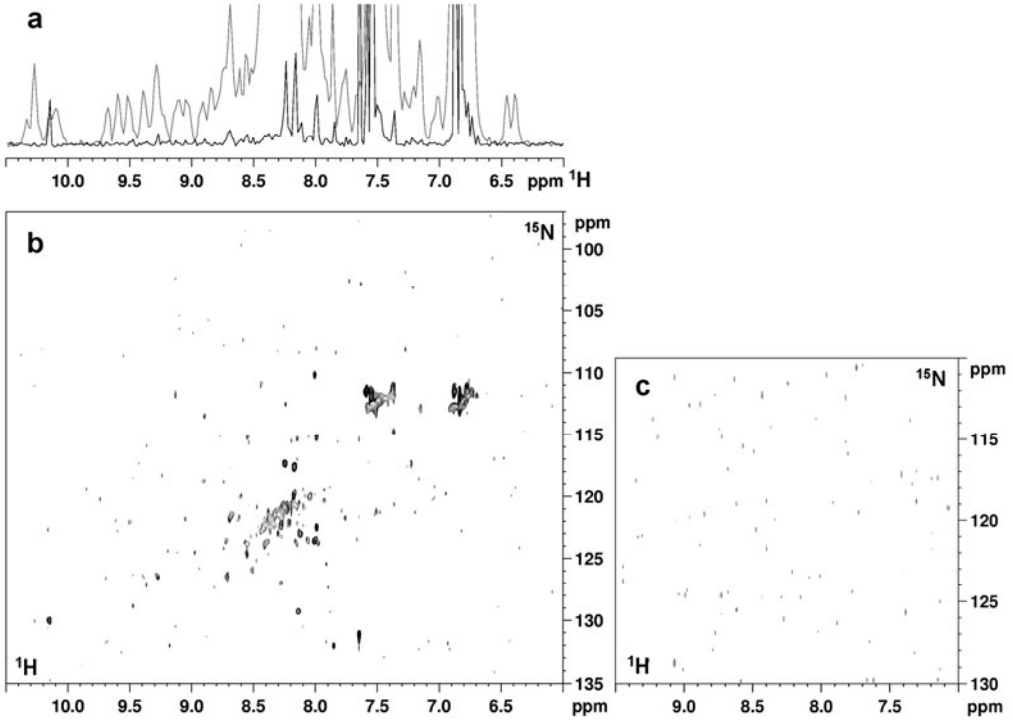

Supplementary Figure 11. NMR spectra of the cell sample supernatants confirm the absence of protein leaked out of the cells. ^{1}H-^{15}N SOFAST HMQC spectra were acquired on the supernatants obtained from each cell sample, after the actual in-cell NMR experiments, to check whether protein leakage has occurred. **a**, ^{1}H projection of the ^{1}H-^{15}N SOFAST HMQC supernatant spectrum (shown in **b**) of cells containing U-^{15}N E,Zn-SOD1 (black line) compared to the ^{1}H projection of the in-cell NMR spectrum (grey line); **b**, 2D ^{1}H-^{15}N SOFAST HMQC supernatant spectrum; **c**, 2D ^{1}H-^{15}N SOFAST HMQC supernatant spectrum of a cell sample containing ^{15}N-cysteine labelled SOD1 and CCS.

3.3. Visualization of redox-controlled protein fold in living cells

Most of the human proteins are encoded by nuclear DNA, and are synthesized in the cytoplasm (or directly targeted to the ER). This is also true for the majority of mitochondrial proteins, and for every protein of the mitochondrial IMS. There are several mechanisms for importing such proteins into the mitochondria, most of which require the proteins to cross the outer membrane through the TOM channel. A class of small proteins of the IMS (which harbour a CHCH structural motif) is imported through the TOM in the unfolded state. Once in the IMS, these proteins are oxidatively folded by Mia40, which is part of the IMS disulfide relay system. These proteins, including Mia40 itself, need to be unfolded and reduced in the cytoplasm in order to be imported, although no atomic-resolution study has proved this. Thiol redox control in the cytoplasm is mainly exerted by the thioredoxin and glutaredoxin systems, which regulate the redox state of protein disulfides exploiting the reducing power of NADPH, through GSH-dependent (Grx1) and independent (Trx1) pathways. In this work, human Mia40 was transiently expressed in the cytoplasm of human cells, the folding and redox states were characterized by NMR and their dependence on the thiol redox systems was investigated. Upon overexpression, Mia40 was found to be oxidized and folded in the cytoplasm, despite the reducing environment given by the high GSH:GSSG ratio. The folding state of Mia40 was then investigated after co-expression of Grx1 or Trx1. Interestingly, Grx1 prevented oxidation of Mia40, decreasing the signal intensity of the folded species in the NMR spectra, while Trx1 had no effect, and only folded Mia40 was detected. As no interaction was observed *in vitro* between Mia40 and Grx1, this effect is likely to occur indirectly, possibly by means of different cellular substrates of the Grx1 system.

Visualization of redox-controlled protein fold in living cells

Lucia Banci[1,2,*], Letizia Barbieri[1], Enrico Luchinat[1], Erica Secci[1]

Affiliations:

[1]Magnetic Resonance Center - CERM, University of Florence, Via Luigi Sacconi 6, 50019, Sesto Fiorentino, Florence, Italy.

[2]Department of Chemistry, University of Florence, Via della Lastruccia 3, 50019, Sesto Fiorentino, Florence, Italy.

Running title: In-cell redox-controlled protein fold

SUBMITTED

Most mitochondrial proteins are encoded by nuclear DNA, thus they are synthesized in the cytoplasm and imported into mitochondria. Several proteins of the intermembrane space (IMS) are imported through an oxidative process, being folded through the formation of structural disulfide bonds catalyzed by Mia40, and then trapped in the IMS. To be imported, these proteins need to be reduced and unfolded; however no structural information *in situ* exists on these proteins in the cytoplasm, prior to their mitochondrial import. In humans, Mia40 itself is imported through the same mechanism, though its folding state in the cytoplasm is unknown. Here we provide atomic-level details on Mia40 folding state in the human cell cytoplasm through in-cell NMR. We showed that overexpressed cytoplasmic Mia40 is folded, and that its folding state is specifically dependent on the glutaredoxin-1 (Grx1) system. Indeed, high Grx1 levels keep Mia40 unfolded, while thioredoxin-1 (Trx1) does not affect Mia40.

The majority of the human proteins is produced by nuclear DNA and is released in the cytoplasm and/or in the ER. These proteins then need to complete their folding and maturation process which could involve several steps, from cofactor binding to cysteine oxidation to other post-translational modifications. Furthermore, if the protein destiny is a cellular compartment other than the cytoplasm, some or all maturation and folding steps could need to take place in the final cellular localization. This is particularly true for a large share of proteins present in the inner membrane space (IMS) of mitochondria, but which do not feature any target sequence for this organelle [1-3]. They are in an unfolded state in the cytoplasm and therefore they can enter mitochondria, thanks to their conformational freedom which allows them to go through the TOM channel [1]. Once entered the IMS they reach the native form by folding, which blocks them in a defined, more rigid conformation, thus preventing them from crossing back the outer membrane [4-6]. It is therefore evident that the folding state of a protein has to be dependent on the cellular compartment where the protein is located, and on its properties. It has been shown that the import of some of these IMS proteins is in fact

modulated by cytosolic thiol-disulfide regulation systems [7]. However no detailed, atomic resolution study has yet confirmed such findings.

In the present work we show, by exploiting in-cell NMR [8-12], that indeed the properties of the cell compartment in terms of redox-regulating components influence the folding state of one of such proteins, whose oxidation state is compartment dependent. We have specifically characterized Mia40, a hub protein for the mitochondrial protein import process. Mia40 is an oxidoreductase which catalyzes in the IMS the formation of internal disulfide bonds on its protein substrates through the intermediate formation of a mixed disulfide bond between the substrate and its catalytic CPC motif [6,13-15]. Together, these proteins constitute the disulfide relay system of the IMS[5,16]. Upon interaction with Mia40 and subsequent formation of their disulfide bonds, the substrates of Mia40 become folded and are trapped in the IMS [17,18]. Interestingly, Mia40 itself obtains its final structure in the IMS upon the formation of two internal disulfide bonds, likely by acting as a substrate of itself [14,19]. Like the other substrates of the disulfide relay system, also Mia40 has to cross the outer mitochondrial membrane in an unfolded, reduced state. Glutaredoxin 1 (Grx1) and thioredoxin 1 (Trx1) are cytoplasmic oxidoreductases involved in the regulation of protein thiol groups and in the cellular defence against oxidative stress [20,21]. Trx1 was recently shown to be responsible for facilitating the mitochondrial import of the small Tim proteins [7]. It can be hypothesized that other small proteins of the IMS sharing the same import mechanism, including Mia40, are regulated by such thiol-regulating proteins.

We show here that Mia40, even in the reducing environment of the cytoplasm, is largely in the oxidized, folded state when it is overexpressed, thus indicating that the high cytoplasmic level of reduced glutathione is not sufficient alone to maintain the reduced state of Mia40. Co-expression of glutaredoxin 1 [20,22] (at comparable level) keeps Mia40 in the unfolded, reduced state, while co-expression of thioredoxin 1, which has a similar role in keeping protein thiols reduced in the cytoplasm [20,23], has no effect on the oxidation state of Mia40. Additionally, glutaredoxin 1 does not catalyze the reduction of Mia40 in presence of reducing agents *in vitro*, implying some effect of the cytoplasmic environment which is not reproduced *in vitro*. These results indicate the presence of a specific redox regulation mechanism involving Grx1, which keeps the endogenous

Mia40 reduced in the cytoplasm, allowing it to reach the outer mitochondrial membrane in the reduced, import-competent state.

Results and Discussion

Mia40, overexpressed in the cytoplasm of human cells, took a folded conformation, as monitored through ^{1}H-^{15}N and ^{1}H NMR spectra, which corresponds to the functional state of Mia40 that is normally found in the IMS (Figure 1a), and is the same conformation of oxidized Mia40 *in vitro* ($Mia40^{2S\text{-}S}$, Supplementary Figure S1a). The central region of the protein is stably folded in two α-helices while the N- and C-terminal regions are intrinsically unfolded. The crosspeaks of the folded part were well dispersed in the spectrum, while the peaks of the intrinsically unfolded regions appeared as strong overlapped signals, which fall in the central part of the spectrum, together with background signals arising from cellular metabolites. The methyl region of the ^{1}H NMR spectrum provided more sensitivity to assess the relative amount of folded Mia40 (Figure 1b). The same species was observed in the cell extracts obtained from cell lysis, with no apparent change in the folding state (Figure 2a,b). The amount of folded protein in the cell extracts was estimated around 51 ± 5 μM by NMR, very close to the total protein amount (60 ± 15 μM) as measured by Western Blot analysis on the same extracts (Figure 3). When Mia40 was co-expressed in the cytoplasm together with glutaredoxin 1 (Grx1), a large fraction of it was present in the reduced, unfolded state. This was clearly monitored through the ^{1}H-^{15}N NMR spectra in which the crosspeaks of the folded part of Mia40 were barely detected, while the crosspeaks of the unfolded parts were still visible, both in intact cells (Figure 1c,d) and in cell extracts (Figure 2c,d). In presence of Grx1, only around 25%, 14 ± 2 μM over a total of 60 ± 10 μM, of Mia40 present in the cytoplasm was in the oxidized state ($Mia40^{2S\text{-}S}$), compared to ~90% in absence of Grx1. In the cytoplasm Grx1 is invisible to NMR, as its signals are broadened beyond detection as a consequence of its slow tumbling rate, which is likely due to interactions with the cellular environment (a similar effect has been reported for several proteins overexpressed in *E. coli* cytoplasm, including wild-type ubiquitin [24], cytochrome c [25], *E. coli* thioredoxin and FKBP [26]). This behaviour was confirmed by the empty ^{1}H-^{15}N spectra when only Grx1 was expressed (Supplementary Figure S2a). The

NMR properties of cytoplasmic Grx1 therefore allowed us to obtain ^{1}H-^{15}N NMR spectra of Mia40 free of interference from Grx1 signals.

The effect of human thioredoxin 1 on Mia40 state was also investigated. Similarly to Grx1, Trx1 in the human cell cytoplasm is not detectable by NMR, consistently with what previously reported in *E. coli* [26] (Supplementary Figure S2c). Contrarily to Grx1, when Trx1 was co-expressed together with Mia40, it did not affect the folding state of Mia40. Indeed, all cytoplasmic Mia40 was found in the folded state (Figure 1e,f and 2e,f) (62 ± 7 µM over a total of 61 ± 18 µM). Therefore, the two thiol-regulating proteins have different effects on Mia40, despite being reported to have overall similar functions in the cytoplasm (Figure 4).

At difference to what was observed in the cells, fully reduced Grx1 had no effect on Mia40 redox state *in vitro*. U-^{15}N Mia40$^{2S\text{-}S}$ was incubated in reducing conditions, either in the presence of dithiothreitol (DTT) or reduced glutathione (GSH), with increasing concentrations of unlabelled, fully reduced Grx1, and each step was monitored by NMR. No change in the spectrum occurred upon addition of up to 2 eq of Grx1 to Mia40$^{2S\text{-}S}$ and 48 h incubation, thus excluding a direct mechanism of reduction of Mia40 by Grx1. In a control experiment, U-^{15}N Mia40$^{2S\text{-}S}$ (Supplementary Figure S1a) was completely reduced by heat denaturation at 95°C in buffer containing either DTT or GSH. No protein degradation occurred. In both cases the protein remained reduced when cooled down at 25°C (Supplementary Figure S1c). The ^{1}H-^{15}N crosspeaks of the α-helical region disappeared, in analogy with what was observed in the cytoplasm in presence of Grx1. The alkylation reaction with AMS visualised on SDS-PAGE confirmed the complete reduction of all cysteines (Supplementary Figure S1b,d). Upon removal of the reducing agent and exposure to air, Mia40 rapidly reverted back to the folded conformation. To test whether Grx1 could bind fully reduced Mia40 and prevent its oxidation, 2 eq of Grx1 were added to a sample of U-^{15}N labelled Mia40 unfolded in presence of GSH. Upon exposure to air Mia40 rapidly folded, thus indicating that Grx1 did not protect reduced Mia40 from oxidation.

The current model of Mia40 maturation pathway requires that the protein, which is natively expressed in the cytoplasm from nuclear mRNA, crosses the outer mitochondrial membrane through the TOM channel in a reduced and unfolded

conformation. No Mia40 has been reported to reside in the cytoplasm, except for the time required to translocate to the mitochondria [27]. However, when Mia40 is overexpressed, it does not translocate quantitatively to the mitochondria, and close to the total of Mia40 remains in the cytoplasm. Our results show that in this situation, cytoplasmic Mia40 reaches the folded state, which is therefore a thermodynamically favoured conformation in the cytoplasm. Therefore, in physiological conditions there is the need for a mechanism to keep Mia40 reduced until it reaches the outer mitochondrial membrane, as the amount and ratio of cytoplasmic GSH is apparently not sufficient for that purpose.

Overexpression of Grx1 allows Mia40 to remain largely in the reduced, unfolded state. Conversely, when oxidized Mia40 is incubated *in vitro* with Grx1 in presence of a reducing agent it does not change its redox state, and the complete reduction of the structural disulfide bonds is only possible upon heat denaturation in reducing conditions. The lack of a direct interaction of Grx1 with Mia40 suggests that the effect of Grx1 on the oxidation state of intracellular Mia40 is not the result of a direct interaction between the two proteins, but is mediated by some other component of the cytoplasm. The action of Grx1 on the folding and the maintenance of the reduced state of Mia40 in the cytoplasm is very specific. Indeed, the behaviour of Mia40 in presence of Trx1 is quite different. Like Grx1, Trx1 regulates the redox state of cytoplasmic proteins, by reducing their disulfide bonds [20,23]. Trx1 has also been reported to act as a co-chaperone to facilitate the folding of its substrates [28,29]. When Trx1 is overexpressed together with Mia40, however, it does not affect the state of Mia40, which folds almost completely. The remarkably different behaviour of Grx1 indicates that the increase of reduced, unfolded Mia40 is not dependent on a generic increase in reducing power in the cytoplasm, which would be provided by both the Grx1 and Trx1 systems. Instead, Grx1 has a specific – although likely indirect – effect on Mia40 redox state, implying a link between the Grx1 redox regulation system and the Mia40 maturation pathway in the cytoplasm.

We have here characterized the folding state of Mia40 in the cytoplasm, obtaining atomic-level information in living human cells by NMR. This approach allowed us to understand how the folding of Mia40 is controlled by the cytoplasmic redox-regulation

system specifically involving Grx1. These results also show the general relevance of atomic resolution studies performed in living cells, which are needed to describe cellular physiological processes such as the redox-controlled protein folding, and to understand how other pathways involved can affect and regulate such processes.

Methods

Overexpression of Mia40, Grx1 and Trx1 in human cells was performed by following a protocol previously established [12,30]. Briefly, the cDNA sequences encoding Mia40 (amino acids 1-142, GenBank accession number: NP_001091972.1), Grx1 (amino acids 1-106, GenBank accession number: NP_001112362.1) and Trx1 (amino acids 1-105, GenBank accession number: NP_003320.2) were amplified by PCR and sub-cloned into the pHLsec vector [12,30] between EcoRI and XhoI restriction enzyme sites. The clones were verified by gene sequencing. Transient transfection was obtained by treating the cells with a DNA:polyethilenimine mixture. The amount of the overexpressed protein in the cells reached a maximum after ~48 hours. Intracellular distribution was assessed by separating the cytoplasmic and the mitochondrial fractions from cell extracts using a mitochondria isolation kit for cultured cells (Thermo Scientific). ~1% of the total Mia40 was estimated to be localized in the mitochondrial fraction.

NMR spectra were acquired on cell samples overexpressing either unlabelled or uniformly U-^{15}N labelled Mia40. The amount of folded Mia40 in the cell extracts was measured by NMR through standard addition of pure, folded Mia40 at known concentration. The ^{1}H resonance at −0.7 ppm of Ile 53 Hγ was used as a marker of the folded conformation of Mia40. Total Mia40 was determined on the same cell extracts by Western Blot analysis, by using the same pure Mia40 sample at increasing dilutions as a reference.

Grx1 was co-expressed with Mia40, either unlabelled or with uniform ^{15}N labelling. The optimal DNA ratio of 1:0.75:2 hMia40:hGrx1:PEI was chosen, which kept the intracellular amount of Mia40 unaltered, and allowed the co-expression of a comparable amount of Grx1 (as estimated by comparing the bands on SDS-PAGE). The relative amount of folded Mia40 was determined as above. Trx1 was co-expressed with Mia40

by transfecting different amounts of hMia40 and hTrx1 DNAs. Three hMia40:hTrx1:PEI ratios were tested (1:0.5:2, 1:0.75:2, 1.25:0.75:2), and about the same intracellular Mia40 levels were obtained, while the amount of Trx1 was estimated to be one order of magnitude lower.

U-^{15}N labelled Mia40 for *in vitro* experiments and unlabelled Mia40 for NMR quantifications were produced as previously described [3]. Glutaredoxin 1 for *in vitro* interaction with Mia40 was produced as follows: a pTH34 vector containing the human Grx1 gene (N-term fused with His-tag and TEV recognition site) was transformed in *E. coli* BL21(DE3) Gold competent cells. Cells were grown at 37 °C in minimal medium until O.D. 0.6 and then induced with 0.5 mM IPTG for 16 h at 25 °C. Glutaredoxin 1 was purified by affinity chromatography using a nickel chelating HisTrap (GE Healthcare) column. After digestion with AcTEV protease (Invitrogen) O/N at 25 °C the protein was separated from the affinity tag in a HisTrap column. The sample buffer was then exchanged with 50 mM potassium phosphate, 0.5 mM EDTA, pH=7.

NMR experiments were acquired at a 950 MHz Bruker Avance™ III spectrometer equipped with a CP TCI CryoProbe™. 1D ^{1}H and 2D ^{1}H,^{15}N-SOFAST-HMQC [31] spectra were acquired at 305K. The total acquisition time for each cell sample ranged from 1 to 2 h. The supernatant of each cell sample was checked for protein leakage in the same experimental conditions. The same NMR spectra were also acquired on the cell extracts. Cell viability before and after NMR experiments was assessed by Trypan Blue staining [32]. Cell viability remained above 90%, as damaged cells ranged from 3% before the experiments to 8% after the experiments.

Acknowledgements:

This work was supported by the Programmi di Ricerca di Rilevante Interesse Nazionale (PRIN) (2009FAKHZT_001 “Biologia strutturale meccanicistica: avanzamenti metodologici e biologici”), and by Ente Cassa di Risparmio di Firenze (“Biologia Strutturale Integrata”).

Associated content

Supporting Information

Supplementary Figures Available: This material is free *via* the Internet.

Author Information:

Corresponding Author

* E-mail: banci@cerm.unifi.it

Notes

The authors declare no competing financial interest.

REFERENCES

(1) Neupert, W., Herrmann, J. M. (2007) Translocation of proteins into mitochondria. *Annu. Rev. Biochem. 76*, 723-749.

(2) Longen, S., Bien, M., Bihlmaier, K., Kloeppel, C., Kauff, F., Hammermeister, M., Westermann, B., Herrmann, J. M., Riemer, J. (2009) Systematic analysis of the twin cx(9)c protein family. *J. Mol. Biol. 393*, 356-368.

(3) Banci, L., Bertini, I., Ciofi-Baffoni, S., Tokatlidis, K. (2009) The coiled coil-helix-coiled coil-helix proteins may be redox proteins. *FEBS Lett. 11*, 1699-1702.

(4) Lu, H., Allen, S., Wardleworth, L., Savory, P., Tokatlidis, K. (2004) Functional TIM10 chaperone assembly is redox-regulated in vivo. *J. Biol. Chem. 279*, 18952-18958.

(5) Mesecke, N., Terziyska, N., Kozany, C., Baumann, F., Neupert, W., Hell, K., Herrmann, J. M. (2005) A disulfide relay system in the intermembrane space of mitochondria that mediates protein import. *Cell 121*, 1059-1069.

(6) Chacinska, A., Pfannschmidt, S., Wiedemann, N., Kozjak, V., Sanjuan Szklarz, L. K., Schulze-Specking, A., Truscott, K. N., Guiard, B., Meisinger, C., Pfanner, N. (2004) Essential role of Mia40 in import and assembly of mitochondrial intermembrane space proteins. *EMBO J. 23*, 3735-3746.

(7) Durigon, R., Wang, Q., Ceh, P. E., Grant, C. M., Lu, H. (2012) Cytosolic thioredoxin system facilitates the import of mitochondrial small Tim proteins. *EMBO Rep. 13*, 916-922.

(8) Reckel, S., Hänsel, R., Löhr, F., Dötsch, V. (2007) In-cell NMR spectroscopy. *Prog. NMR Spectrosc. 51*, 91-101.

(9) Inomata, K., Ohno, A., Tochio, H., Isogai, S., Tenno, T., Nakase, I., Takeuchi, T., Futaki, S., Ito, Y., Hirokai, H., Shirakawa, M. (2009) High-resolution multi-dimensional NMR spectroscopy of proteins in human cells. *Nature 458*, 106-109.

(10) Ogino, S., Kubo, S., Umemoto, R., Huang, S., Nishida, N., Shimada, I. (2009) Observation of NMR signals from proteins introduced into living mammalian cells by reversible membrane permeabilization using a pore-forming toxin, streptolysin O. *J. Am. Chem. Soc. 131*, 10834-10835.

(11) Selenko, P., Frueh, D. P., Elsaesser, S. J., Haas, W., Gygi, S. P., Wagner, G. (2009) In situ observation of protein phosphorylation by high-resolution NMR spectroscopy. *Nat. Struct. Mol. Biol. 15*, 321-329.

(12) Banci, L., Barbieri, L., Bertini, I., Luchinat, E., Secci, E., Zhao, Y., and Aricescu, A. R. Monitoring protein maturation steps in living cells with atomic resolution by NMR. The case of human superoxide dismutase. *Unpublished work.*

(13) Naoe, M., Ohwa, Y., Ishikawa, D., Ohshima, C., Nishikawa, S. I., Yamamoto, H., Endo, T. (2004) Identification of Tim40 that mediates protein sorting to the mitochondrial intermembrane space. *J. Biol. Chem. 279*, 47815-47821.

(14) Grumbt, B., Stroobant, V., Terziyska, N., Israel, L., Hell, K. (2007) Functional characterization of Mia40p, the central component of the disulfide relay system of the mitochondrial intermembrane space. *J. Biol. Chem. 282*, 37461-37470.

(15) Banci, L., Bertini, I., Cefaro, C., Ciofi-Baffoni, S., Gallo, A., Martinelli, M., Sideris, D. P., Katrakili, N., Tokatlidis, K. (2009) MIA40 is an oxidoreductase that catalyzes oxidative protein folding in mitochondria. *Nat. Struct. Mol. Biol. 16*, 198-206.

(16) Tokatlidis, K. (2005) A disulfide relay system in mitochondria. *Cell 121*, 965-967.

(17) Gabriel, K., Milenkovic, D., Chacinska, A., Muller, J., Guiard, B., Pfanner, N., Meisinger, C. (2007) Novel mitochondrial intermembrane space proteins as substrates of the MIA import pathway. *J Mol Biol 365*, 612-620.

(18) Banci, L., Bertini, I., Cefaro, C., Cenacchi, L., Ciofi-Baffoni, S., Felli, I. C., Gallo, A., Gonnelli, L., Luchinat, E., Sideris, D. P., Tokatlidis, K. (2010) Molecular chaperone function of Mia40 triggers consecutive induced folding steps of the substrate in mitochondrial protein import. *Proc. Natl. Acad. Sci. USA 107*, 20190-20195.

(19) Chacinska, A., Guiard, B., Muller, J. M., Schulze-Specking, A., Gabriel, K., Kutik, S., Pfanner, N. (2008) Mitochondrial biogenesis, switching the sorting pathway of the intermembrane space receptor Mia40. *J Biol. Chem. 283*, 29723-29729.

(20) Meyer, Y., Buchanan, B. B., Vignols, F., Reichheld, J. P. (2009) Thioredoxins and glutaredoxins: unifying elements in redox biology. *Annu. Rev. Genet. 43*, 335-367.

(21) Holmgren, A. (1989) Thioredoxin and glutaredoxin systems. *J. Biol. Chem. 264*, 13963-13966.

(22) Sagemark, J., Elgan, T. H., Burglin, T. R., Johansson, C., Holmgren, A., Berndt, K. D. (2007) Redox properties and evolution of human glutaredoxins. *Proteins 68*, 879-892.

(23) Holmgren, A. (1979) Reduction of disulfides by thioredoxin. Exceptional reactivity of insulin and suggested functions of thioredoxin in mechanism of hormone action. *J. Biol. Chem. 254*, 9113-9119.

(24) Sakai, T., Tochio, H., Tenno, T., Ito, Y., Kokubo, T., Hiroaki, H., Shirakawa, M. (2006) In-cell NMR spectroscopy of proteins inside Xenopus laevis oocytes. *J. Biomol. NMR 36*, 179-188.

(25) Crowley, P. B., Chow, E., Papkovskaia, T. (2011) Protein interactions in the Escherichia coli cytosol: an impediment to in-cell NMR spectroscopy. *Chembiochem. 12*, 1043-1048.

(26) Reckel, S., Lopez, J. J., Löhr, F., Glaubitz, C., Dötsch, V. (2012) In-cell solid-state NMR as a tool to study proteins in large complexes. *ChemBioChem 13*, 534-537.

(27) Hofmann, S., Rothbauer, U., Muhlenbein, N., Baiker, K., Hell, K., Bauer, M. F. (2005) Functional and mutational characterization of human MIA40 acting during import into the mitochondrial intermembrane space. *J Mol Biol 353*, 517-528.

(28) Berndt, C., Lillig, C. H., Holmgren, A. (2008) Thioredoxins and glutaredoxins as facilitators of protein folding. *Biochim. Biophys. Acta 1783*, 641-650.

(29) Jurado, P., de, L., V, Fernandez, L. A. (2006) Thioredoxin fusions increase folding of single chain Fv antibodies in the cytoplasm of Escherichia coli: evidence that chaperone activity is the prime effect of thioredoxin. *J. Mol. Biol. 357*, 49-61.

(30) Aricescu, A. R., Lu, W., Jones, E. Y. (2006) A time- and cost-efficient system for high-level protein production in mammalian cells. *Acta Crystallogr. D. Biol. Crystallogr. 62*, 1243-1250.

(31) Schanda, P., Brutscher, B. (2005) Very Fast Two-Dimensional NMR Spectroscopy for Real-Time Investigation of Dynamic Events in Proteins on the Time Scale of Seconds. *J. Am. Chem. Soc. 127*, 8014-8015.

(32) Freshney, R. *Culture of Animal Cells: A Manual of Basic Technique*; Alan R. Liss, Inc., New York: 1987.

Figures:

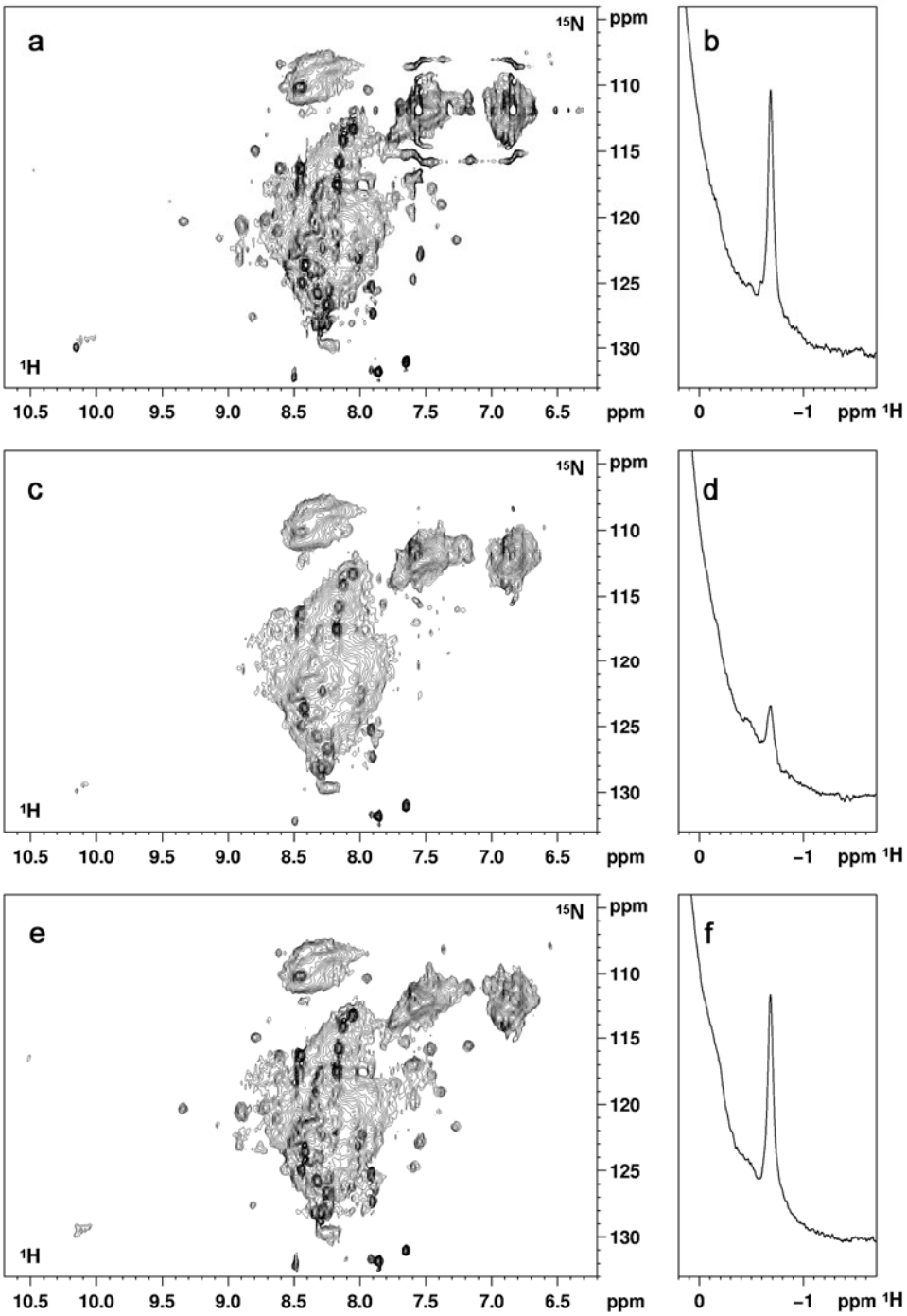
a
b
c
d
e
f
15N
1H
ppm
110
115
120
125
130
10.5
10.0
9.5
9.0
8.5
8.0
7.5
7.0
6.5
0
−1
ppm 1H

Figure 1. The folding state of Mia40 in the cytoplasm is dependent on the presence of different redox-regulating proteins. NMR spectra were acquired on human cells expressing uniformly ^{15}N-labelled Mia40 in the cytoplasm. (a, c, e) ^{1}H-^{15}N SOFAST HMQC spectra. The strong, overlapped crosspeaks between 8.0 and 8.5 ppm (^{1}H) correspond to the unfolded regions, while the weaker, dispersed crosspeaks belong to the residues of the folded region of Mia40. (b, d, f) aliphatic region of ^{1}H spectra showing the ^{1}Hγ peak of Ile 53, which is a marker of the folded conformation of Mia40 and falls in a cellular background-free region. (a, b) Spectra of cells expressing Mia40. (c, d) Spectra of cells co-expressing Mia40 and Grx1. (e, f) Spectra of cells co-expressing Mia40 and Trx1.

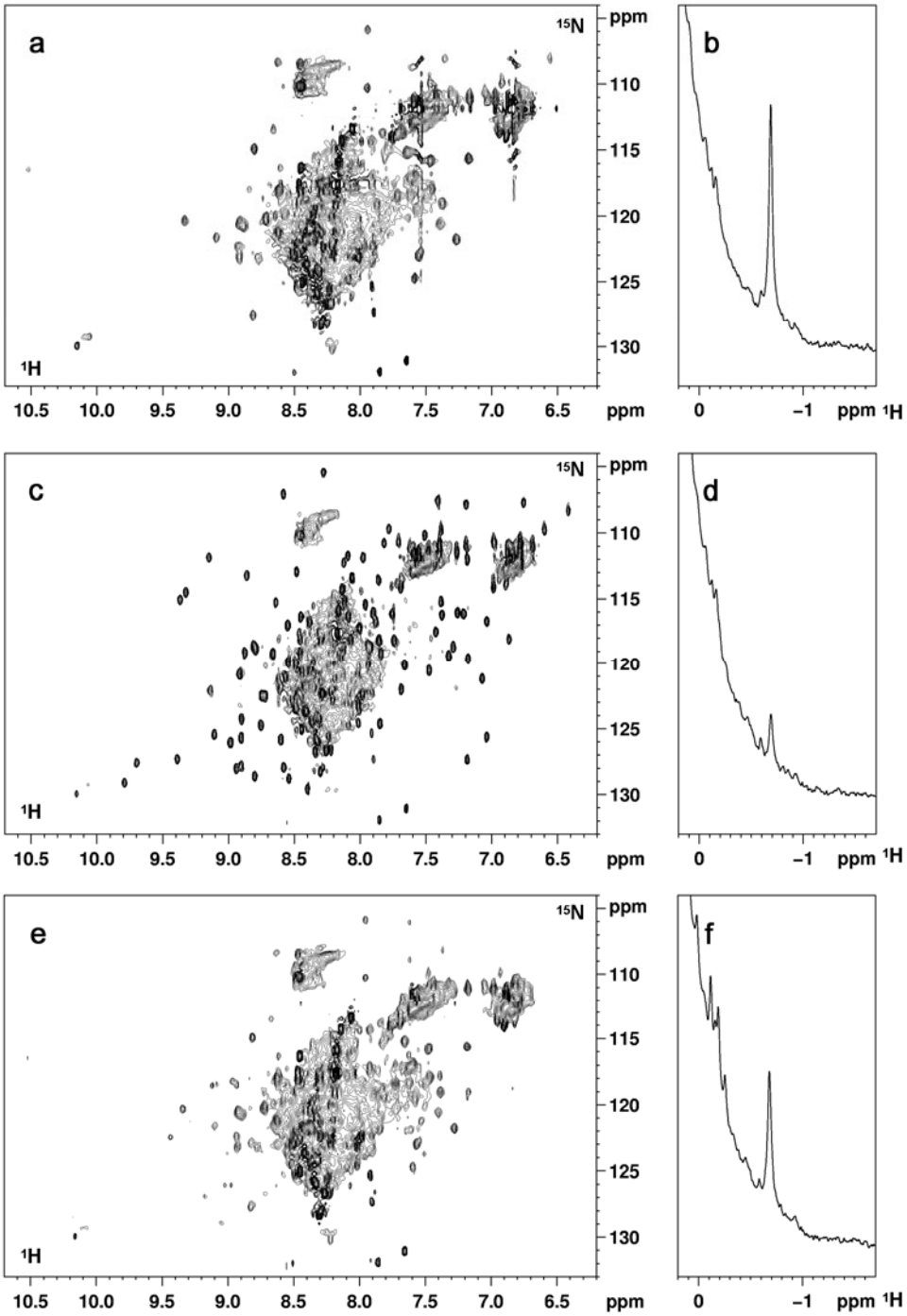
a
b
c
d
e
f
15N
1H
ppm
110
115
120
125
130
10.5
10.0
9.5
9.0
8.5
8.0
7.5
7.0
6.5
0
−1

Figure 2. NMR spectra acquired on the cell extracts corresponding to the samples in Figure 1. NMR spectra were acquired on the cell extract of samples expressing uniformly ^{15}N-labelled Mia40. The relative amounts of the two Mia40 folding states remained unchanged upon cell lysis. (a, b) Spectra of cell extract containing Mia40. (c, d) Spectra of cell extract containing Mia40 and Grx1. (e, f) Spectra of cell extract containing Mia40 and Trx1. Upon cell lysis, both Grx1 and Trx1 became visible in the ^{1}H-^{15}N spectra (c, e).

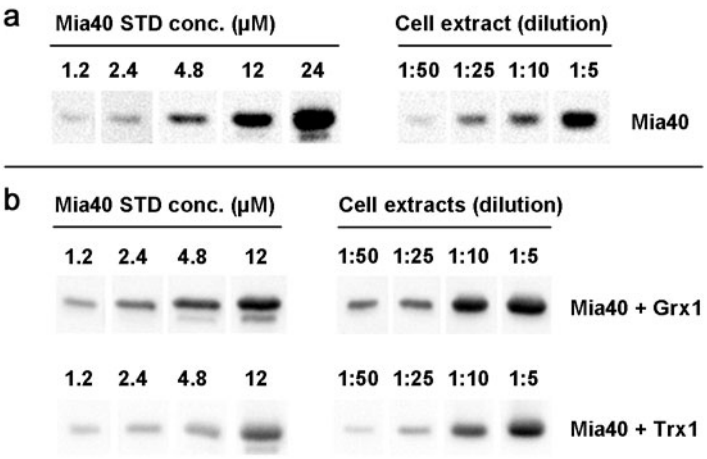

Figure 3. The total amount of Mia40 in the cell extracts is measured by Western Blot analysis. Samples of cell extracts were blotted at increasing dilutions together with samples of pure Mia40 at known concentrations. (a) Cell extract from cells expressing Mia40 alone. (b) Cell extracts from cells expressing Mia40 + Grx1 and Mia40 + Trx1. The blots were stained with a primary antibody against Mia40 (Abcam). A calibration curve was obtained for each blot from the intensities of the standard Mia40 samples. The concentration of Mia40 in the cell extracts was calculated for each dilution from the calibration curve, and averaged.

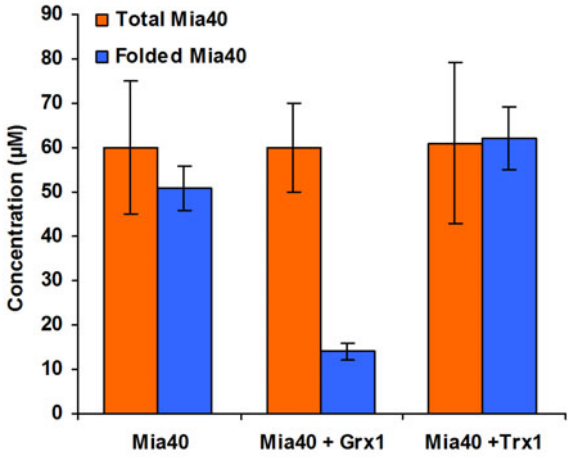

Figure 4. Effect of Grx1 and Trx1 on Mia40 folding state in the cytoplasm. Total Mia40 (orange bars) measured on cell extracts by Western Blot analysis is compared with folded Mia40 (blue bars) measured by NMR. When only Mia40 is expressed, it is largely present in the folded state in the cytoplasm. Co-expression of Grx1 causes a decrease of folded Mia40. Co-expression of Trx1 has no effect on the folding state of Mia40.

Supporting Information

Visualization of redox-controlled protein fold in living cells

Lucia Banci[1,2,*], Letizia Barbieri[1], Enrico Luchinat[1], Erica Secci[1]

Affiliations:

[1]Magnetic Resonance Center - CERM, University of Florence, Via Luigi Sacconi 6, 50019, Sesto Fiorentino, Florence, Italy.

[2]Department of Chemistry, University of Florence, Via della Lastruccia 3, 50019, Sesto Fiorentino, Florence, Italy.

*Corresponding Author

Supplementary Figures:

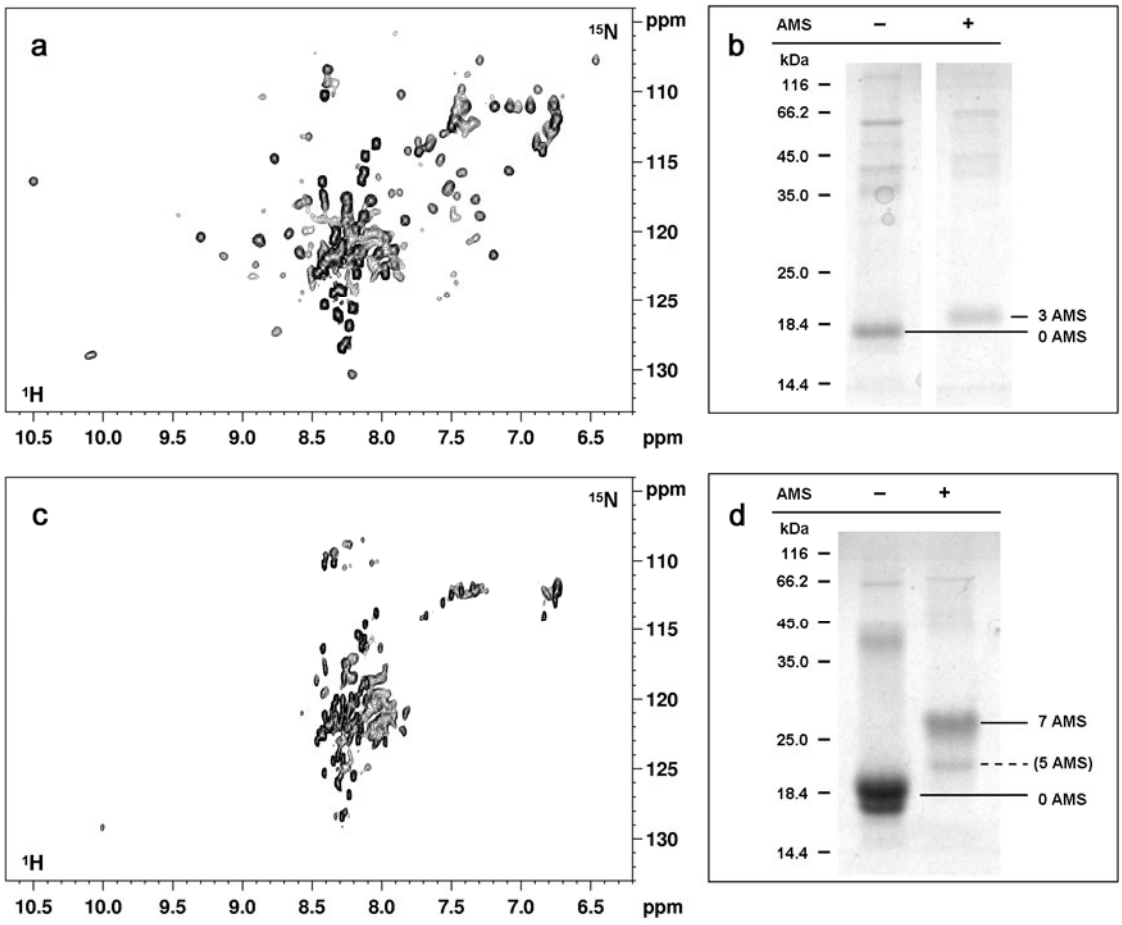

Supplementary Figure S1: Oxidized, folded Mia40 is reduced *in vitro* upon heat denaturation in reducing conditions. ^{1}H-^{15}N SOFAST HMQC spectra were acquired on pure U-^{15}N Mia40$^{2S\text{-}S}$ (a) before and (c) after denaturation at 95°C in presence of 10 mM GSH. After denaturation, the crosspeaks of the N- and C-terminal unfolded segments of Mia40 are still visible (with sharper lines), while those corresponding to the core segment of oxidized Mia40 disappear. AMS reaction was performed on Mia40 samples before and after denaturation, which were run on Coomassie-stained SDS-PAGE (b, d), confirming the reduction of the two structural disulfide bonds.

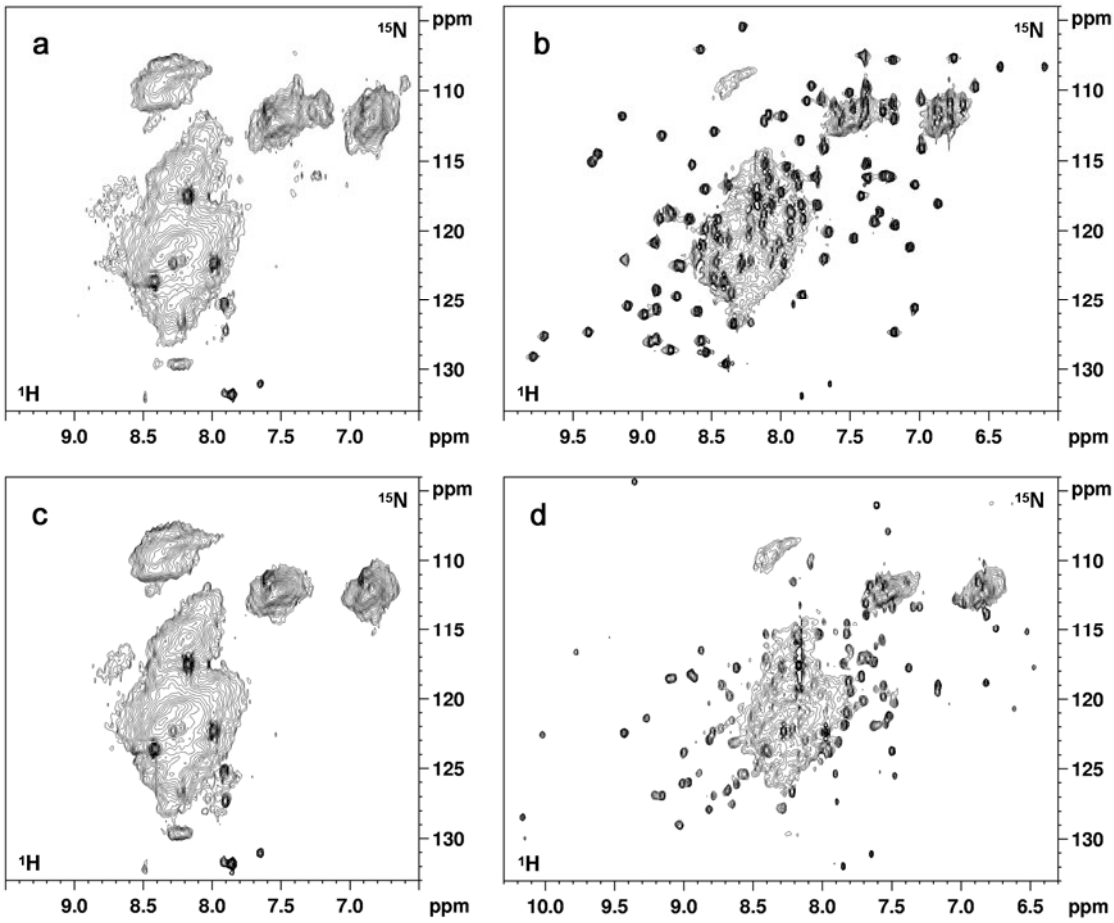

Supplementary Figure S2: The amide signals of cytoplasmic Grx1 and Trx1 are broadened beyond detection. ^{1}H-^{15}N SOFAST-HMQC spectra were acquired on samples of human cells expressing (a) Grx1 and (c) Trx1, and on the corresponding cell extracts (b, d). Only the cellular background signals were visible in the spectra of intact cells, where the amide crosspeaks of Grx1 and Trx1 are broadened beyond detection. Upon cell lysis, the crosspeaks of both proteins were detected.

3.4 Impaired folding and metal binding of SOD1 fALS mutants

Impaired folding and metal binding of SOD1 fALS mutants

Lucia Banci[1,2,*], Letizia Barbieri[1], Francesca Cantini[1,2], Enrico Luchinat[1]

Affiliations:

[1]CERM, Magnetic Resonance Center, University of Florence, Via Luigi Sacconi 6, 50019, Sesto Fiorentino, Florence, Italy.

[2]Department of Chemistry, University of Florence, Via della Lastruccia 3, 50019, Sesto Fiorentino, Florence, Italy.

* To whom correspondence should be addressed. L.B. (banci@cerm.unifi.it)

IN PREPARATION

Introduction

Cu,Zn-SOD1 is strongly implicated in the onset of the familial form of amyotrophic lateral sclerosis (fALS), as SOD1 protein aggregates have been found in dead motor neurons of ALS patients and transgenic mice[1]. Furthermore, 20% of fALS cases have been linked to mutations in the SOD1 gene[2]. More than 100 fALS-linked SOD1 mutations have been described, which are scattered throughout SOD1 amino acid sequence[3]. The pathogenicity of SOD1 has been demonstrated to be due to a gain of toxic function, and it has been linked to the presence of protein aggregates rich in SOD1 content at the late stage of the ALS disease[1]. As in other neurodegenerative diseases, the insoluble aggregates are not the toxic species, which causes motor neuron death and triggers the onset of the disease. Instead, soluble oligomeric intermediates in SOD1 aggregation process are thought to be responsible of the toxic gain of function[4]. In one hypothesis, the oligomers are formed through oxidation of the two free cysteines of SOD1 (6 and 111), forming amyloid-like structures[5].

Mature Cu,Zn-SOD1 is stably folded in a dimeric quaternary structure, and is not prone to aggregation, whereas the intermediate species of the maturation process (i.e. metal-depleted SOD1 species) are more likely to lose their quaternary structure and to oligomerize[6]. Therefore, an impaired maturation process leads to accumulation of immature SOD1 species, which are prone to oligomerization.

In this work currently in progress, the maturation process of a set of fALS mutants is studied through the in-human-cell NMR approach, which was previously applied to wild-type SOD1[7]. The outcome of the maturation process in different cellular conditions (e.g. presence of metals and/or CCS chaperone) will be compared with the wild-type scenario, providing direct atomic-level information on how each mutation affects the ability of intracellular SOD1 to acquire its mature state. Currently, two SOD1 fALS mutants – T54R and I113T – are being characterized in the cytoplasm of human cells. These two mutations occur close to the homodimer interface of SOD1. The previous *in vitro* studies show that T54R and I113T mutations have opposite effect on the oligomerization rate of the apo species[8]. T54R SOD1 has an oligomerization rate slightly slower than WT SOD1, likely due to the Arg54-Asn19 interaction which

stabilizes the homodimeric state[9]. I113T instead has an oligomerization rate more than twice that of WT SOD1[8]. Both mutants have similar folding properties to WT SOD1: the apo state is partially unstructured, while the zinc-bound species is dimeric and more stably folded.

Results

T54R and I113T SOD1 mutants were overexpressed in HEK293T cells in zinc-supplemented U-^{15}N labelled medium, and their folding and metallation state were determined. Cytoplasmic T54R SOD1 quantitatively bound one zinc ion per monomer (**Figure 1a**), and was in the dimeric state. This finding is consistent with the reported wild-type-like (WTL) behaviour of T54R SOD1 *in vitro*[8,9]. Instead, cytoplasmic I113T SOD1 in the same zinc-supplemented medium remained mostly in the apo state, which is largely unstructured and likely monomeric (**Figure 1b**). This outcome is consistent with the reported lower zinc affinity *in vitro* of I113T SOD1 compared to WT SOD1[10]. Other studies reported a WTL behaviour also for I113T SOD1, which was able to rescue SOD1 activity in *sod1Δ* yeast mutants[3], implying that copper insertion in the mutant protein had occurred. The formation of copper-containing, zinc-deficient mutant SOD1 species (which have been reported to be toxic[11]) can be hypothesized.

Further experiments will elucidate the role of CCS and copper in the maturation of T54R and I113T SOD1 mutants. Concurrently, the intracellular behaviour of other fALS mutants will be investigated (e.g. A4V, G37R, G93A).

Figures

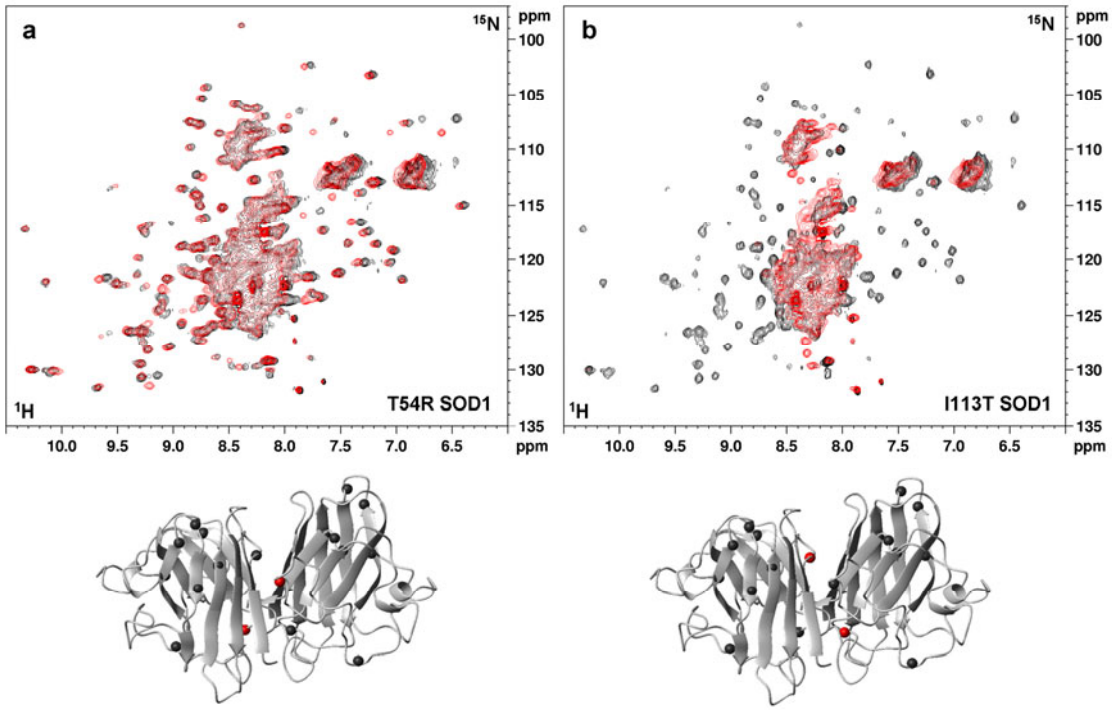

Figure 1: SOD1 fALS mutants were characterized in the human cell cytoplasm in zinc-supplemented U-^{15}N medium. (a) T54R SOD1 ^{1}H-^{15}N correlation spectrum (red) overlayed to the WT SOD1 spectrum (black); (b) I113T SOD1 ^{1}H-^{15}N correlation spectrum (red) overlayed to the WT SOD1 spectrum (black). Below each spectrum, the position of the mutation on the surface of SOD1 homodimer is shown [adapted from (8)]. T54R SOD1 behaves like WT SOD1, as one zinc per monomer is bound, and a homodimer is formed. I113T on the contrary does not bind zinc, and remains in the apo state, likely as a monomer.

References

1. Bruijn,L.I. *et al.* Aggregation and motor neuron toxicity of an ALS-linked SOD1 mutant independent from wild-type SOD1. *Science* **281**, 1851-1854 (1998).

2. Rosen,D.R. *et al.* Mutations in Cu/Zn superoxide dismutase gene are associated with familial amyotrophic lateral sclerosis. *Nature* **362**, 59-62 (1993).

3. Valentine,J.S., Doucette,P.A. & Potter,S.Z. Copper-zinc superoxide dismutase and amyotrophic lateral sclerosis. *Ann. Rev. Biochem.* **74**, 563-593 (2005).

4. Ross,C.A. & Poirier,M.A. Protein Aggregation and Neurodegenerative Disease. *Nat. Med.* **10**, S10-17 (2006).

5. Banci,L. *et al.* Metal-free SOD1 forms amyloid-like oligomers: a possible general mechanism for familial ALS. *Proc. Natl. Acad. Sci. USA* **104**, 11263-11267 (2007).

6. Lindberg,M.J., Tibell,L. & Oliveberg,M. Common denominator of Cu/Zn superoxide dismutase mutants associated with amyotrophic lateral sclerosis: Decreased stability of the apo state. *Proc. Natl. Acad. Sci. USA* **99**, 16607-16612 (2002).

7. Banci,L. *et al.* Atomic resolution monitoring of protein maturation in live human cells. *Unpublished work.*

8. Banci,L. *et al.* SOD1 and amyotrophic lateral sclerosis: mutations and oligomerization. *Plos ONE* **3**, e1677 (2008).

9. Banci,L. *et al.* Structural and dynamic aspects related to oligomerization of apo SOD1 and its mutants. *Proc. Natl. Acad. Sci. U. S. A* **106**, 6980-6985 (2009).

10. Crow,J.P., Sampson,J.B., Zhuang,Y., Thomson,J.A. & Beckman,J.S. Decreased zinc affinity of amyotrophic lateral sclerosis-associated superoxide dismutase mutants leads to enhanced catalysis of tyrosine nitration by peroxynitrite. *J. Neurochem.* **69**, 1936-1944 (1997).

11. Roberts,B.R. *et al.* Structural characterization of zinc-deficient human superoxide dismutase and implications for ALS. *J. Mol. Biol.* **373**, 877-890 (2007).

4. CONCLUSIONS AND PERSPECTIVES

In this doctorate project, the in-cell NMR approach was applied to follow protein functional processes, such as binding of metals and changes in the folding and cysteine redox state. Starting from a single protein expressed in *E. coli* cells, the approach was then extended to human cells, where multiple maturation steps were followed, some of which were dependent on the strictly regulated metal homeostasis of human cells, and as such would not be reproduced faithfully in bacterial cells. Finally, by simultaneously expressing two proteins, the effect of a partner on the final state of the maturating protein was investigated.

The sequence of events that allow human SOD1 to reach the mature state was thoroughly investigated. It was shown in *E. coli* cells that SOD1 spontaneously binds zinc, when this is added to the external medium, and reaches a folded, dimeric – and still reduced – state. In human cells, the effects of copper supplementation and co-expression of the chaperone CCS were studied, and the crucial role of CCS in catalyzing SOD1 internal disulfide bond formation without simultaneous copper transfer to SOD1 was shown for the first time. By following the same approach, a set of fALS-linked mutants of SOD1 is currently being characterized in the human cell cytoplasm, and the effects of each mutation at different steps of SOD1 maturation pathway are investigated.

Through the protein expression approach for in-human-cell NMR, the folding and redox state in the cytoplasm of the mitochondrial protein Mia40 was studied, obtaining clues on how the Grx1 redox regulation system has a specific role in keeping Mia40 unfolded, so that it can be imported into the mitochondria.

The newly developed protein expression approach in cultured human cells proved feasible for protein detection by NMR, and should be applicable to a range of soluble proteins. Additionally it gives the advantage, compared to protein insertion from outside, of being able to follow a protein maturation sequence starting right after its biosynthesis. Hopefully, it will complement the other in-cell NMR approaches, and may be integrated with them, to shed light on functional processes of increasing complexity in human cells, at atomic resolution.

Further development should focus on improving the sensitivity of the NMR experiments, by developing fast pulse sequences specifically optimized for cell samples.

The selectivity of the labelling should also be improved, to increase the ratio between protein and background signals. Importantly, both this factors will help decreasing the lower limit of protein concentration in the cell needed for NMR detection, hopefully reaching levels closer to the physiological conditions.

A further direction for development would be the extension of in-cell NMR to specific cell lines, which are already used as a model of tissues or for studying specific pathologies. If applied to such cellular systems, in-cell NMR could be combined with other cell biology techniques, such as live cell imaging techniques, protein functional assays, cell function assays and immunoblotting or immunoprecipitation techniques, thus providing direct correlation between the whole-cell view and the structural features of the underlying components. In this context, the approach of in-cell NMR by protein expression in human cells should easily integrate with those cell biology techniques, which already rely on the overexpression of proteins in cultured cells, that would complement the atomic-level description with information on the cellular localization of the protein and on the functional and metabolic state of the cell.

5. REFERENCE LIST

1. Gierasch,L.M. & Gershenson,A. Post-reductionist protein science, or putting Humpty Dumpty back together again. *Nature Chemical Biology* **5**, 774-777 (2009).

2. Li,C.W., Negendank,W.G., Murphy-Boesch,J., Padavic-Shaller,K. & Brown,T.R. Molar quantitation of hepatic metabolites in vivo in proton-decoupled, nuclear Overhauser effect enhanced 31P NMR spectra localized by three-dimensional chemical shift imaging. *NMR Biomed.* **9**, 141-155 (1996).

3. Kanamori,K. & Ross,B.D. Glial alkalinization detected in vivo by 1H-15N heteronuclear multiple-quantum coherence-transfer NMR in severely hyperammonemic rat. *J. Neurochem.* **68**, 1209-1220 (1997).

4. Serber,Z. *et al.* High-resolution macromolecular NMR spectroscopy inside living cells. *J. Am. Chem. Soc.* **123**, 2446-2447 (2001).

5. Barnes,C.O., Monteith,W.B. & Pielak,G.J. Internal and global protein motion assessed with a fusion construct and in-cell NMR spectroscopy. *Chembiochem.* **12**, 390-391 (2011).

6. Wang,Q., Zhuravleva,A. & Gierasch,L.M. Exploring weak, transient protein--protein interactions in crowded in vivo environments by in-cell nuclear magnetic resonance spectroscopy. *Biochemistry* **50**, 9225-9236 (2011).

7. Dedmon,M.M., Patel,C.N., Young,G.B. & Pielak,G.J. FlgM gains structure in living cells. *Proc. Natl. Acad. Sci. U. S. A* **99**, 12681-12684 (2002).

8. McNulty,B.C., Young,G.B. & Pielak,G.J. Macromolecular crowding in the Escherichia coli periplasm maintains alpha-synuclein disorder. *J. Mol. Biol.* **355**, 893-897 (2006).

9. Sakakibara,D. *et al.* Protein structure determination in living cells by in-cell NMR spectroscopy. *Nature* **458**, 102-105 (2009).

10. Schlesinger,A.P., Wang,Y., Tadeo,X., Millet,O. & Pielak,G.J. Macromolecular crowding fails to fold a globular protein in cells. *J. Am. Chem. Soc.* **133**, 8082-8085 (2011).

11. Binolfi,A., Theillet,F.X. & Selenko,P. Bacterial in-cell NMR of human alpha-synuclein: a disordered monomer by nature? *Biochem. Soc. Trans.* **40**, 950-954 (2012).

12. Burz,D.S., Dutta,K., Cowburn,D. & Shekhtman,A. Mapping structural interactions using in-cell NMR spectroscopy (STINT-NMR). *Nat. Methods* **3**, 91-93 (2006).

13. Burz,D.S. & Shekhtman,A. In-cell biochemistry using NMR spectroscopy. *Plos ONE* **3**, e2571 (2008).

14. Xie,J., Thapa,R., Reverdatto,S., Burz,D.S. & Shekhtman,A. Screening of small molecule interactor library by using in-cell NMR spectroscopy (SMILI-NMR). *J. Med. Chem.* **52**, 3516-3522 (2009).

15. Inomata,K. *et al.* High-resolution multi-dimensional NMR spectroscopy of proteins in human cells. *Nature* **458**, 106-109 (2009).

16. Augustus,A.M., Reardon,P.N. & Spicer,L.D. MetJ repressor interactions with DNA probed by in-cell NMR. *Proc. Natl. Acad. Sci. U. S. A* **106**, 5065-5069 (2009).

17. Crowley,P.B., Chow,E. & Papkovskaia,T. Protein interactions in the Escherichia coli cytosol: an impediment to in-cell NMR spectroscopy. *Chembiochem.* **12**, 1043-1048 (2011).

18. Bodart,J.F. *et al.* NMR observation of Tau in Xenopus oocytes. *J. Magn Reson.* **192**, 252-257 (2008).

19. Selenko,P. *et al.* In situ observation of protein phosphorylation by high-resolution NMR spectroscopy. *Nat. Struct. Mol. Biol.* **15**, 321-329 (2008).

20. Selenko,P., Serber,Z., Gadea,B., Ruderman,J. & Wagner,G. Quantitative NMR analysis of the protein G B1 domain in Xenopus laevis egg extracts and intact oocytes. *Proc. Natl. Acad. Sci. U. S. A* **103**, 11904-11909 (2006).

21. Sakai,T. *et al.* In-cell NMR spectroscopy of proteins inside Xenopus laevis oocytes. *J. Biomol. NMR* **36**, 179-188 (2006).

22. Ogino,S. *et al.* Observation of NMR signals from proteins introduced into living mammalian cells by reversible membrane permeabilization using a pore-forming toxin, streptolysin O. *J. Am. Chem. Soc.* **131**, 10834-10835 (2009).

23. Bertrand,K., Reverdatto,S., Burz,D.S., Zitomer,R. & Shekhtman,A. Structure of proteins in eukaryotic compartments. *J. Am. Chem. Soc.* **134**, 12798-12806 (2012).

24. McCord,J.M. & Fridovich,I. Superoxide dismutase. Enzymic function for erythrocuprein. *J. Biol. Chem.* **244**, 6049-6055 (1969).

25. Kobayashi,T. *et al.* Ultrastructural localization of superoxide dismutase in human skin. *Acta Derm. Venereol.* **73**, 41-45 (1993).

26. Crapo,J.D., Oury,T., Rabouille,C., Slot,J.W. & Chang,L.Y. Copper,zinc superoxide dismutase is primarily a cytosolic protein in human cells. *Proc. Natl. Acad. Sci. USA* **89**, 10405-10409 (1992).

27. Lindenau,J., Noack,H., Possel,H., Asayama,K. & Wolf,G. Cellular distribution of superoxide dismutases in the rat CNS. *Glia* **29**, 25-34 (2000).

28. Field,L.S., Furukawa,Y., O'Halloran,T.V. & Culotta,V.C. Factors controlling the uptake of yeast copper/zinc superoxide dismutase into mitochondria. *J. Biol. Chem.* **278**, 28052-28059 (2003).

29. Sturtz,L.A., Diekert,K., Jensen,L.T., Lill,R. & Culotta,V.C. A fraction of yeast Cu,Zn-superoxide dismutase and its metallochaperone, CCS, localize to the intermembrane space of mitochondria. A physiological role for SOD1 in guarding against mitochondrial oxidative damage. *J. Biol. Chem.* **276**, 38084-38089 (2001).

30. Forman,H.J. & Fridovich,I. On the stability of bovine superoxide dismutase. *J. Biol. Chem.* **248**, 2645-2649 (1973).

31. Roe,J.A. *et al.* Differential Scanning Calorimetry of Cu,Zn-Superoxide Dismutase, the Apoprotein, and Its Zinc-Substituted Derivatives. *Biochemistry* **27**, 950-958 (1988).

32. Bertini,I., Mangani,S. & Viezzoli,M.S. Advanced Inorganic Chemistry. Sykes,A.G. (ed.), pp. 127-250 (Academic Press, San Diego, CA, USA,1998).

33. Arnesano,F. *et al.* The unusually stable quaternary structure of human SOD1 is controlled by both metal occupancy and disulfide status. *J. Biol. Chem.* **279**, 47998-48003 (2004).

34. Banci,L. *et al.* Solution structure of reduced monomeric Q133M2 Copper, Zinc Superoxide Dismutase. Why is SOD a dimeric enzyme? *Biochemistry* **37**, 11780-11791 (1998).

35. Banci,L., Bertini,I., Cantini,F., D'Onofrio,M. & Viezzoli,M.S. Structure and dynamics of copper-free SOD: The protein before binding copper. *Protein Sci.* **11**, 2479-2492 (2002).

36. Banci,L., Bertini,I., Cramaro,F., Del Conte,R. & Viezzoli,M.S. Solution structure of Apo Cu,Zn superoxide dismutase: role of metal ions in protein folding. *Biochemistry* **42**, 9543-9553 (2003).

37. Banci,L. *et al.* Human SOD1 maturation through interaction with human CCS. *Proc. Natl. Acad. Sci. USA* **109**, 13555-13560 (2012).

38. Wong,P.C. *et al.* Copper chaperone for superoxide dismutase is essential to activate mammalian Cu/Zn superoxide dismutase. *Proc. Natl. Acad. Sci. USA* **97**, 2886-2891 (2000).

39. Jensen,L.T. & Culotta,V.C. Activation of CuZn Superoxide Dismutases from Caenorhabditis elegans Does Not Require the Copper Chaperone CCS. *J. Biol. Chem.* **280**, 41373-41379 (2005).

40. Furukawa,Y., Torres,A.S. & O'Halloran,T.V. Oxygen-induced maturation of SOD1: a key role for disulfide formation by the copper chaperone CCS. *EMBO J.* **23**, 2872-2881 (2004).

41. Wang,J. *et al.* Copper-binding-site-null SOD1 causes ALS in transgenic mice: aggregates of non-native SOD1 delineate a common feature. *Hum. Mol. Genet.* **12**, 2753-2764 (2003).

42. Banci,L. *et al.* Metal-free SOD1 forms amyloid-like oligomers: a possible general mechanism for familial ALS. *Proc. Natl. Acad. Sci. USA* **104**, 11263-11267 (2007).

43. Lelie,H.L. *et al.* Copper and Zinc Metallation Status of Copper-Zinc Superoxide Dismutase from Amyotrophic Lateral Sclerosis Transgenic Mice. *Journal of Biological Chemistry* **286**, 2795-2806 (2011).

44. Banci,L. *et al.* NMR characterization of a "fibril-ready" state of demetallated wild-type superoxide dismutase. *J. Am. Chem. Soc.* **133**, 345-349 (2011).

45. Rosen,D.R. *et al.* Mutation in Cu,Zn superoxide dismutase gene are associated with familial amyotrophyc lateral sclerosis. *Nature* **362**, 59-62 (1993).

46. Lindberg,M.J., Bystrom,R., Boknas,N., Andersen,P.M. & Oliveberg,M. Systematically perturbed folding patterns of amyotrophic lateral sclerosis (ALS)-associated SOD1 mutants. *Proc. Natl. Acad. Sci. USA* **102**, 9754-9759 (2005).

47. Culotta,V.C. *et al.* The copper chaperone for superoxide dismutase. *J. Biol. Chem.* **272**, 23469-23472 (1997).

48. Rae,T.D., Torres,A.S., Pufahl,R.A. & O'Halloran,T.V. Mechanism of Cu,Zn-superoxide dismutase activation by the human metallochaperone hCCS. *J. Biol. Chem.* **276**, 5166-5176 (2001).

49. Carroll,M.C. *et al.* Mechanisms for activating Cu- and Zn-containing superoxide dismutase in the absence of the CCS Cu chaperone. *Proc. Natl. Acad. Sci. USA* **101**, 5964-5969 (2004).

50. Leitch,J.M., Yick,P.J. & Culotta,V.C. The right to choose: multiple pathways for activating copper,zinc superoxide dismutase. *J. Biol. Chem.* **284**, 24679-24683 (2009).

51. Caruano-Yzermans,A.L., Bartnikas,T.B. & Gitlin,J.D. Mechanisms of the copper-dependent turnover of the copper chaperone for superoxide dismutase. *J. Biol. Chem.* **281**, 13581-13587 (2006).

52. Lamb,A.L. *et al.* Crystal structure of the copper chaperone for superoxide dismutase. *Nature Struct. Biol.* **6**, 724-729 (1999).

53. Allen,S., Badarau,A. & Dennison,C. Cu(I) Affinities of the Domain 1 and 3 Sites in the Human Metallochaperone for Cu,Zn-Superoxide Dismutase. *Biochemistry* **51**, 1439-1448 (2012).

54. Henze,K. & Martin,W. Evolutionary biology: essence of mitochondria. *Nature* **426**, 127-128 (2003).

55. McBride,H.M., Neuspiel,M. & Wasiak,S. Mitochondria: more than just a powerhouse. *Curr. Biol. 2006. Jul. 25. ;16. (14):R551. -60.* **16**, R551-R560 (2006).

56. Hajnoczky,G. *et al.* Mitochondrial calcium signalling and cell death: approaches for assessing the role of mitochondrial Ca2+ uptake in apoptosis. *Cell Calcium* **40**, 553-560 (2006).

57. Wang,C. & Youle,R.J. The role of mitochondria in apoptosis*. *Annu. Rev. Genet.* **43**, 95-118 (2009).

58. Herrmann,J.M. & Neupert,W. Protein transport into mitochondria. *Curr. Opin. Microbiol.* **3**, 210-214 (2000).

59. Pfanner,N. & Geissler,A. Versatility of the mitochondrial protein import machinery. *Nat. Rev. Mol. Cell Biol.* **2**, 339-349 (2001).

60. Truscott,K.N. *et al.* A presequence- and voltage-sensitive channel of the mitochondrial preprotein translocase formed by Tim23. *Nat. Struct. Biol.* **8**, 1074-1082 (2001).

61. Kovermann,P. *et al.* Tim22, the essential core of the mitochondrial protein insertion complex, forms a voltage-activated and signal-gated channel. *Mol. Cell* **9**, 363-373 (2002).

62. Westerman,B.A., Poutsma,A., Steegers,E.A. & Oudejans,C.B. C2360, a nuclear protein expressed in human proliferative cytotrophoblasts, is a representative member of a novel protein family with a conserved coiled coil-helix-coiled coil-helix domain. *Genomics* **83**, 1094-1104 (2004).

63. Stojanovski,D. *et al.* The MIA system for protein import into the mitochondrial intermembrane space. *Biochim. Biophys. Acta* **1783**, 610-617 (2008).

64. Cobine,P.A., Pierrel,F. & Winge,D.R. Copper trafficking to the mitochondrion and assembly of copper metalloenzymes. *Biochim. Biophys. Acta* **1763**, 759-772 (2006).

65. Banci,L. *et al.* Mitochondrial copper(I) transfer from Cox17 to Sco1 is coupled to electron transfer. *Proc. Natl. Acad. Sci. USA* **105**, 6803-6808 (2008).

66. Banci,L., Bertini,I., Cavallaro,G. & Rosato,A. The functions of Sco proteins from genome-based analysis. *J. Proteome Res.* **6**, 1568-1579 (2007).

67. Bauer,M.F., Hofmann,S., Neupert,W. & Brunner,M. Protein translocation into mitochondria: the role of TIM complexes. *Trends in Cell Biology* **10**, 25-31 (2000).

68. Endres,M., Neupert,W. & Brunner,M. Transport of the ADP/ATP carrier of mitochondria from the TOM complex to the TIM22.54 complex. *EMBO J.* **18**, 3214-3221 (1999).

69. Vial,S. *et al.* Assembly of Tim9 and Tim10 into a functional chaperone. *J. Biol. Chem.* **277**, 36100-36108 (2002).

70. Mesecke,N. *et al.* A disulfide relay system in the intermembrane space of mitochondria that mediates protein import. *Cell* **121**, 1059-1069 (2005).

71. Grumbt,B., Stroobant,V., Terziyska,N., Israel,L. & Hell,K. Functional characterization of Mia40p, the central component of the disulfide relay system of the mitochondrial intermembrane space. *J. Biol. Chem.* **282**, 37461-37470 (2007).

72. Banci,L. *et al.* MIA40 is an oxidoreductase that catalyzes oxidative protein folding in mitochondria. *Nat. Struct. Mol. Biol.* **16**, 198-206 (2009).

73. Banci,L. *et al.* Molecular chaperone function of Mia40 triggers consecutive induced folding steps of the substrate in mitochondrial protein import. *Proc. Natl. Acad. Sci. USA* **107**, 20190-20195 (2010).

74. Sideris,D.P. *et al.* A novel intermembrane space-targeting signal docks cysteines onto Mia40 during mitochondrial oxidative folding. *J. Cell Biol.* **187**, 1007-1022 (2009).

75. Banci,L. *et al.* An electron-transfer path through an extended disulfide relay system: the case of the redox protein ALR. *J. Am. Chem. Soc.* **134**, 1442-1445 (2012).

76. Tokatlidis,K. A disulfide relay system in mitochondria. *Cell* **121**, 965-967 (2005).

77. Naoe,M. *et al.* Identification of Tim40 that mediates protein sorting to the mitochondrial intermembrane space. *J. Biol. Chem.* **279**, 47815-47821 (2004).

78. Terziyska,N. *et al.* Mia40, a novel factor for protein import into the intermembrane space of mitochondria is able to bind metal ions. *FEBS Lett.* **579**, 179-284 (2005).

79. Hofmann,S. *et al.* Functional and mutational characterization of human MIA40 acting during import into the mitochondrial intermembrane space. *J Mol Biol* **353**, 517-528 (2005).

80. Chacinska,A. *et al.* Mitochondrial biogenesis, switching the sorting pathway of the intermembrane space receptor Mia40. *J Biol. Chem.* **283**, 29723-29729 (2008).

81. Hu,J., Dong,L. & Outten,C.E. The redox environment in the mitochondrial intermembrane space is maintained separately from the cytosol and matrix. *J. Biol. Chem.* **283**, 29126-29134 (2008).

82. Holmgren,A. *et al.* Thiol redox control via thioredoxin and glutaredoxin systems. *Biochem. Soc. Trans.* **33**, 1375-1377 (2005).

83. Meyer,Y., Buchanan,B.B., Vignols,F. & Reichheld,J.P. Thioredoxins and glutaredoxins: unifying elements in redox biology. *Annu. Rev. Genet.* **43**, 335-367 (2009).

84. Holmgren,A. Thioredoxin and glutaredoxin systems. *J. Biol. Chem.* **264**, 13963-13966 (1989).

85. Berndt,C., Lillig,C.H. & Holmgren,A. Thiol-based mechanisms of the thioredoxin and glutaredoxin systems: implications for diseases in the cardiovascular system. *Am. J. Physiol Heart Circ. Physiol* **292**, H1227-H1236 (2007).

86. Lind,C. *et al.* Identification of S-glutathionylated cellular proteins during oxidative stress and constitutive metabolism by affinity purification and proteomic analysis. *Arch. Biochem. Biophys.* **406**, 229-240 (2002).

87. Lu,H., Allen,S., Wardleworth,L., Savory,P. & Tokatlidis,K. Functional TIM10 chaperone assembly is redox-regulated in vivo. *J. Biol. Chem.* **279**, 18952-18958 (2004).

88. Durigon,R., Wang,Q., Ceh,P.E., Grant,C.M. & Lu,H. Cytosolic thioredoxin system facilitates the import of mitochondrial small Tim proteins. *EMBO Rep.* **13**, 916-922 (2012).

89. Aricescu,A.R., Lu,W. & Jones,E.Y. A time- and cost-efficient system for high-level protein production in mammalian cells. *Acta Crystallogr. D. Biol. Crystallogr.* **62**, 1243-1250 (2006).

90. Bodenhausen,G. & Ruben,D.J. Natural abundance nitrogen-15 NMR by enhanced heteronuclear spectroscopy. *Chem. Phys. Lett.* **69**, 185-188 (1980).

91. Schanda,P. & Brutscher,B. Very Fast Two-Dimensional NMR Spectroscopy for Real-Time Investigation of Dynamic Events in Proteins on the Time Scale of Seconds. *J. Am. Chem. Soc.* **127**, 8014-8015 (2005).